Applying InSAR to volcano deformation

Matt Pritchard,
Falk Amelung &
Susanna Ebmeier

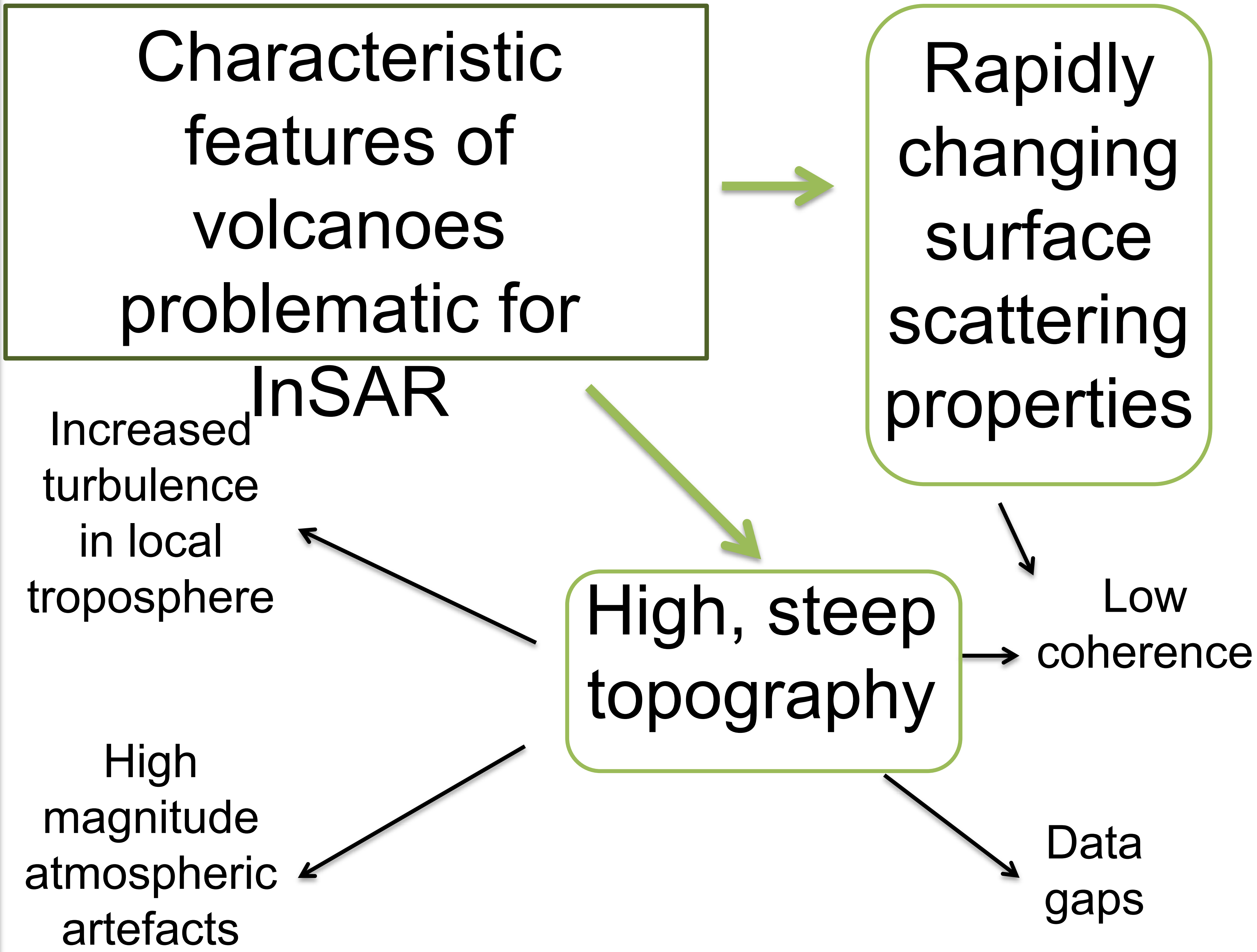
Characteristic features of volcanoes problematic for InSAR
Rapidly changing surface scattering properties
High, steep topography
Increased turbulence in local troposphere
High magnitude atmospheric artefacts
Low coherence
Data gaps

Application of InSAR to volcano deform

Volcanic vs. earthquake cycle deformation

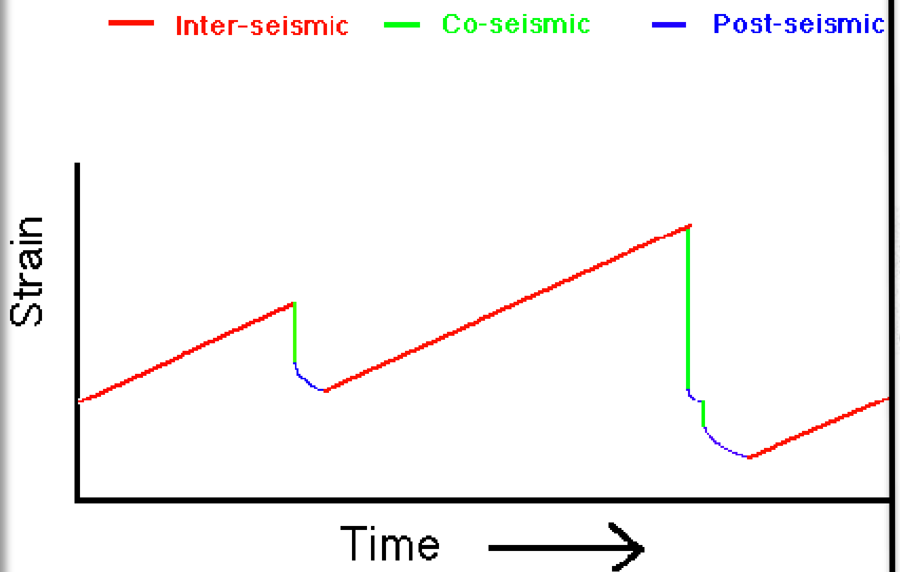

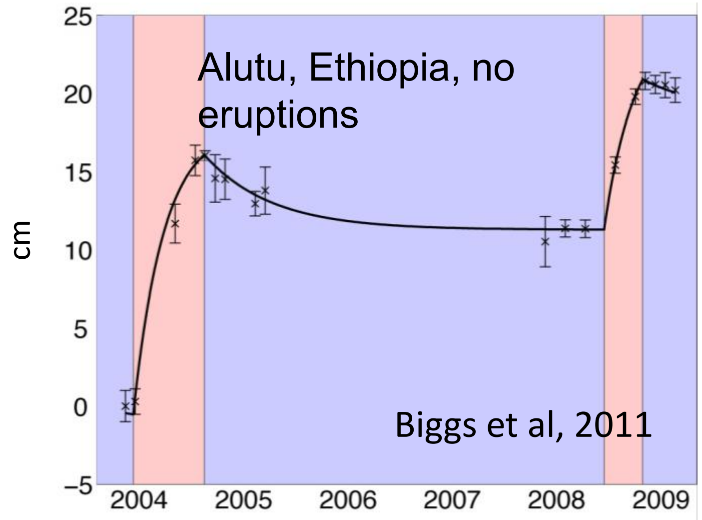

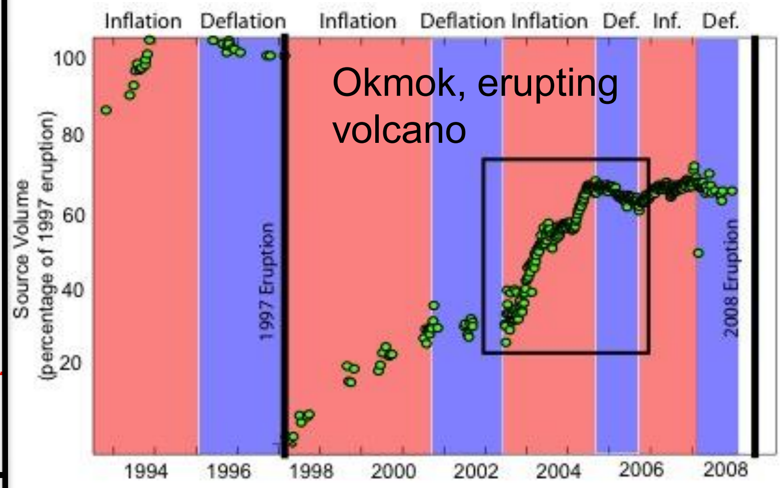

78 ' +(- ,(65(9: ; : 3(<2#"&8 "(- ,(65(9: : =3(>#(- ,(65(9: : ?(

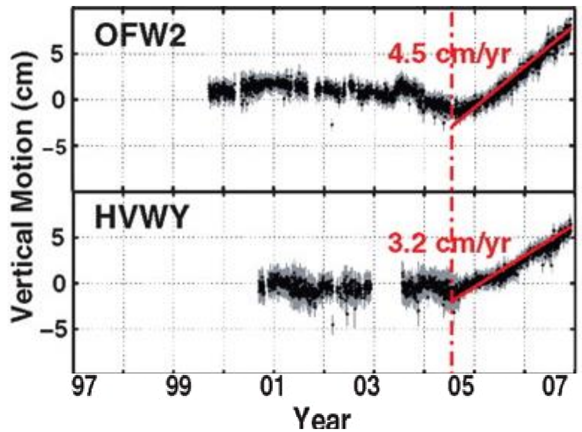

Yellowstone Caldera

Chang et al., 2007

Application of InSAR to volcano deform

Volcanic vs. earthquake cycle deformation

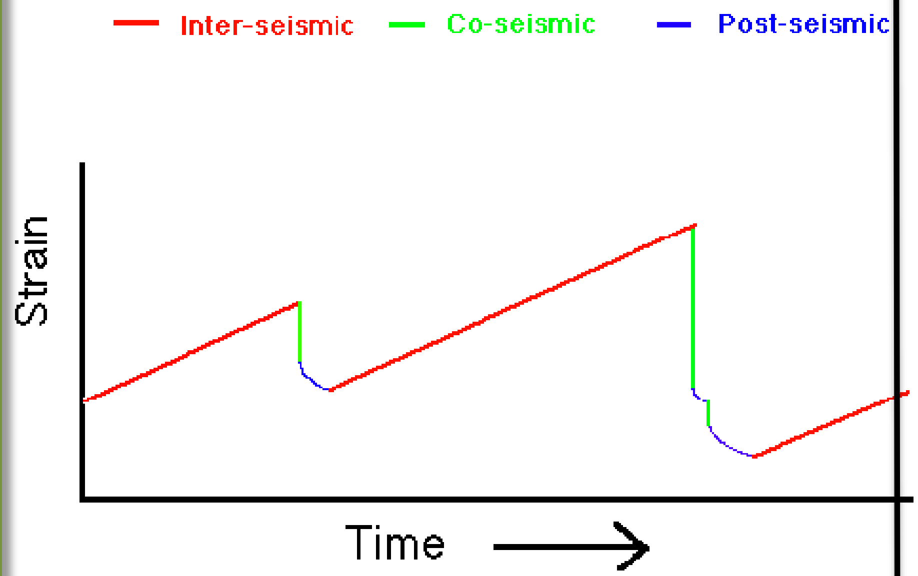

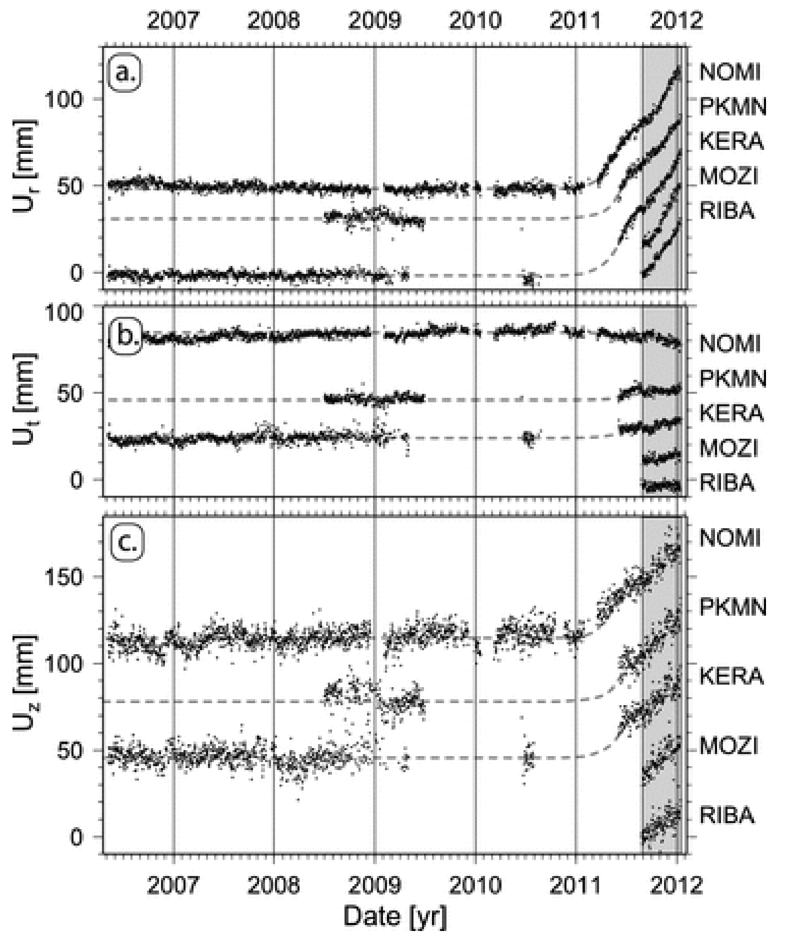

Newman et al., 2012

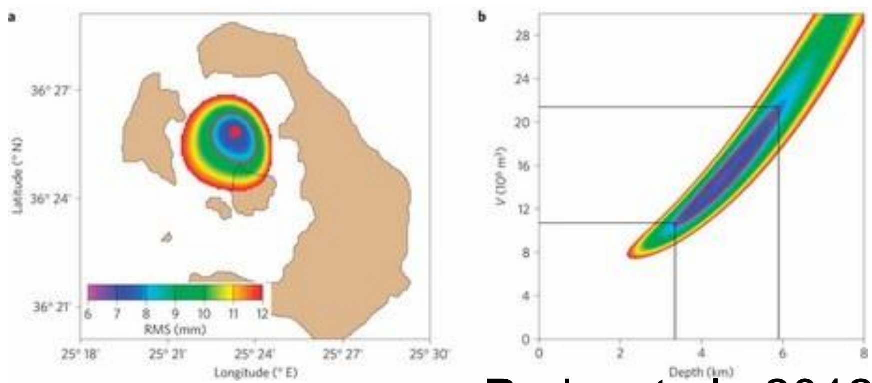

Parks et al., 2012

Tropospheric water vapour

Atmospheric contributions to phase : the impact of high topography

Turbulent atmosphere

- Orographic effects induce local overturning and condensation (e.g. Webley et al., 2004)
- The spatial dimensions of turbulent water vapour signals are on the scale of kms in mountainous regions, but 10s kms over flatter topography.

Stable atmosphere

- Water vapour concentrations vary the most low in the atmosphere, so there are large spatial differences in total path water vapour over steep topography.

Tropospheric water vapour

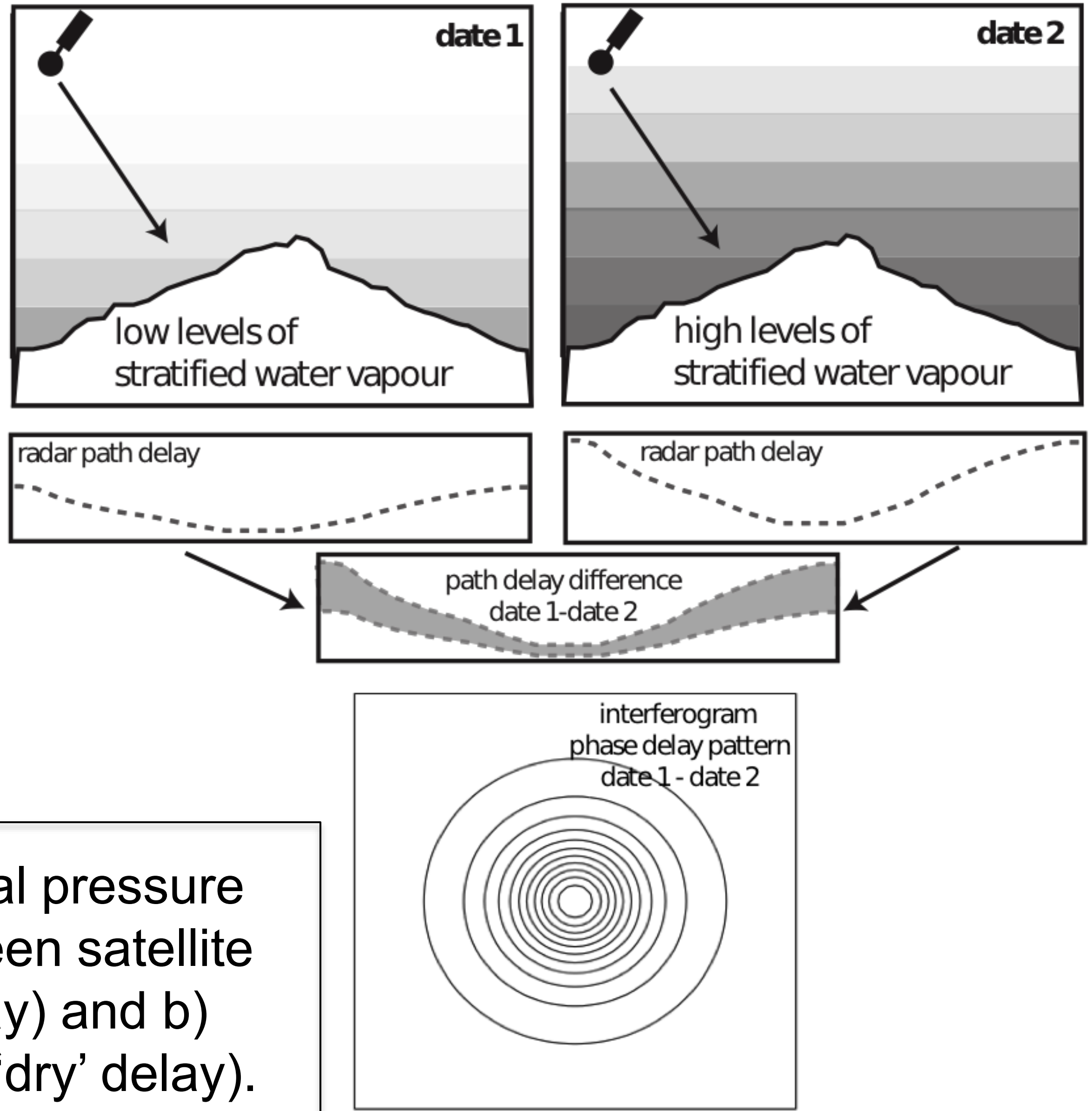

Differences in a) partial pressure of water vapour between satellite and ground ('wet' delay) and b) hydrostatic pressure ('dry' delay).

Tropospheric water vapour

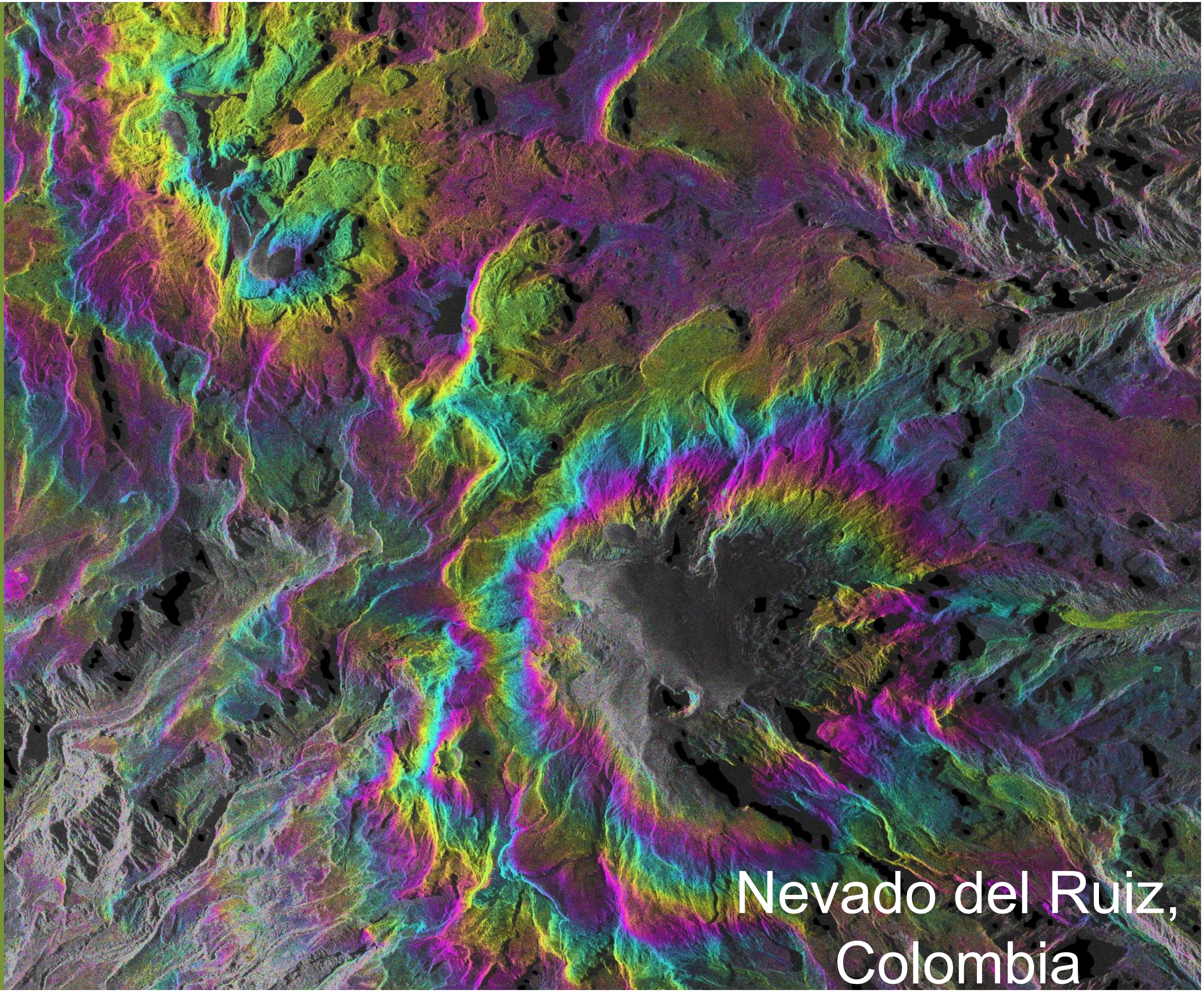

Tropospheric water vapour

Identifying atmospheric artefacts

	Tests	Category 4a: **stratified water vapour**	Category 4b: **turbulent water vapour**
Individual interferograms	phase topography correlation	phase is dependent on elevation	no correlation
sets of interferograms over the same volcano	pair-wise logic	← feature is associated with particular acquisitions →	
	stacking	← feature disappears/ significantly reduced in magnitude in stack →	
	time series	phase is seasonally dependent	phase is independent of time

Tropospheric water vapour

Phase-topography correlation

Correlation of topography with height
San Miguel, El Salvador

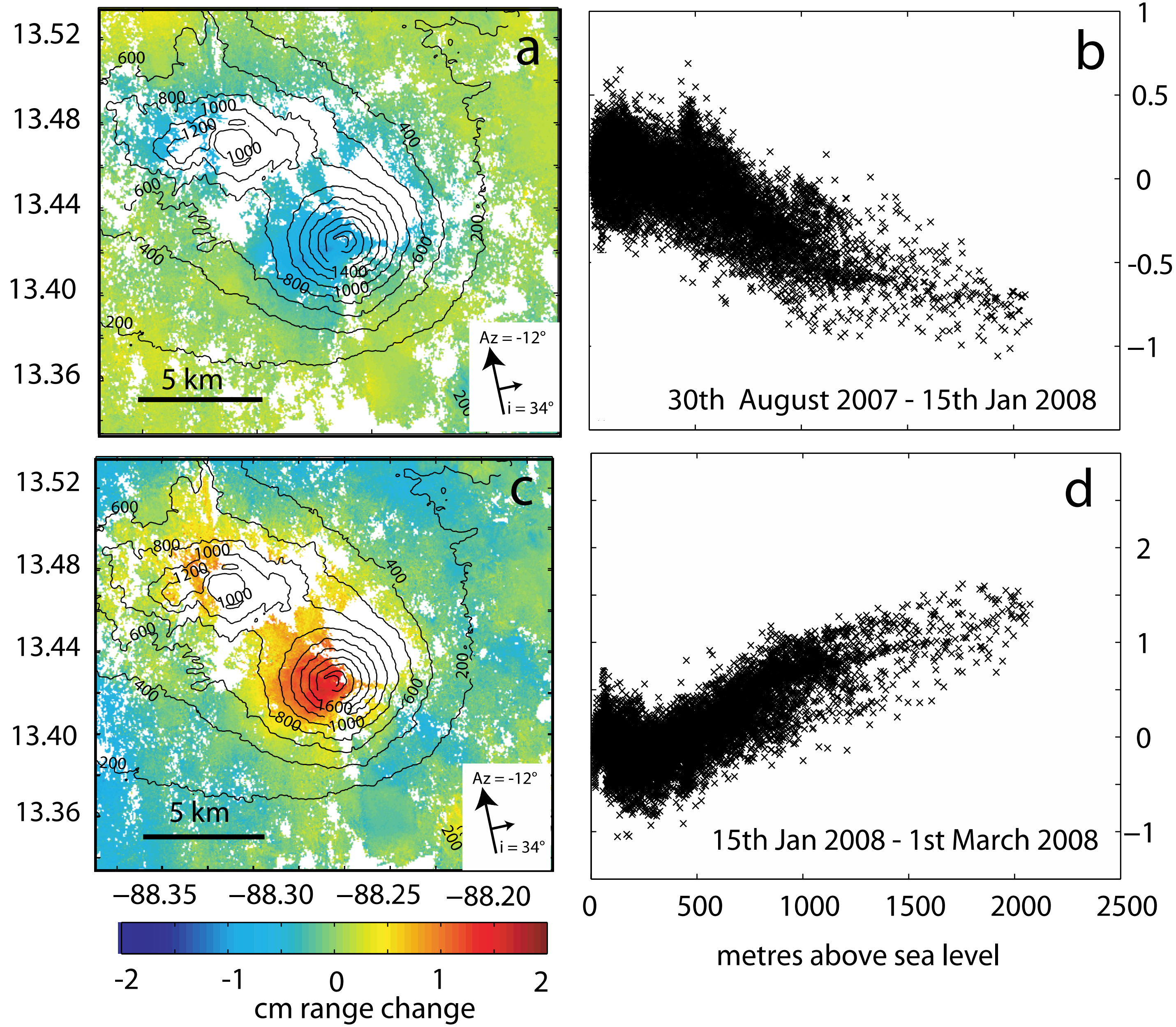

Tropospheric water vapour

Pairwise Logic

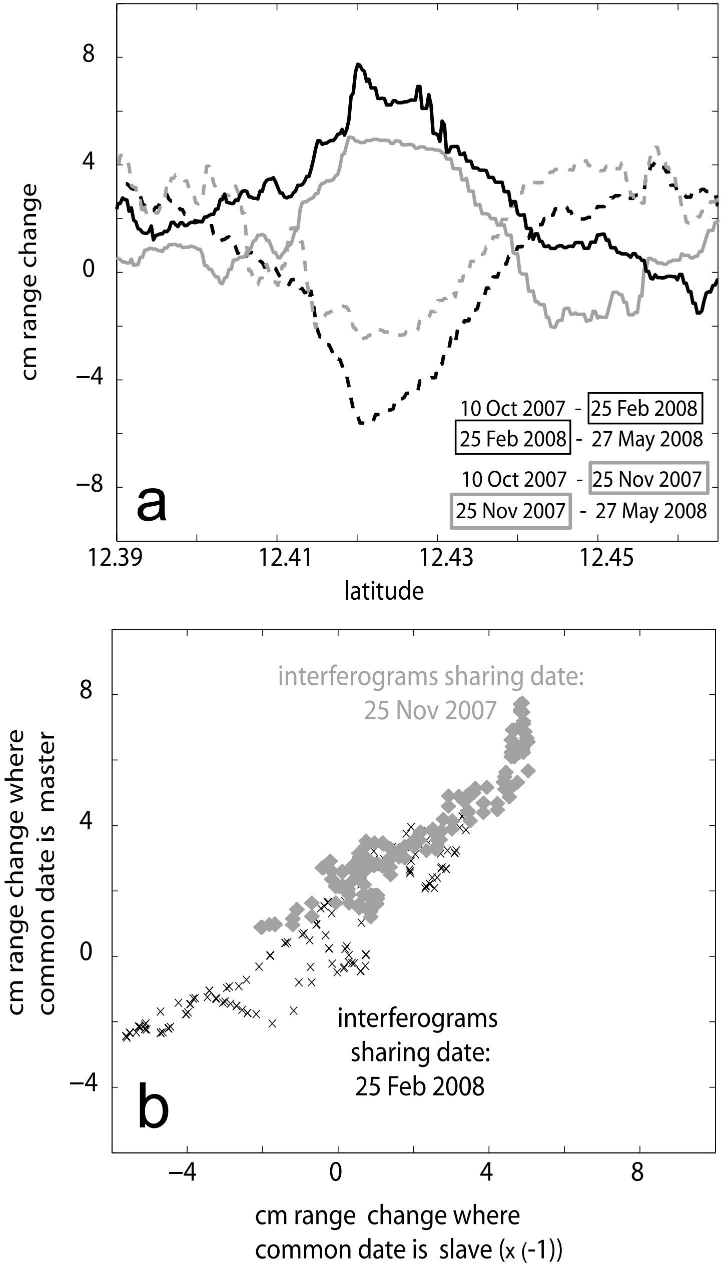

A high water vapour signal in image 'B', but not 'A' and 'C' can result in characteristic pattern:

$$\phi_{AB} = - \phi_{BC}$$

Tropospheric water vapour

Temporal development of signal

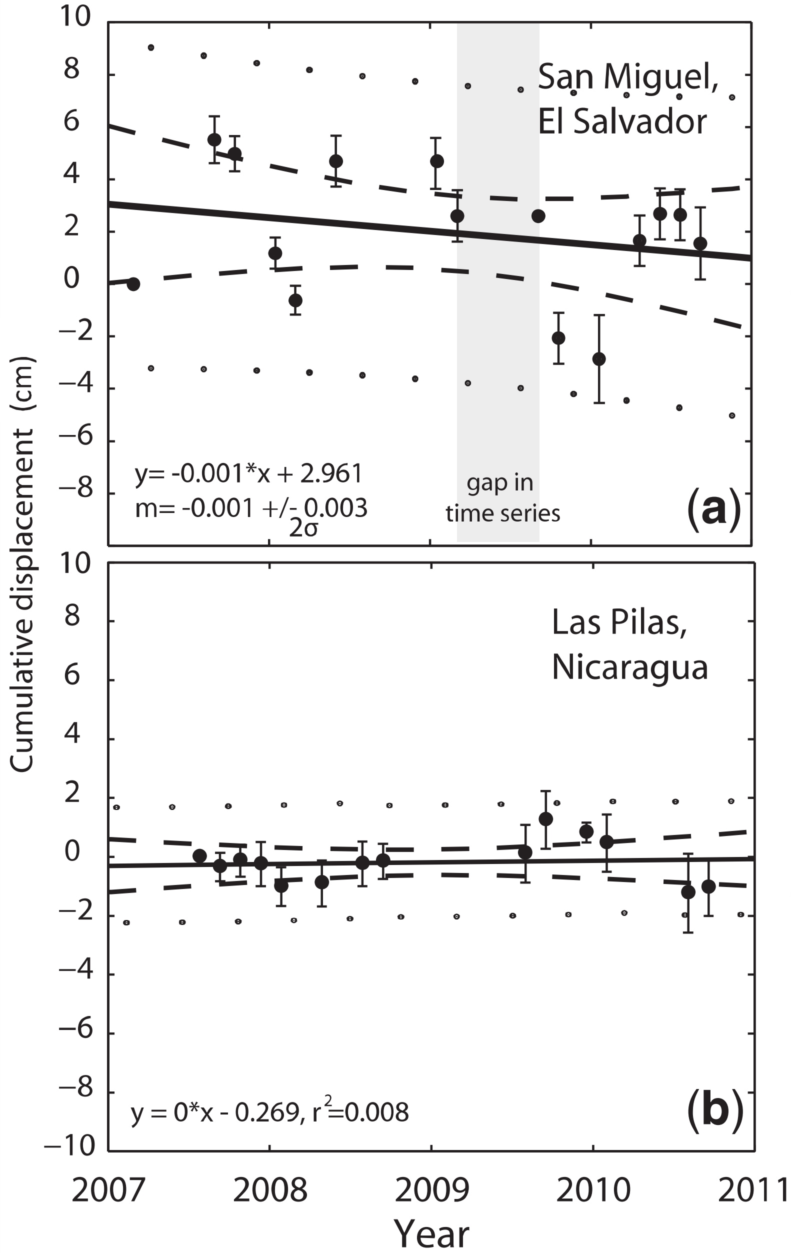

root mean squared variability = 4.7cm

root mean squared variability = 1.1cm

Tropospheric water vapour

Increase in variability with topographic height = ~ 2cm/k

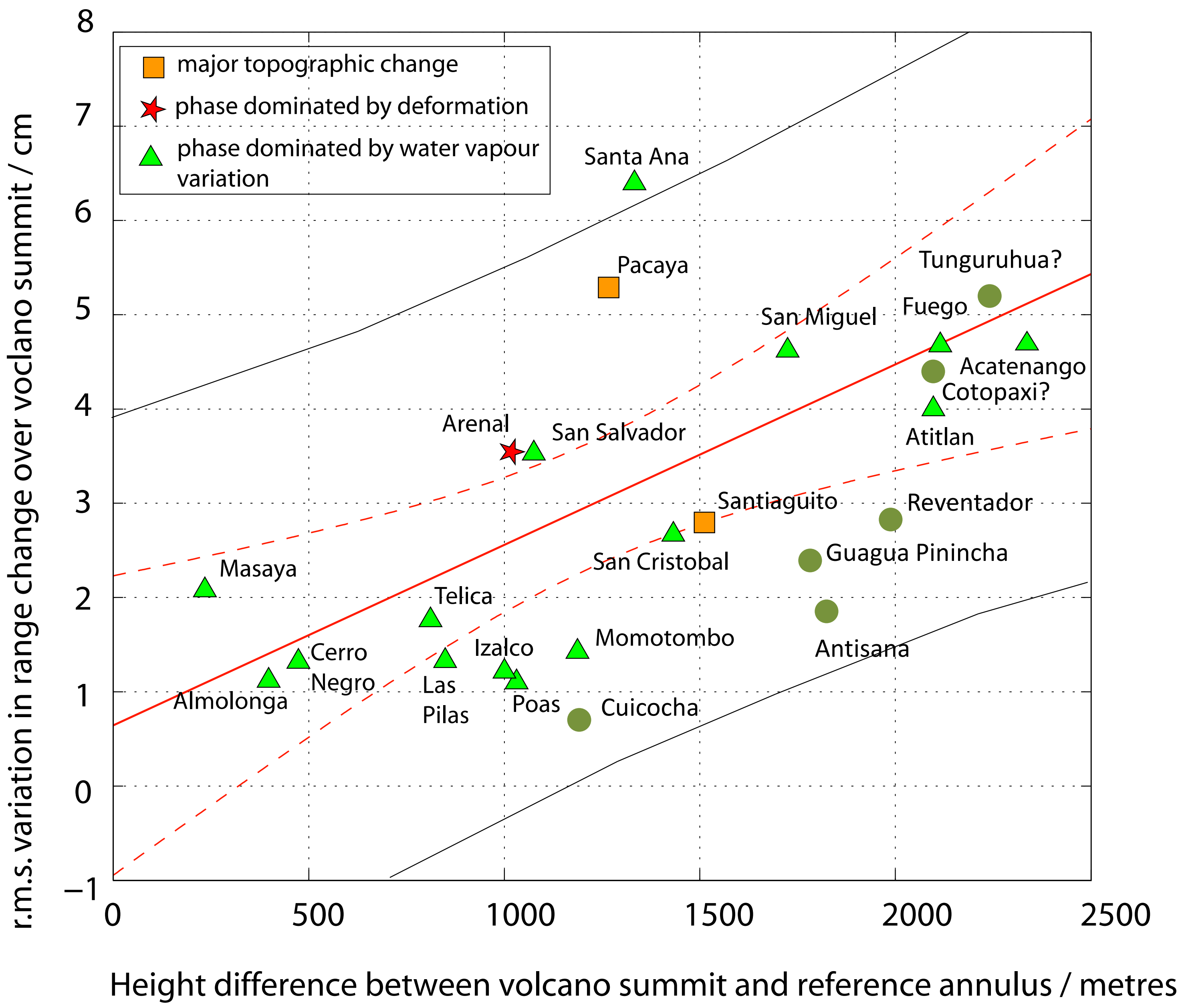

Tropospheric water vapour

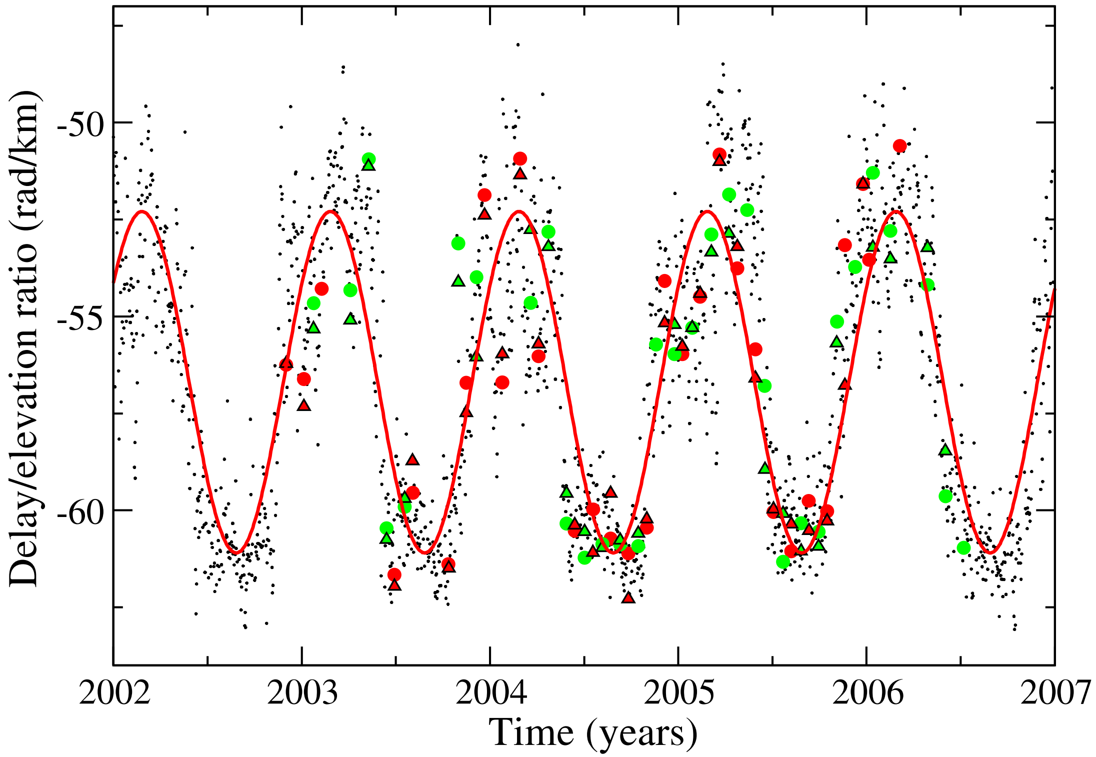

Pinel et al., 2011

Average ratio of phase delay to elevation over 400-1000m elevation range at Colima, Mexico

Black dots are meteorological reanalysis data and coloured symbols from interferograms

Seasonal variations in phase delay caused by stratospheric water vapour.

Tropospheric water vapour

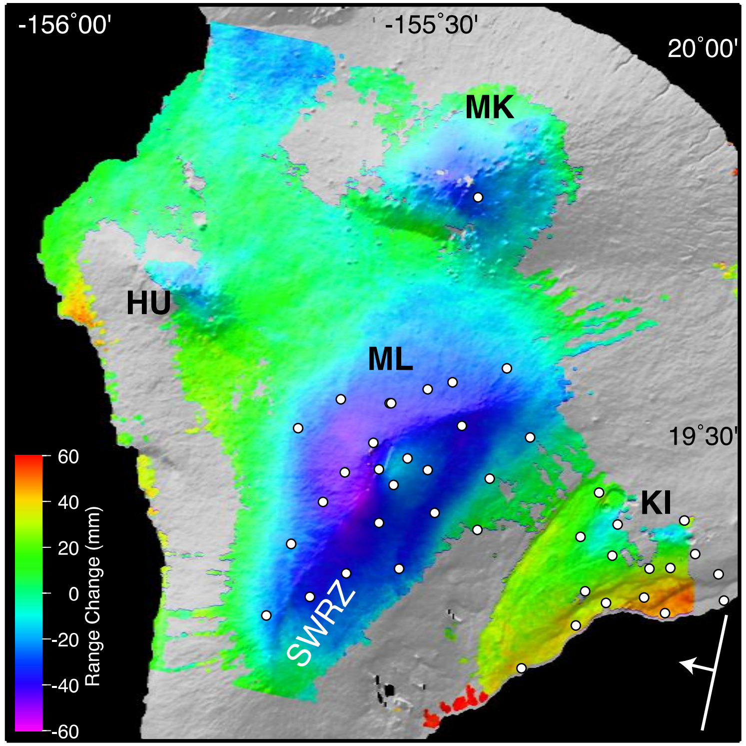

Interferogram, Big Island, Hawai'i
Foster et al., 2006

High resolution weather model from Mauna Kea weather centre
- reduces variance by 60% at 30 km scale in best cases
- Highly dependent on the model initial conditions

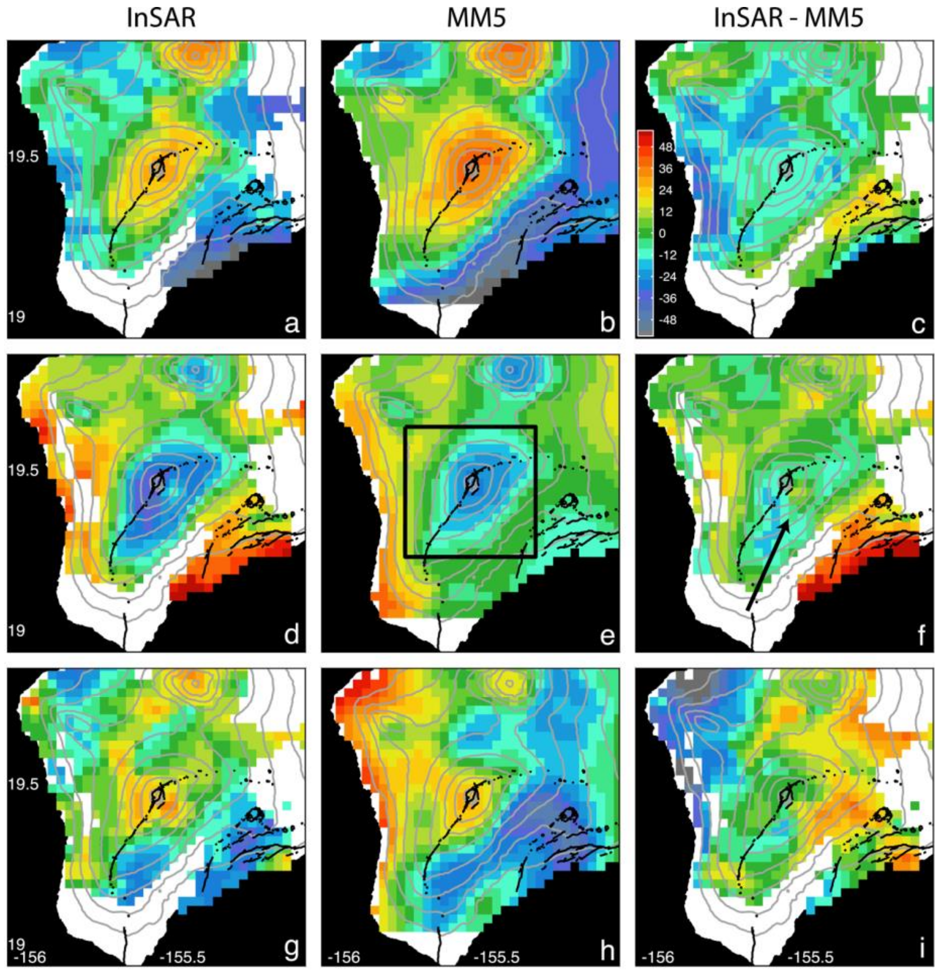

InSAR Model Residual

Tropospheric water vapour

Etna deformation field 2004-2005 , after correction with nested atmospheric model

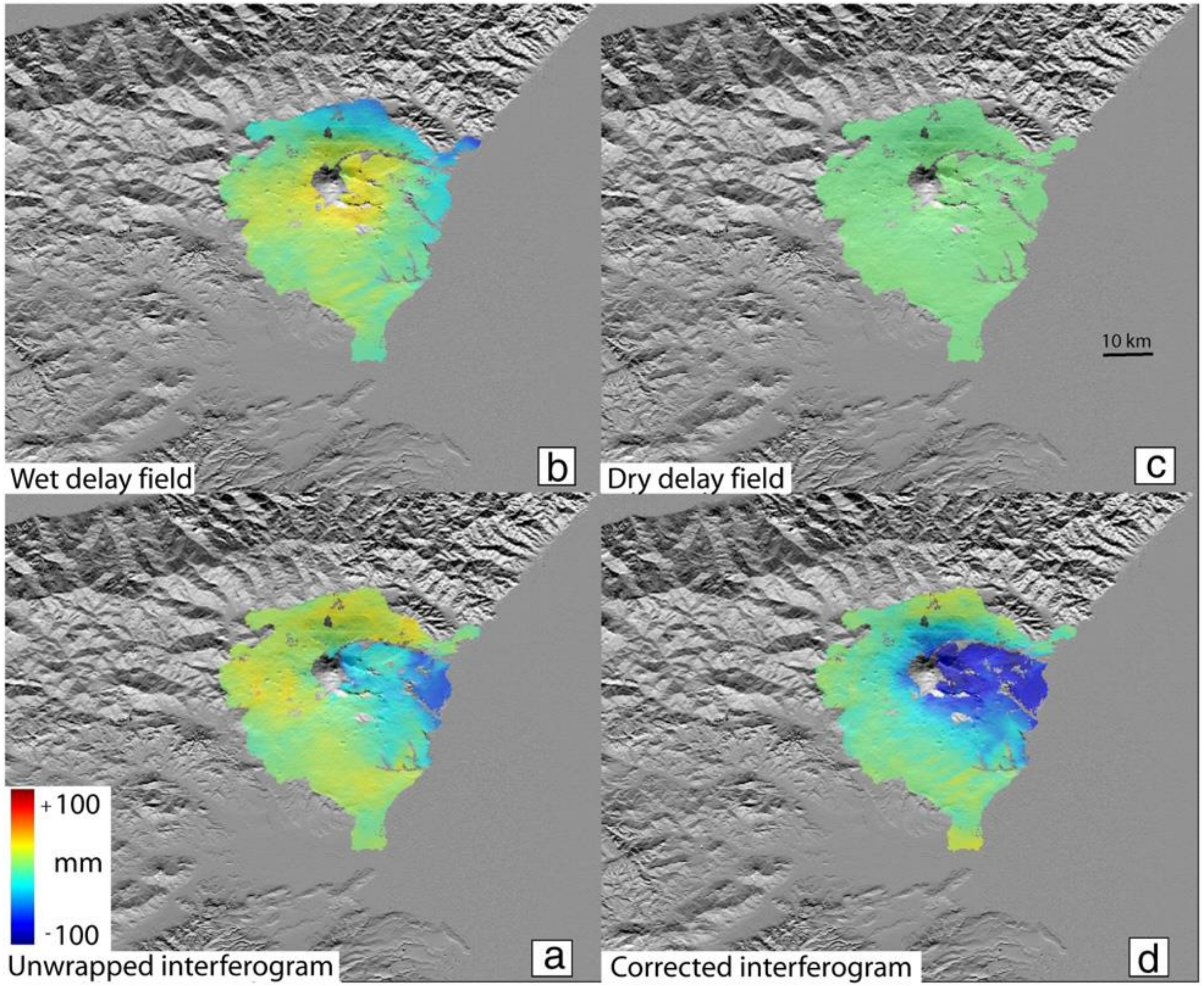

Wadge et al., 2010

Coherence: changes to pixel scattere

Coherence at volcanoes	geometric	temporal
High coherence	Flat topography Small perpendicular baseline	Stable surfaces, e.g. bare rock, desert, no snowfall, little or no vegetation, urban area
Low coherence	Steep topography Large perpendicular baselines	Dense, fast growing vegetation, high elevation (=snowy), intensive agriculture, water

The impact of radar wavelength

The impact of radar wavelength:

L-band radar penetrates forest, vegetation much more successfully than shorter wavelengths

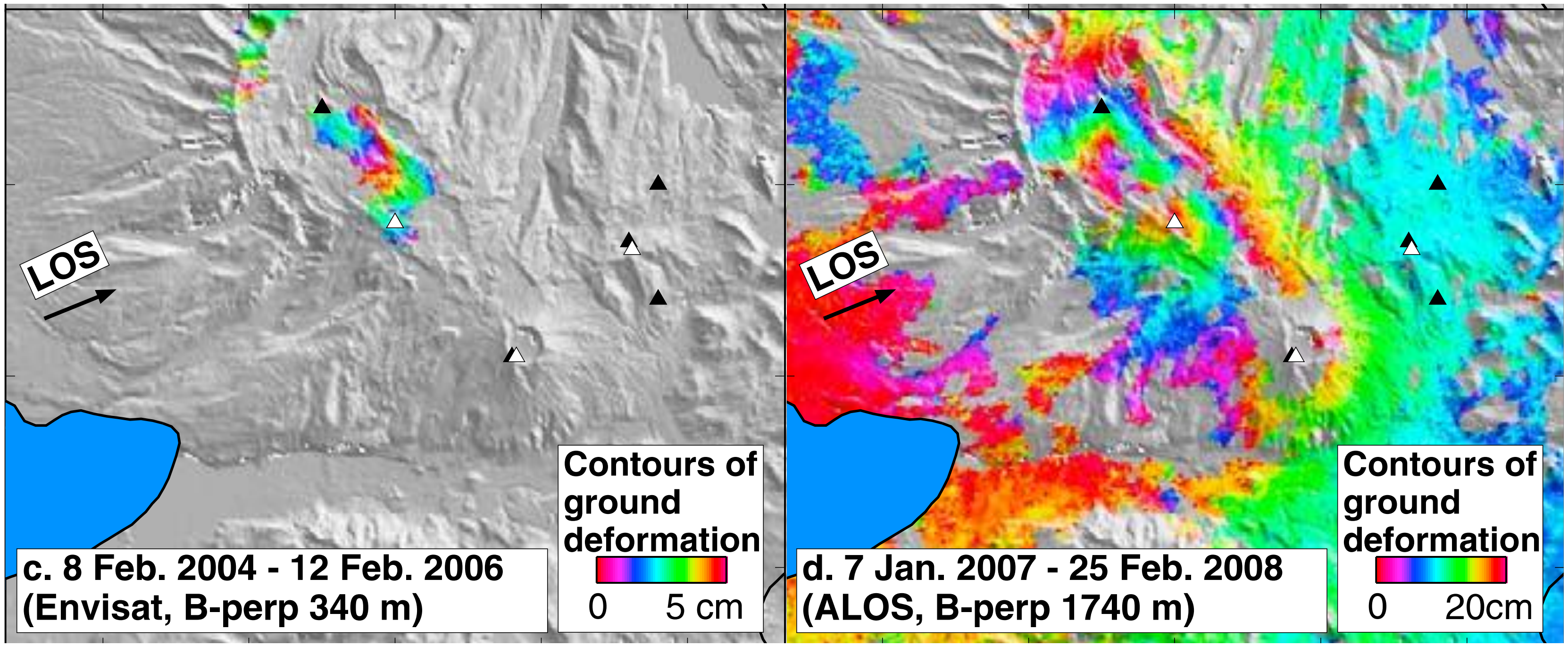

Fournier et al., 2010; Cordon Caulle, Chile

The impact of radar wavelength: C-band compared with L-band

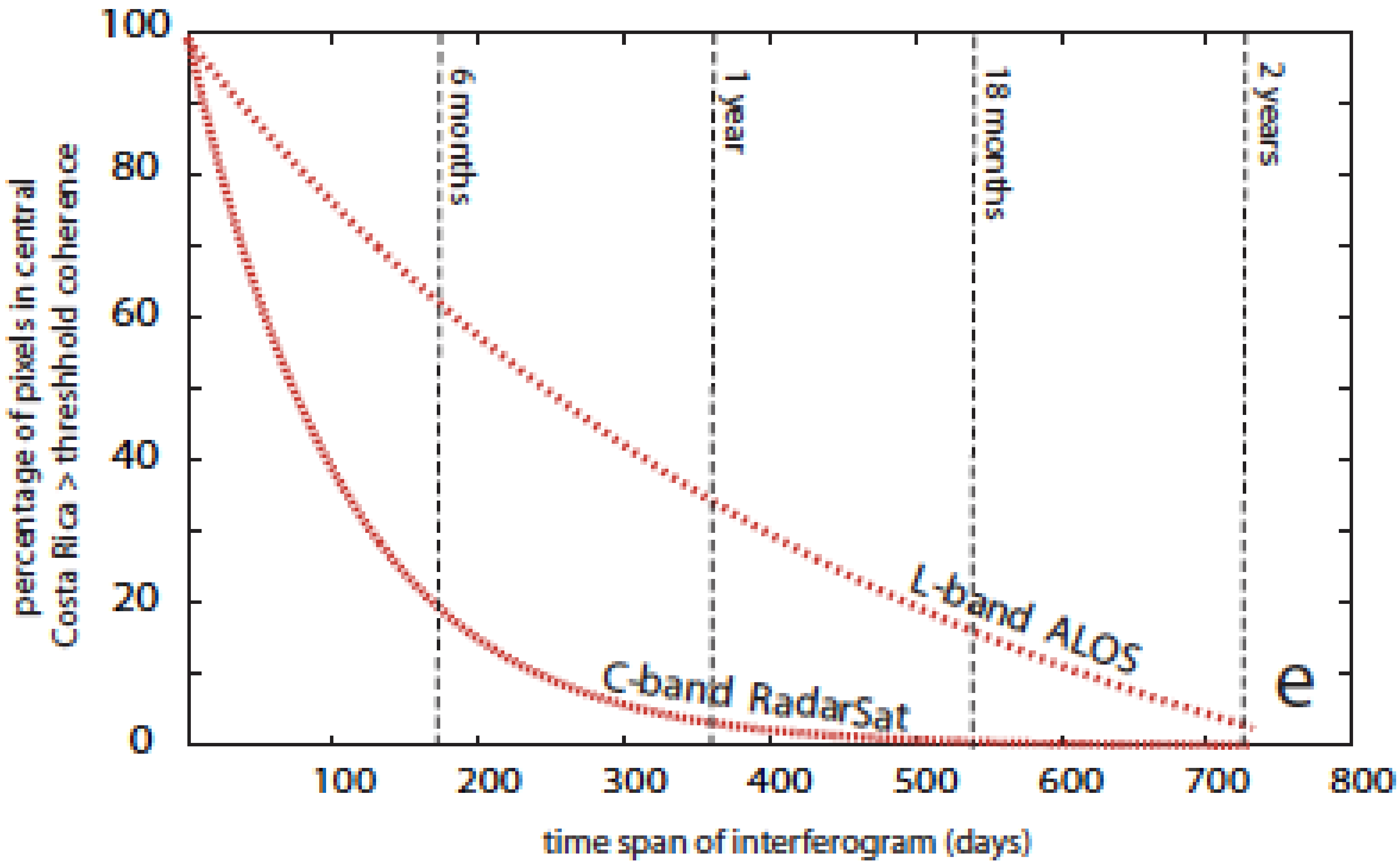

The impact of radar wavelength

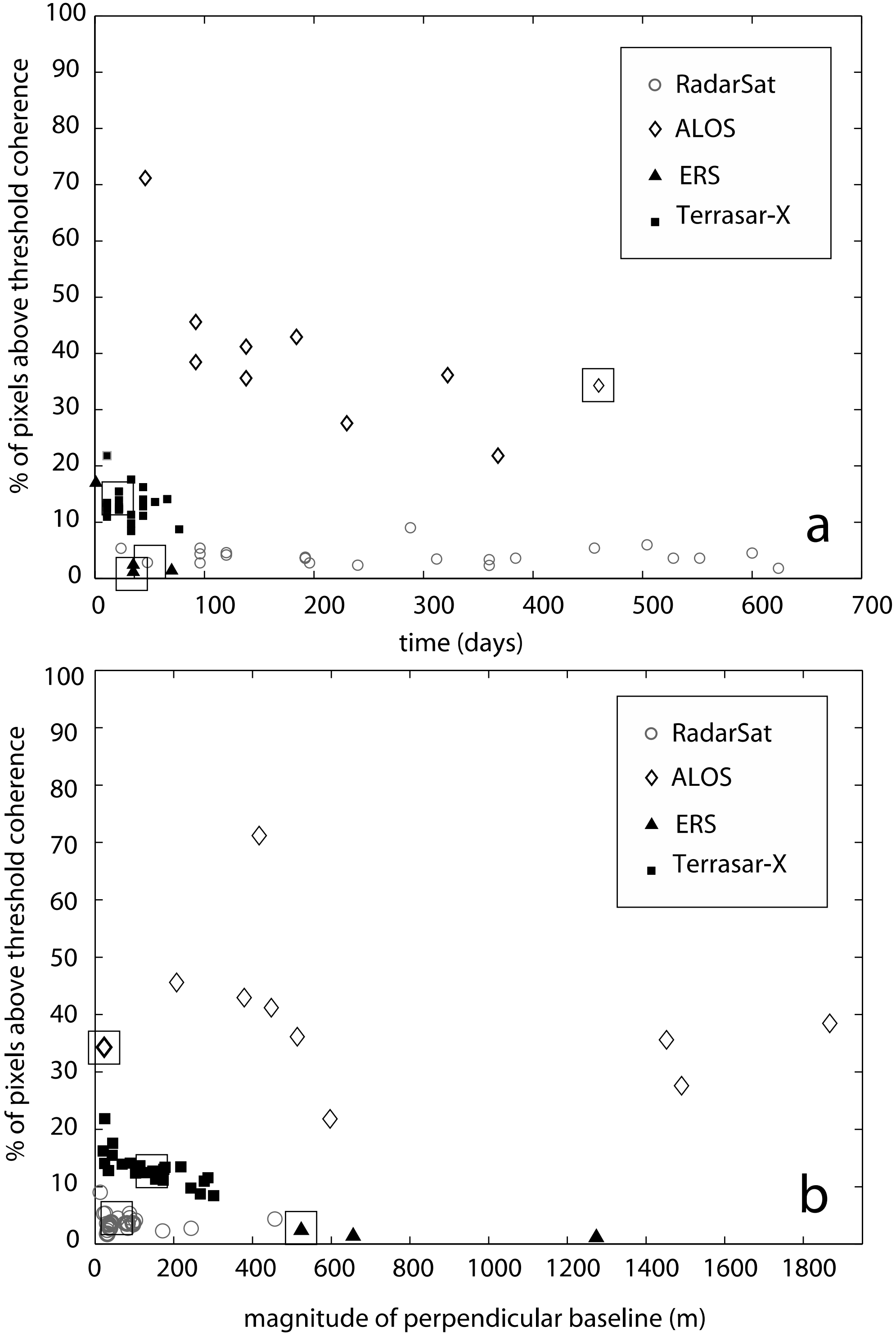

- only L-band data can be used to make interferograms covering more than 6 months, or for baselines of more than ~500 metres.

The impact of radar wavelength

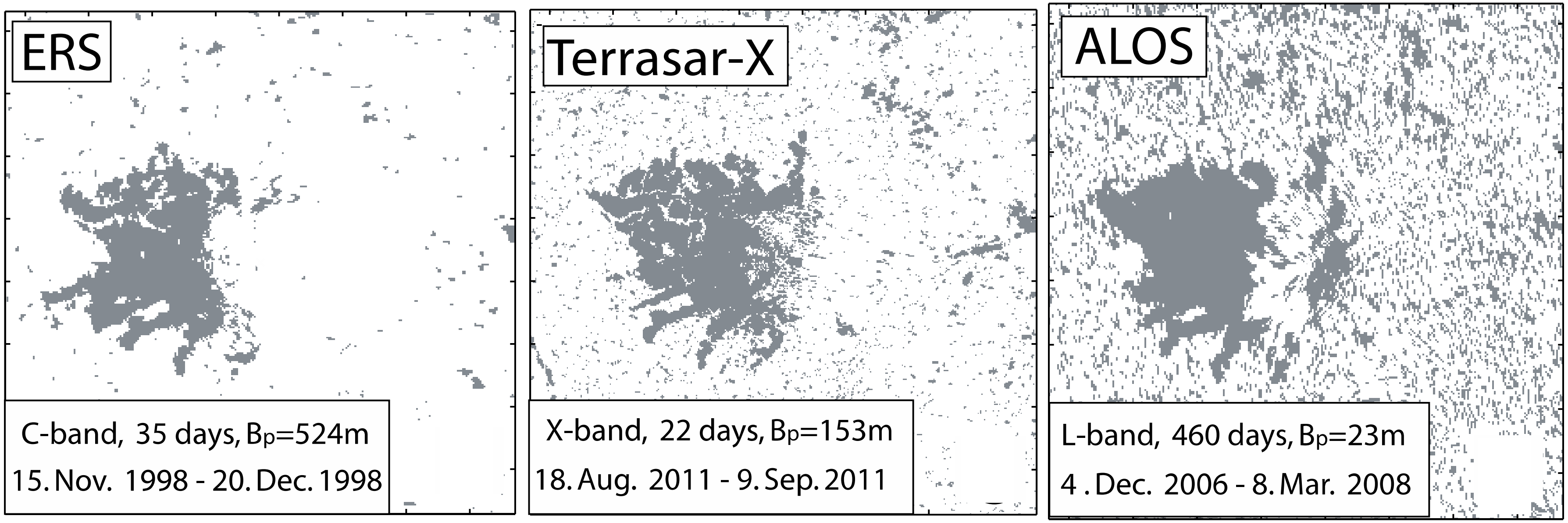

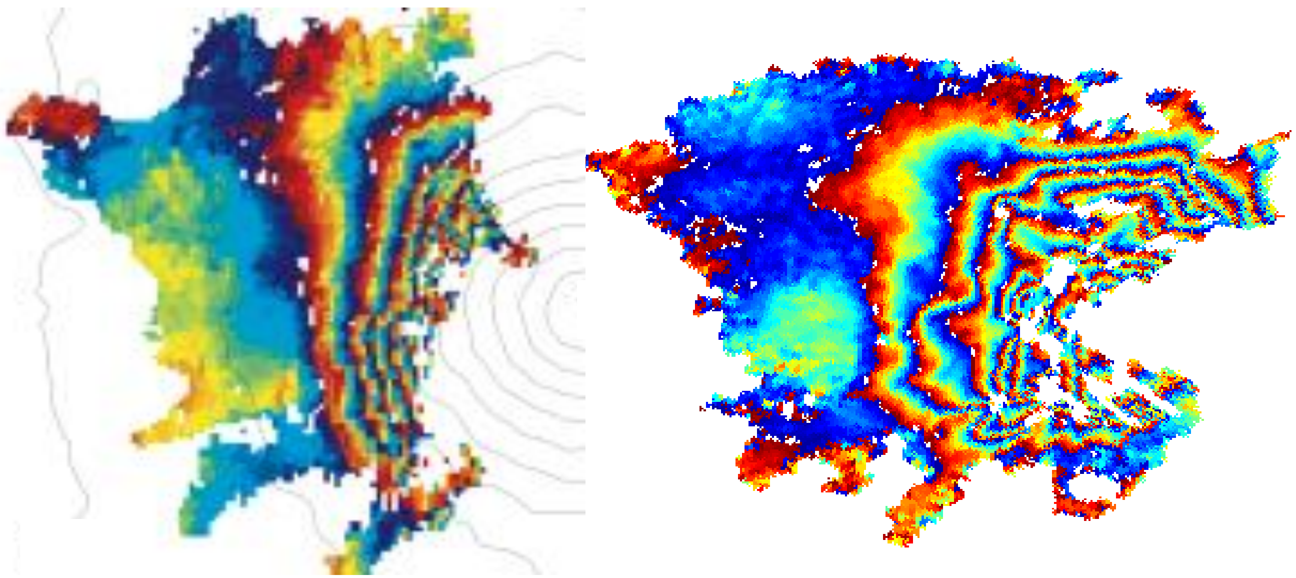

The impact of radar viewing topograp

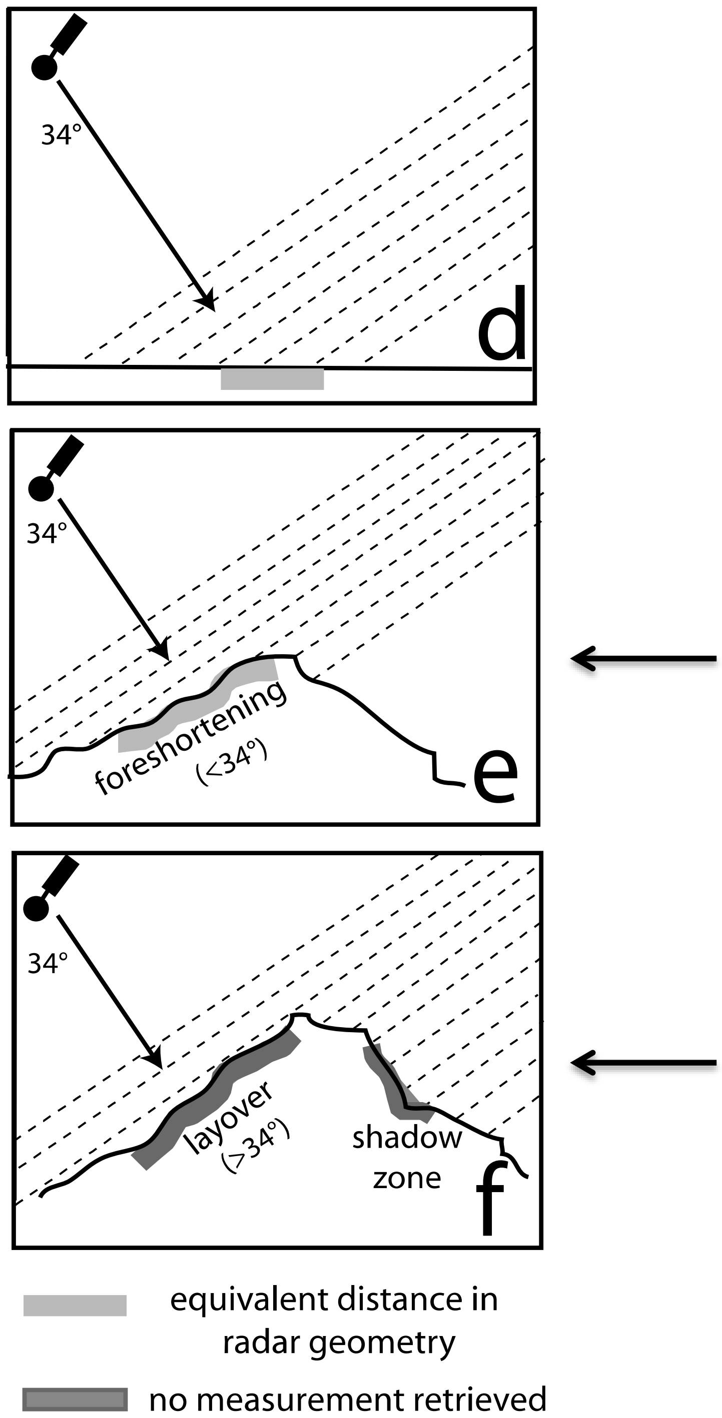

Geocoded image of a volcano is foreshortened on slopes facing the satellite

No measurement is possible on slopes exceeding the satellite incidence angle

The impact of radar viewing topograp

ascending

decending

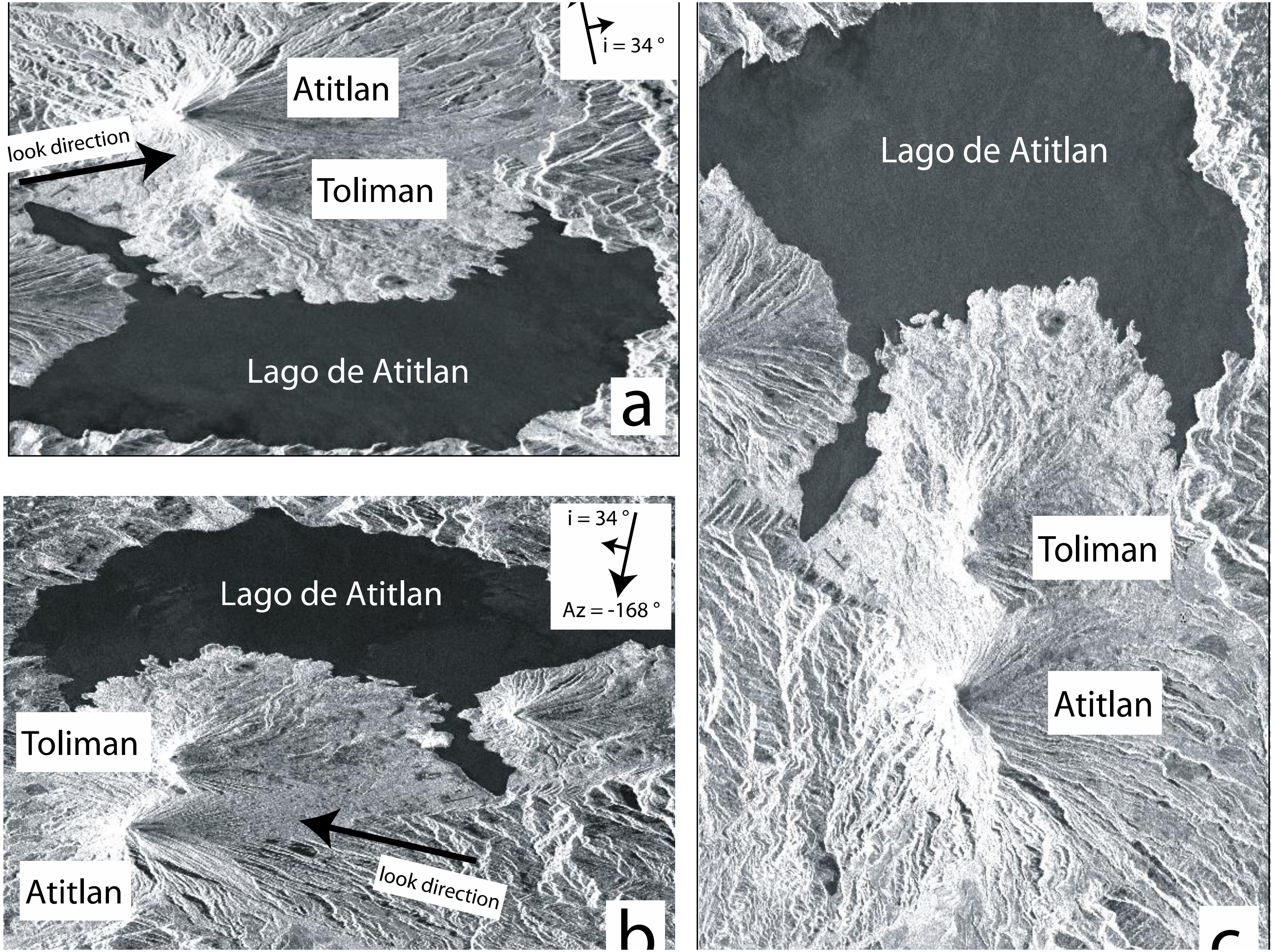

Radar geometry

Geocoded image

Errors in digital elevation models

Particularly common in over mountains:

- layover in SRTM data
- fewer ASTER images contributing to high topography regions in GDEM due to high §number of cloudy images

DEM errors can be corrected given a set of interferograms, but for volcanoes can sometimes include useful information about topographic change.

Topographic phase artefacts

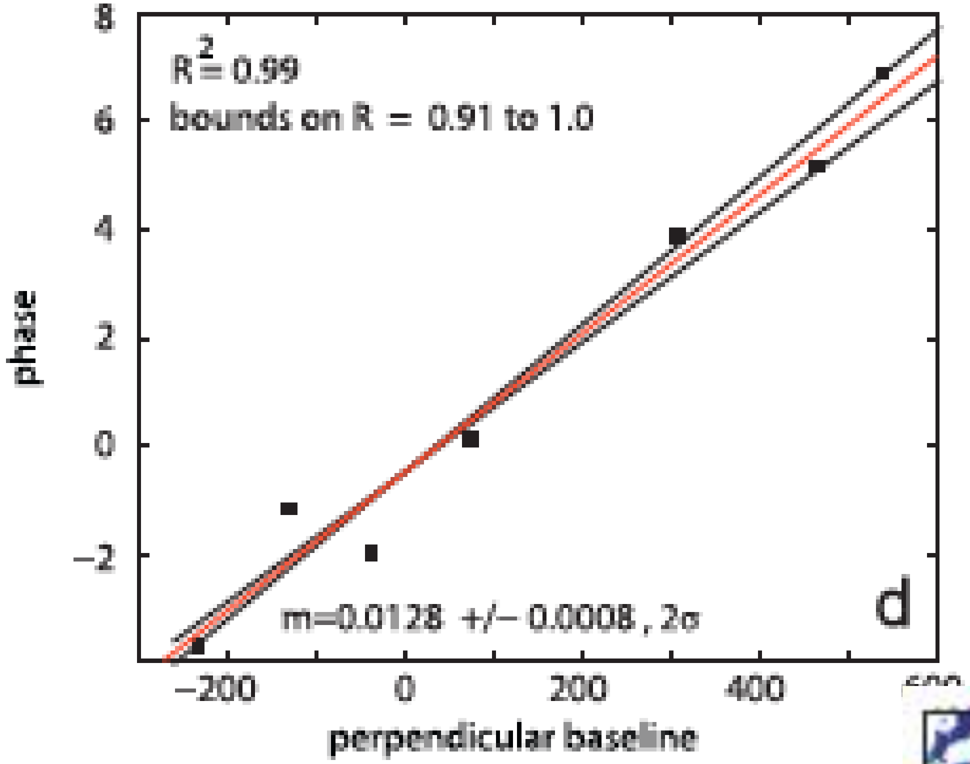

$$\delta z = \frac{r\lambda \sin v}{4\pi B_{perp}} \delta\phi_{topo}$$

Calculation of lava thicknesses from interferometric phase

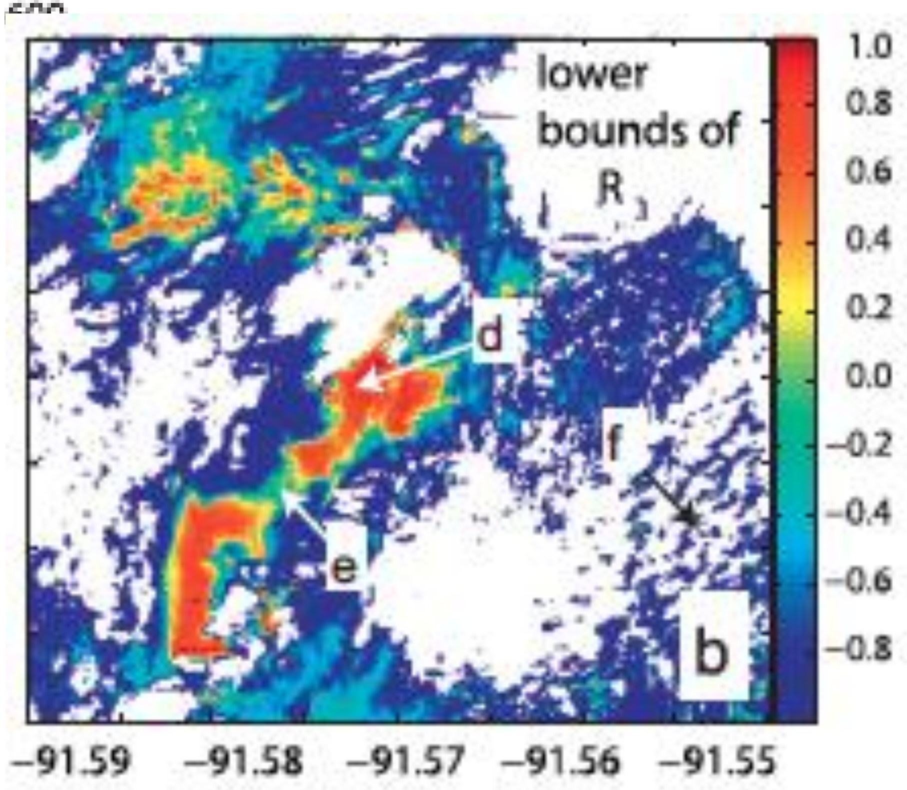

Topographic phase artefacts

Santiaguito lavas, Guatemala

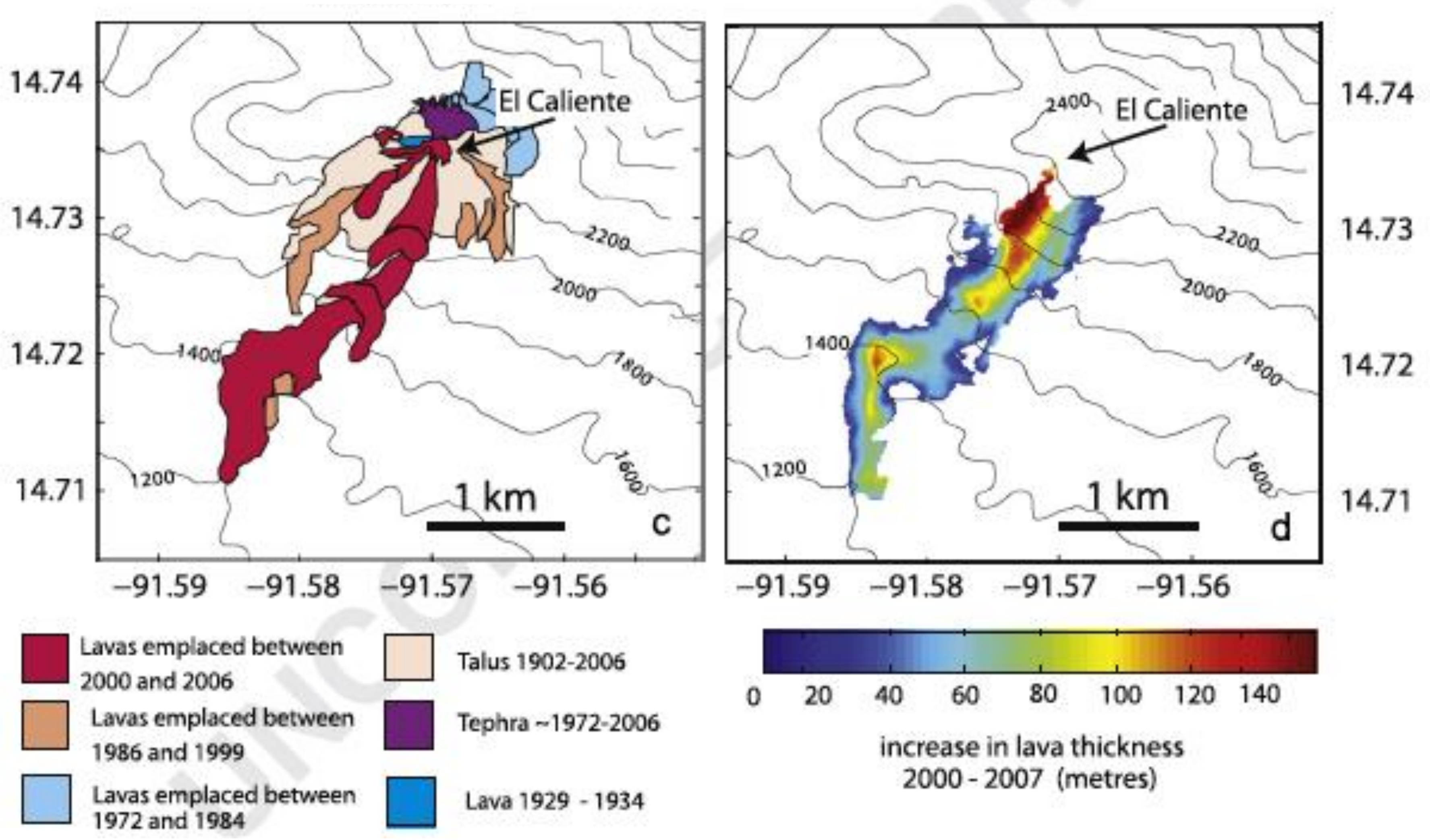

Topographic phase artefacts

Reventador lavas, Guatemala

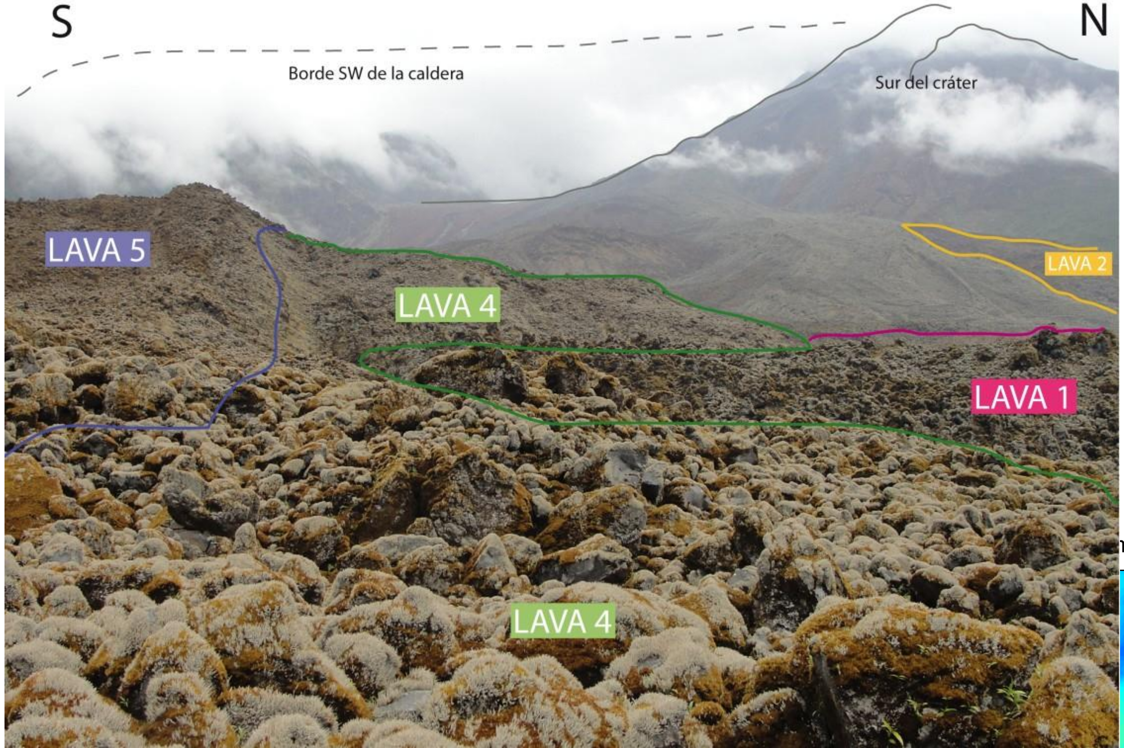

Maria Fernanda Narajo Hidalgo, MSc thesis 2013

11 separate lava flows 2004-2005

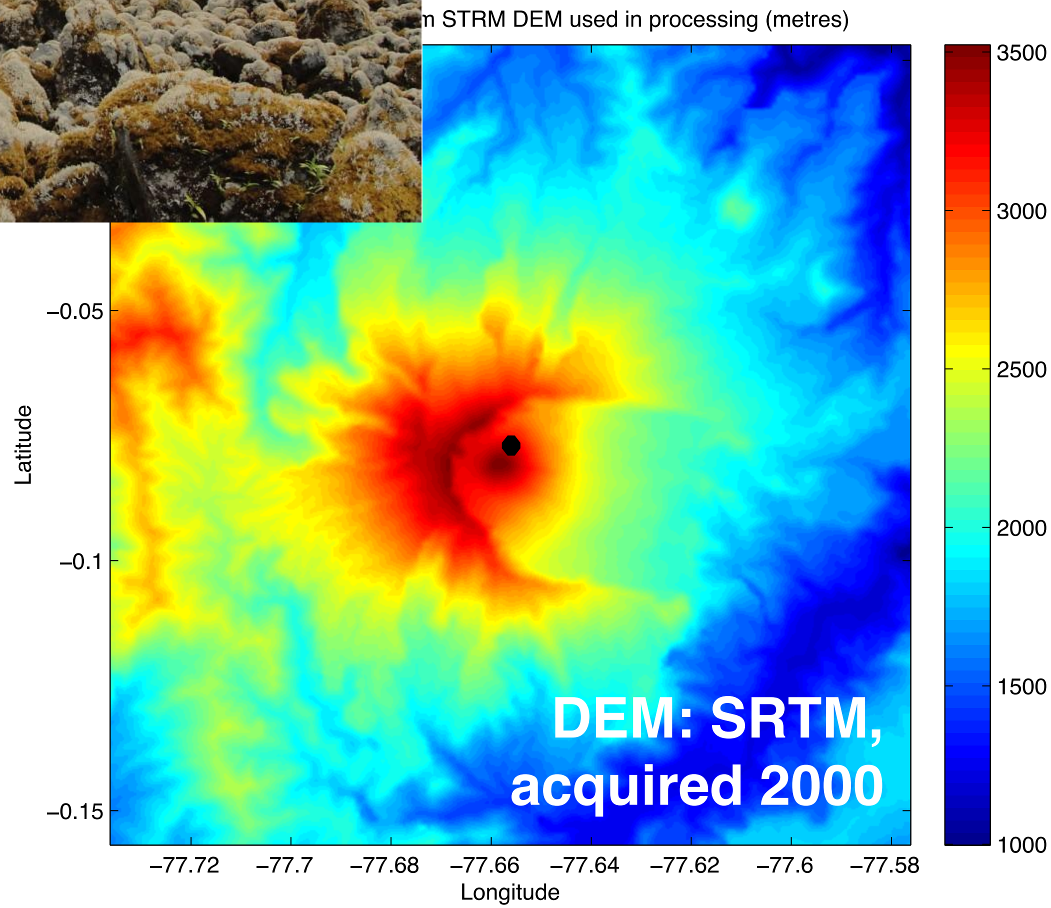

Topographic phase artefacts

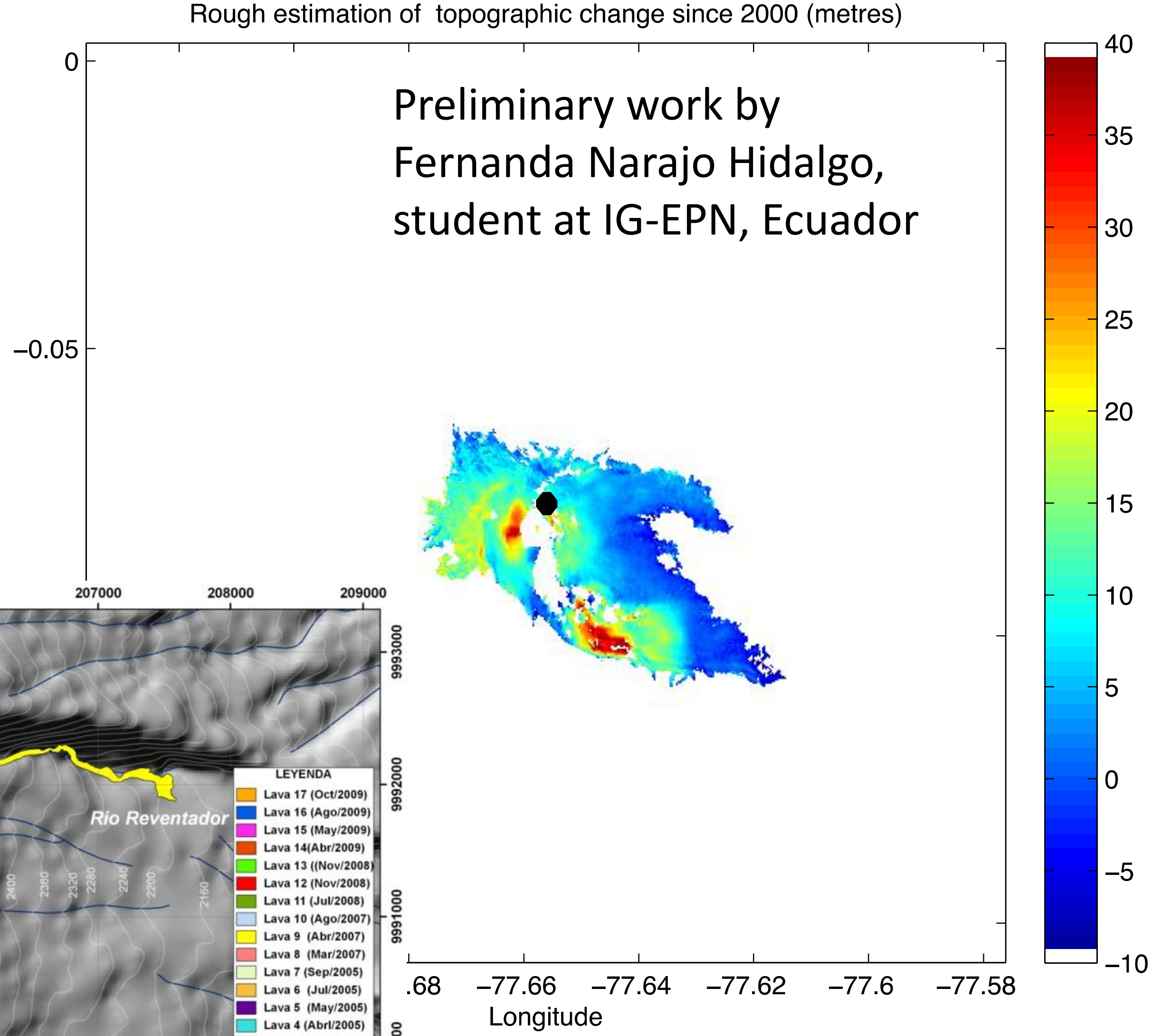

Maria Fernanda Narajo Hidalgo, MSc thesis 2013

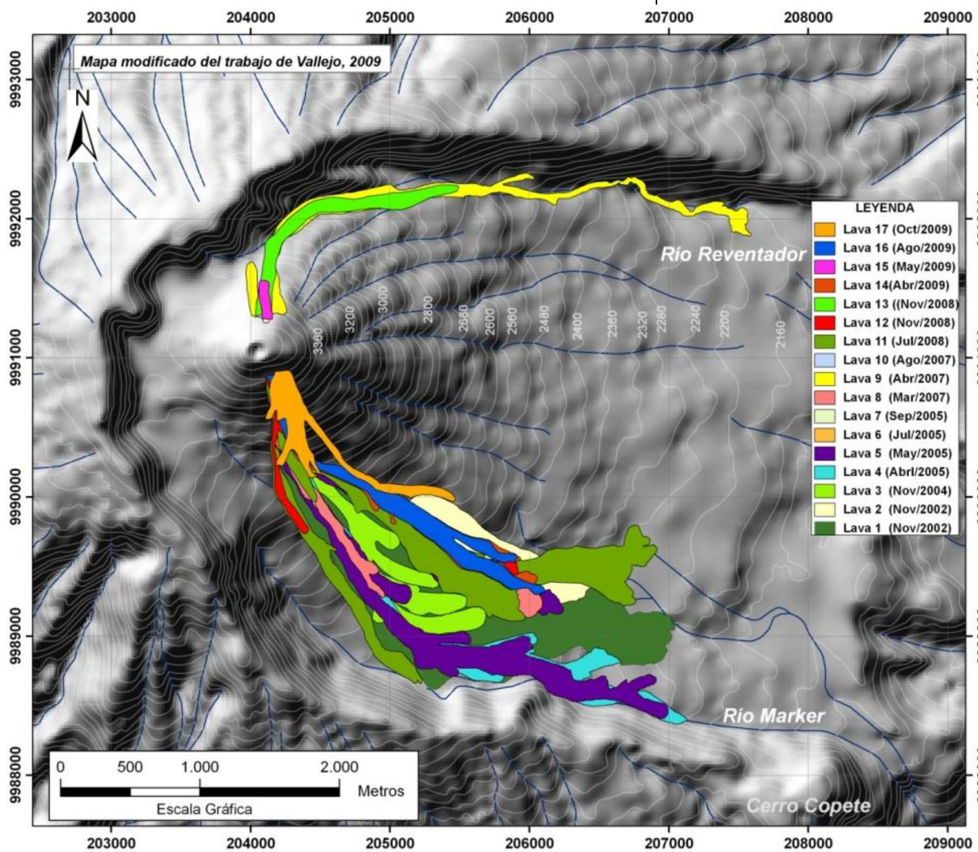

Volcano deformation models

- Uplift is caused by increased pressure on "magma reservoir" walls:
  1. What is the depth?
  2. What is dP?
  3. What else?
     non-spherical shape?
     non-point source size?
     more than 1 source?
     elastic/viscoelastic structure, etc.

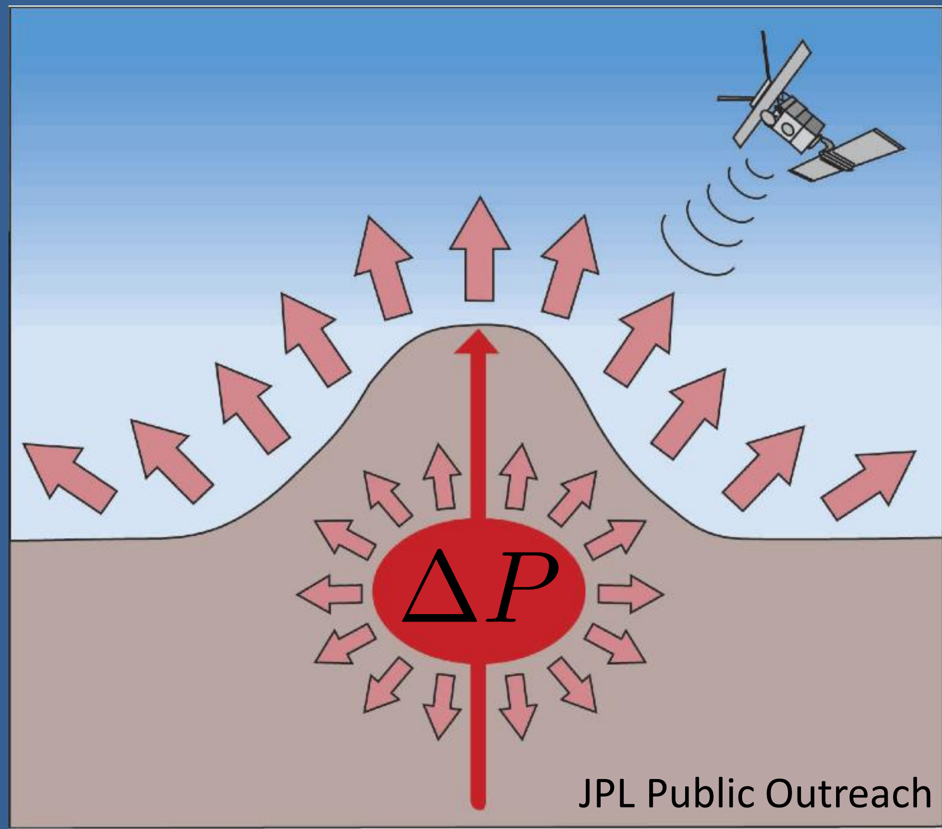

What is the physical cause of the deformation?

- What causes uplift/subsidence?
  Fluid/gas movements
  melting of country rock
  viscoelastic movement of country rock
  poroelasticity
  thermoelasticity

- Fluids movements: magmatic or hydrothermal?
  New magma injection or volatile exsolution
  Need gravity data to constrain

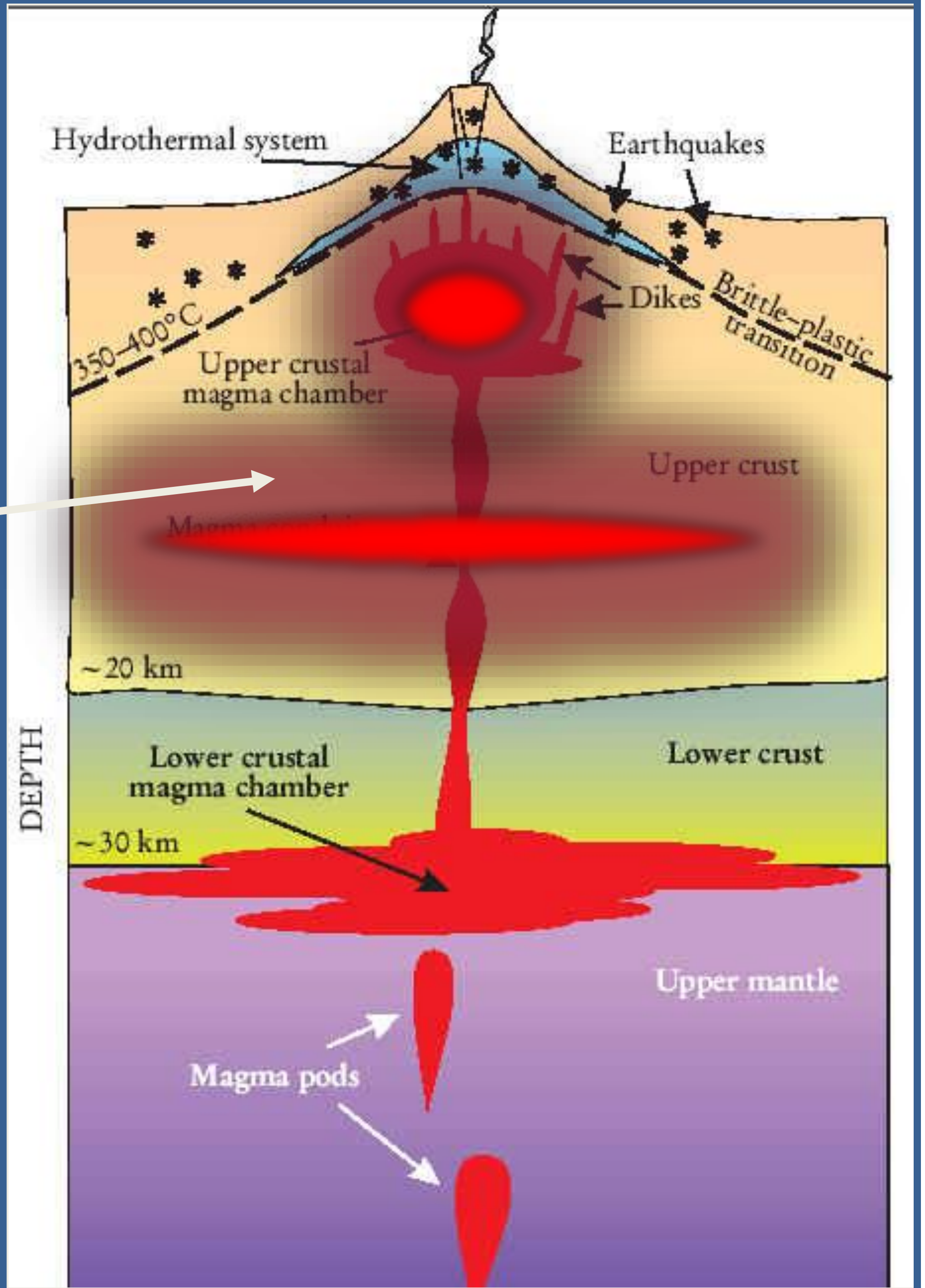

Modified from Hill et al., 2002

Yellowstone 2004-2008 uplift

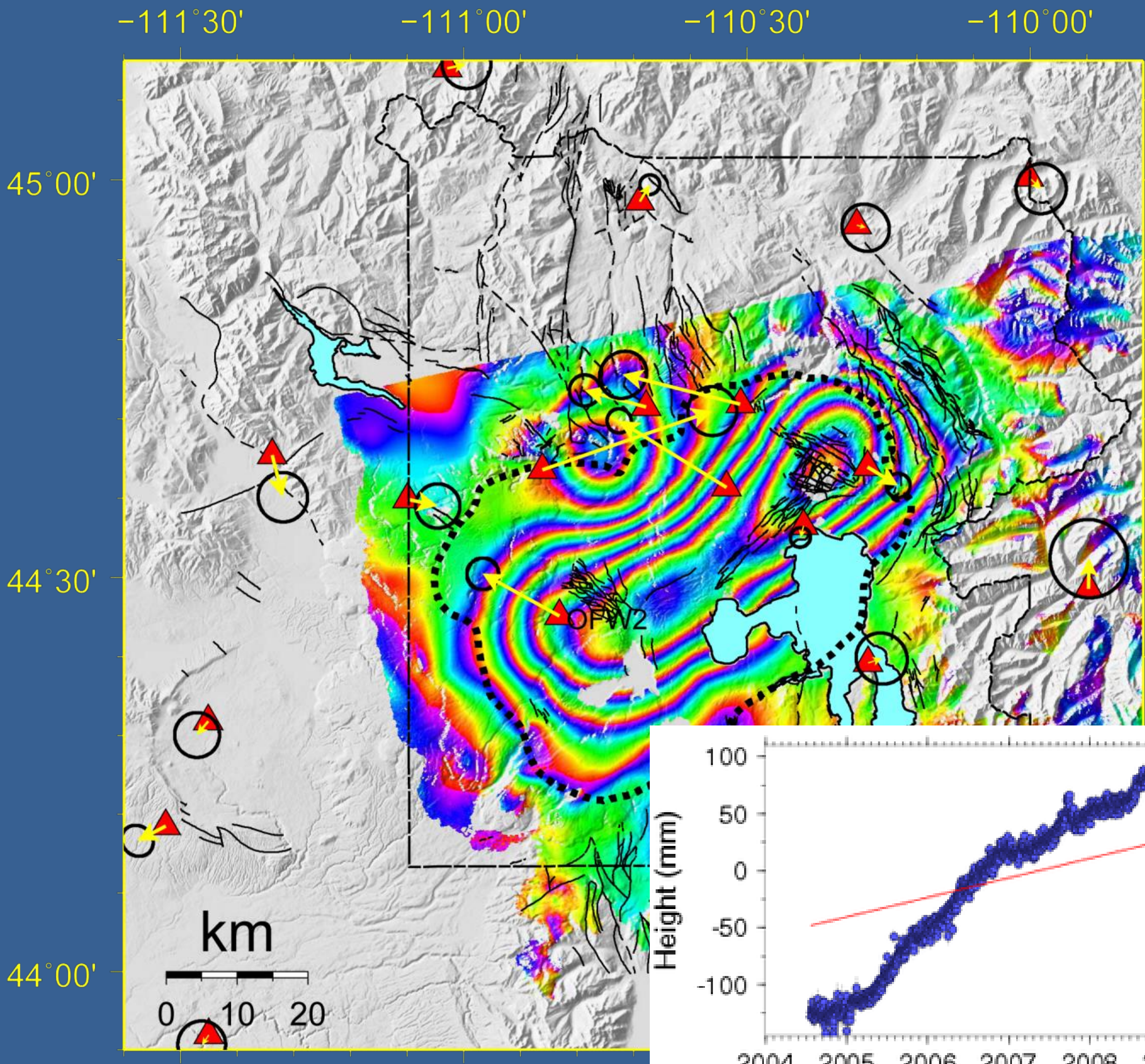

ENVISAT IS2 2004-2006 interferogram with Continuous GPS vectors (Chang et al., 2007)

Modified from Chuck Wicks

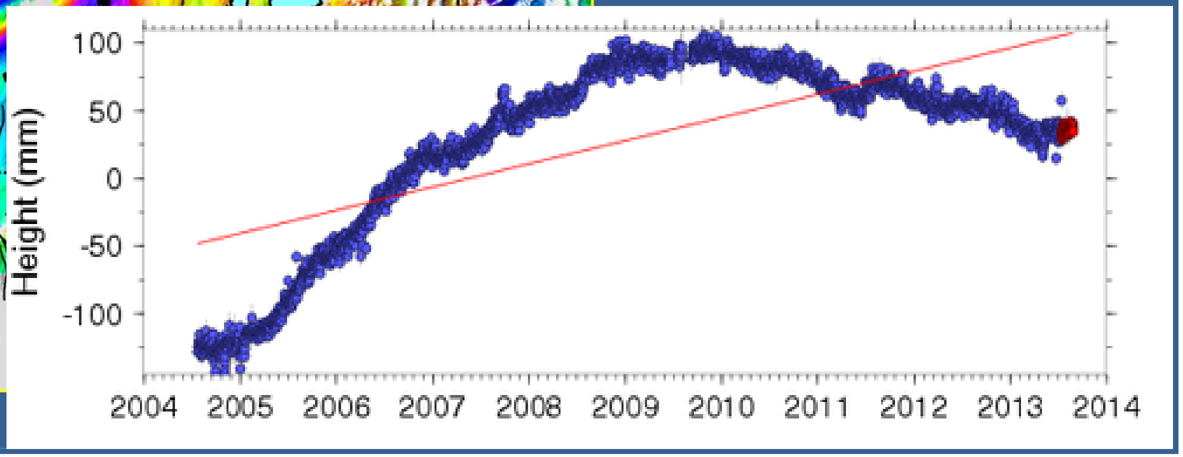

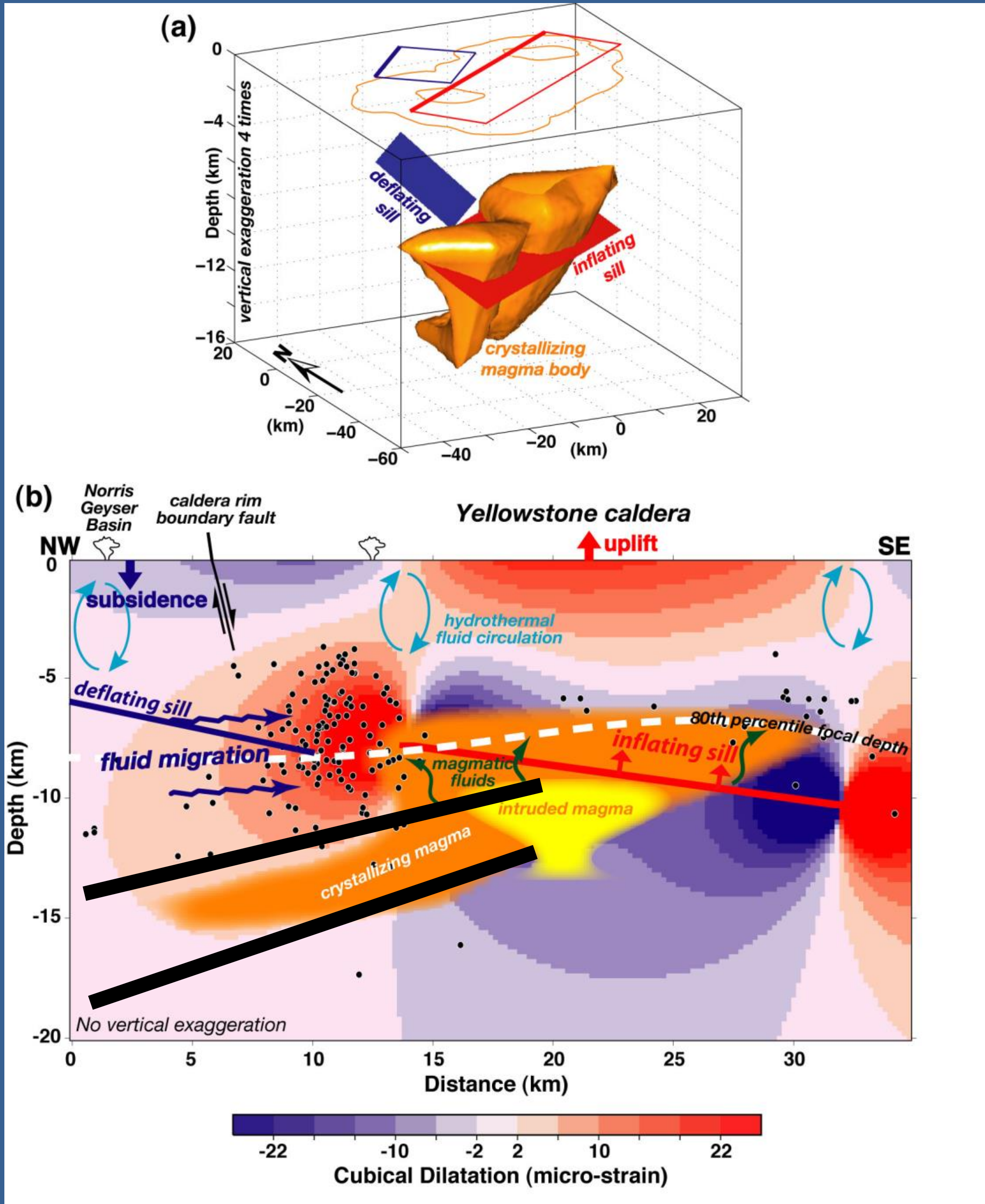

Inferred subsurface from deformation & other measurements

Sources for 2004-2006 deformation (InSAR plus GPS)

Combined with earthquakes, Coloumb stress change modeling and inferences from seismic tomography

From: Chang et al., 2007

Analytic Source Types

- Point Source (Mogi)
- Spherical Source (McTigue)
- Prolate Spheroid (Yang)
- Dislocation Crack (Okada)
- Realistic Crack (Fialko)

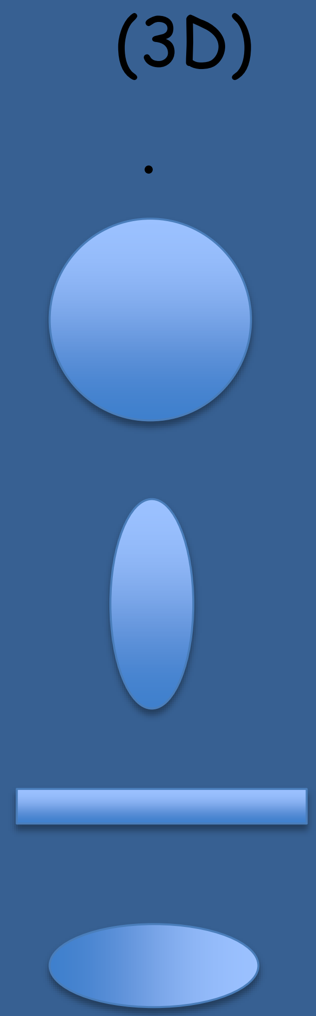

Brief Mogi Source History

Date	Publication	Author
1931	The plastico-elastic deformation of a semi-infinite solid body due to an internal force	Sezawa, K.
1936	The dynamics of the formation of cone-sheets, ring-dykes, and caldron subsidence	Anderson, E.M.
1955	On the strain produced in a semi-infinite elastic solid by an interior source of stress	Yamakawa, N.
1958	Relations between the eruptions of various volcanoes and the deformations of the ground surfaces around them	Mogi, K.
1987	Elastic stress and deformation near a finite spherical magma body: resolution of the point source paradox	McTigue, D.F.

When is Elastic Mogi Model OK?

- 20 cm of uplift at Darwin volcano (Galapagos Islands) during 1992±98
- Best-fit Mogi model with depth of 3km
  - But, implies ΔP=100-1000 GPa

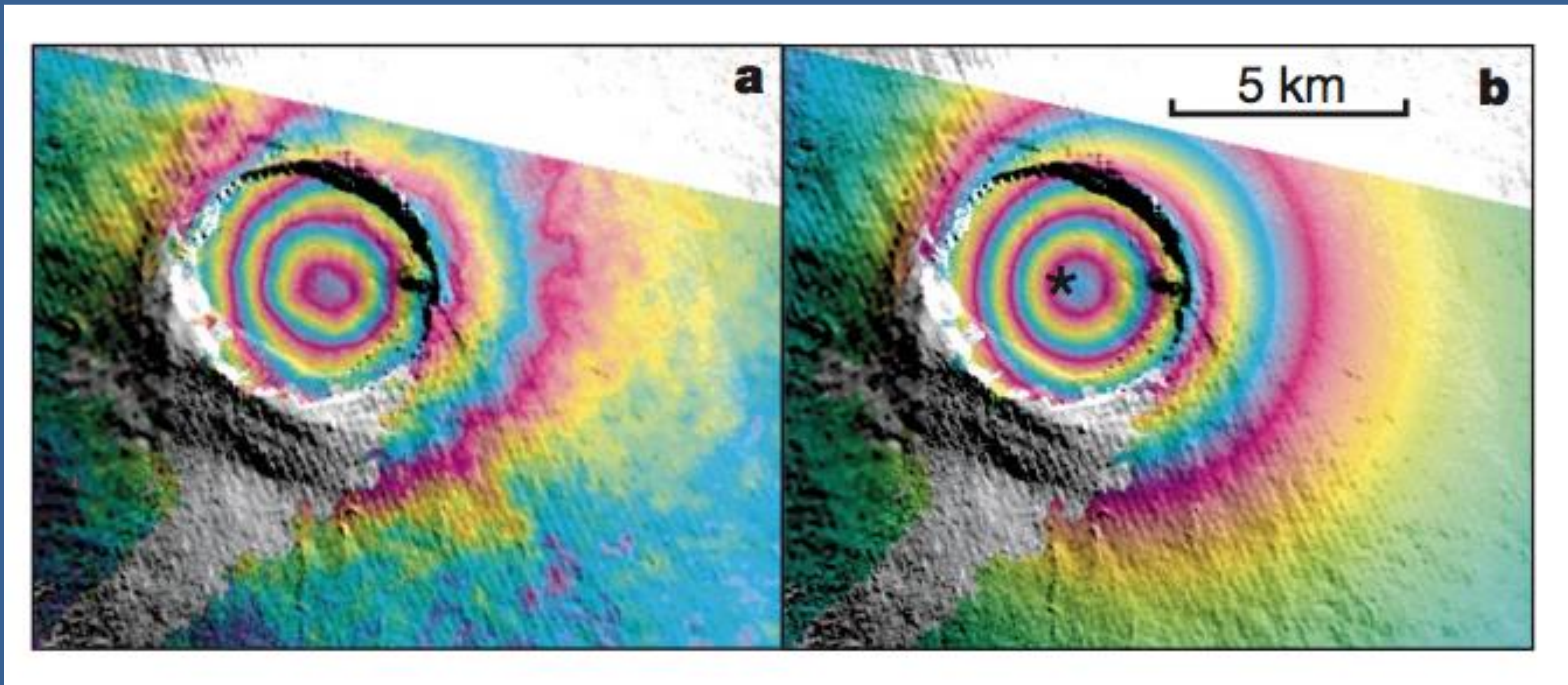

Amelung et al 2000 (Nature)

Mogi Source properties

$$u_z = \frac{(1-\nu)pa^3}{4\mu}\left[\frac{d}{(\rho^2+d^2)^{3/2}}\right]$$

$$\Delta V = \frac{\pi p a^3}{.\,\mu}$$

$$u_\rho = \frac{(1-\nu)pa^3}{4\mu}\left[\frac{\rho}{(\rho^2+d^2)^{3/2}}\right]$$

Mogi-predicted surface displacements

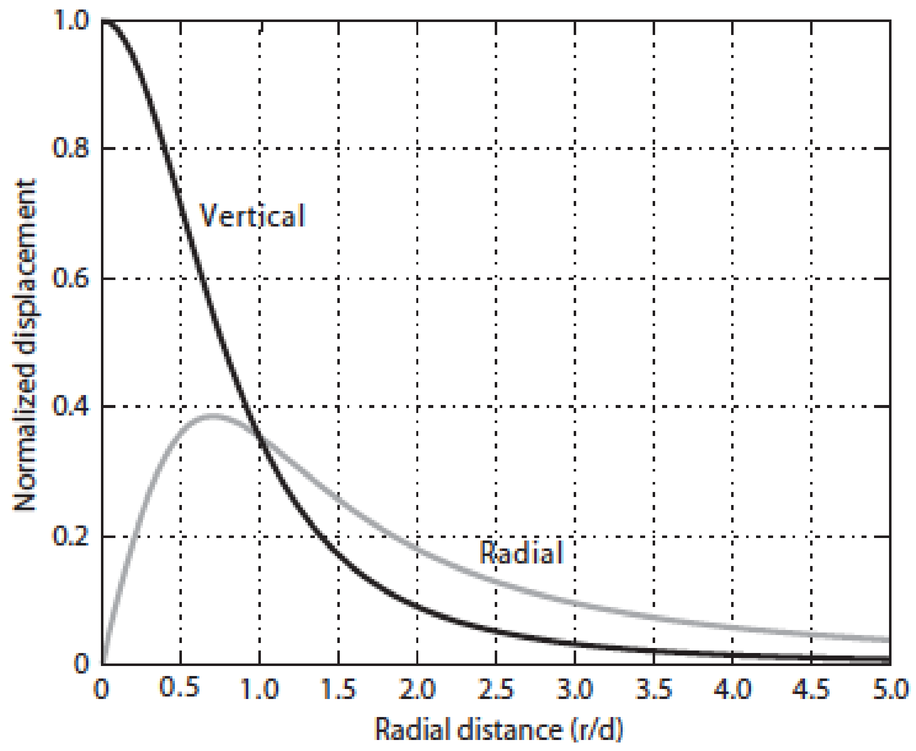

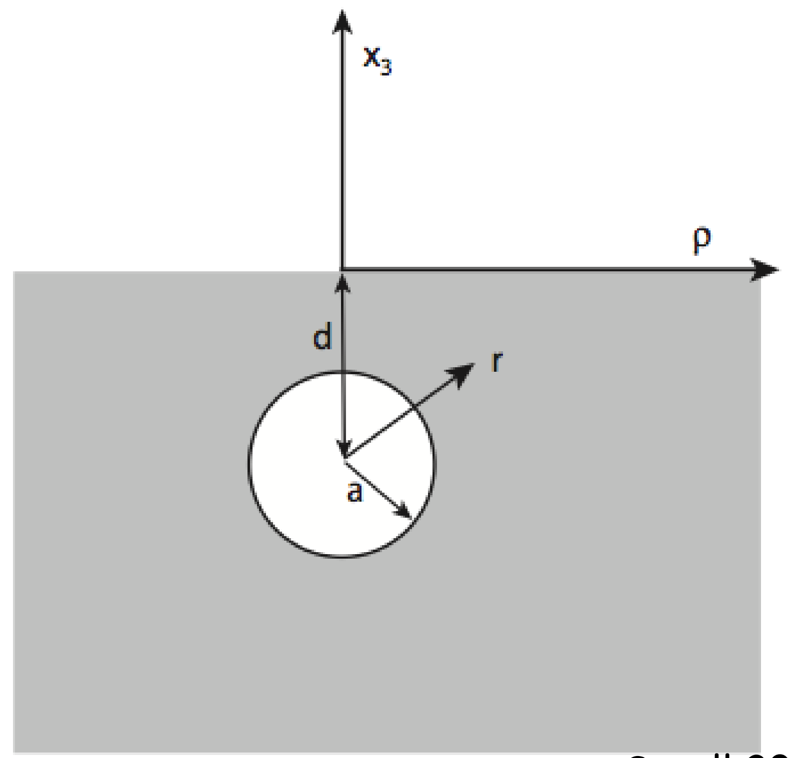

Segall 2010

Vary shape of "magma chamber"

- Bottom line:

With only one component of deformation: all shapes can fit data, but have different depths

Consider:

- Spherical point source
- Prolate ellipsoid (football)
- Oblate ellipsoid (frisbee)
- Finite sphere

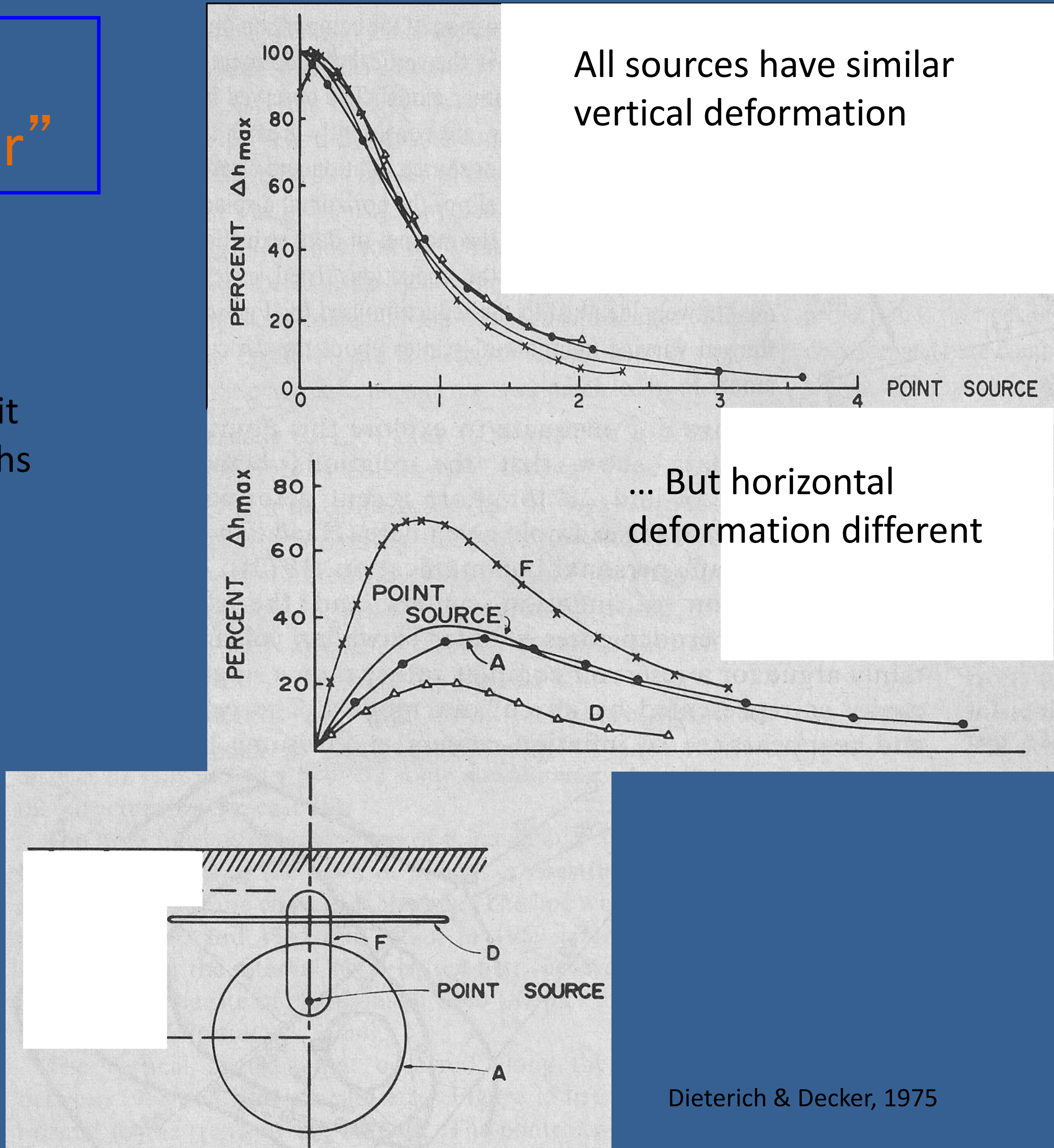

All sources have similar vertical deformation

… But horizontal deformation different

Dieterich & Decker, 1975

Mogi source Pros

- **Analytic** and **fast** to compute
- Matches axis-symmetric data well
- First-order mathematical approximation to a more physically-realistic finite spherical source (McTigue 1987)

Mogi Source Cons

- "**HIPSHS**" Assumptions:
  - **H**omogeneous
  - **I**sotropic
  - **P**ossion-**S**olid (υ=0.25)
  - **H**alf-**S**pace
  - elastic
- In most volcanic areas, there assumptions are probably all **wrong**…

Masterlark 2007 Review

JOURNAL OF GEOPHYSICAL RESEARCH, VOL. 112, B06419, doi:10.1029/2006JB004860, 2007

Click Here for Full Article

Magma intrusion and deformation predictions: Sensitivities to the Mogi assumptions

Timothy Masterlark[1]

Received 16 November 2006; revised 29 January 2007; accepted 15 February 2007; published 26 June 2007.

Gist:

- Okmok, AK subsided up to 1.5m as a result of the 1997 eruption
- Quantitatively assess each of the "HIPSHS" assumptions on Okmok deformation data

Paper Outline

$$\mathbf{m} = \hat{\mathbf{G}}^{-1}\mathbf{d}$$

1) Invert InSAR data for best-fit Mogi model
2) Run forward Mogi model with different parameters

$$\mathbf{G}\mathbf{m} = \mathbf{d}$$

   a) Add topography
   b) Vary Poisson's ratio
   c) Anisotropy
   d) Heterogeneity

Analytic (a–b)

Finite Element Models (c–d)

Okmok, AK


Kelly Reeves, Alaskan A

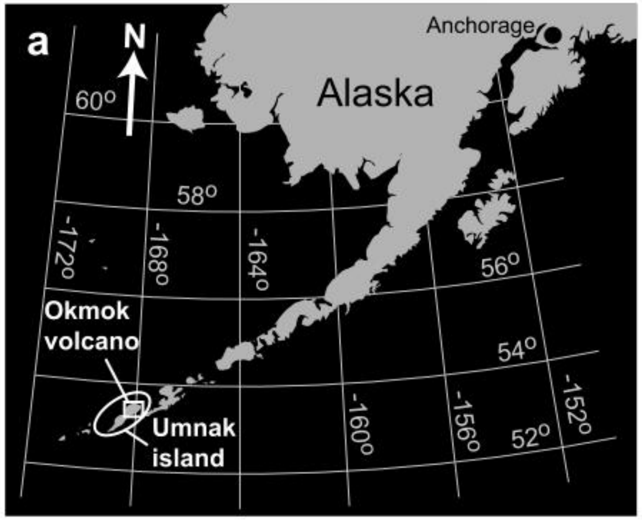
a
N
Anchorage
Alaska
60°
58°
56°
54°
52°
-172°
-168°
-164°
-160°
-156°
-152°
Okmok
volcano
Umnak
island

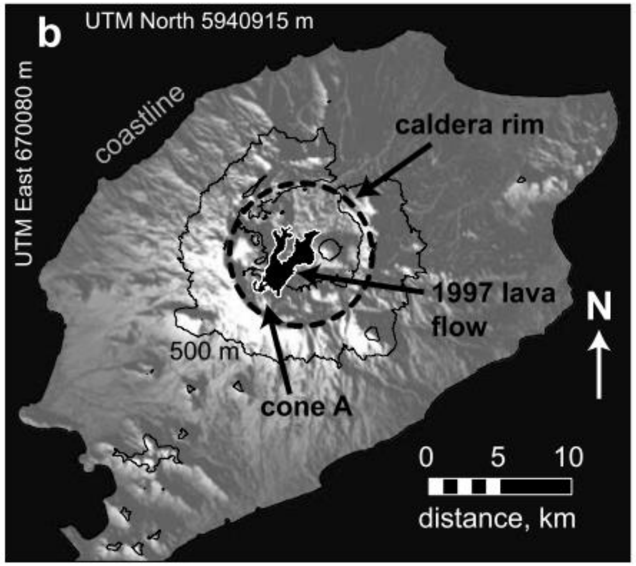
b
UTM North 5940915 m
UTM East 670080 m
coastline
caldera rim
1997 lava
flow
500 m
cone A
N
0
5
10
distance, km

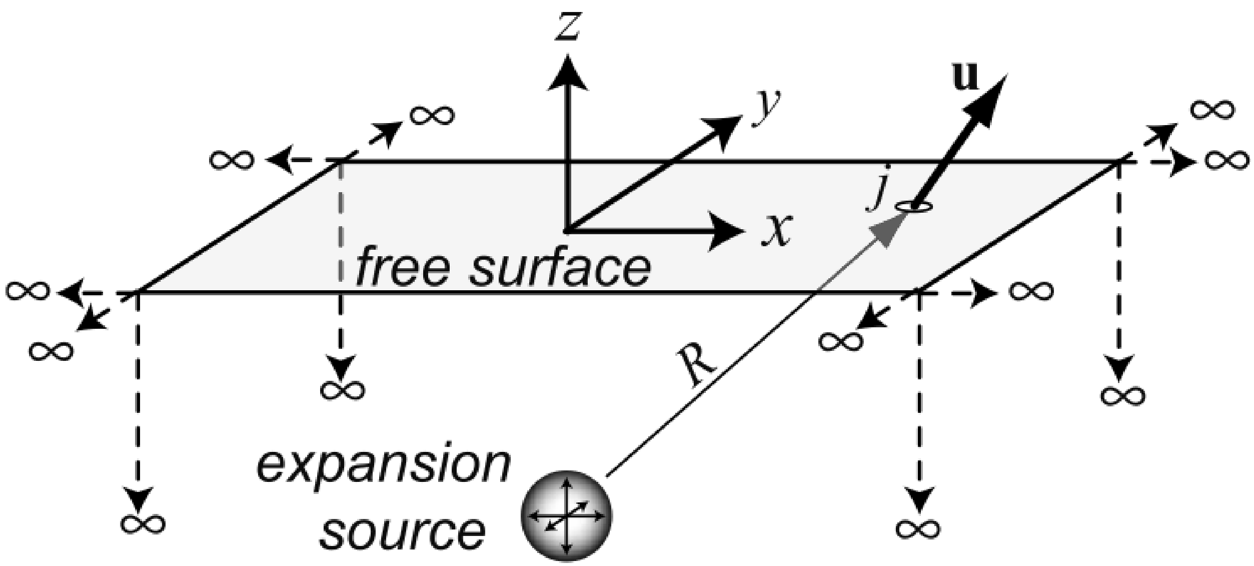
z
y
x
u
j
free surface
R
expansion
source
∞

1) Mogi Model

$G = 15\,\mathrm{GPa}$

$\nu = 0.25$

RMSE = 11.0mm

93.5 % data matched

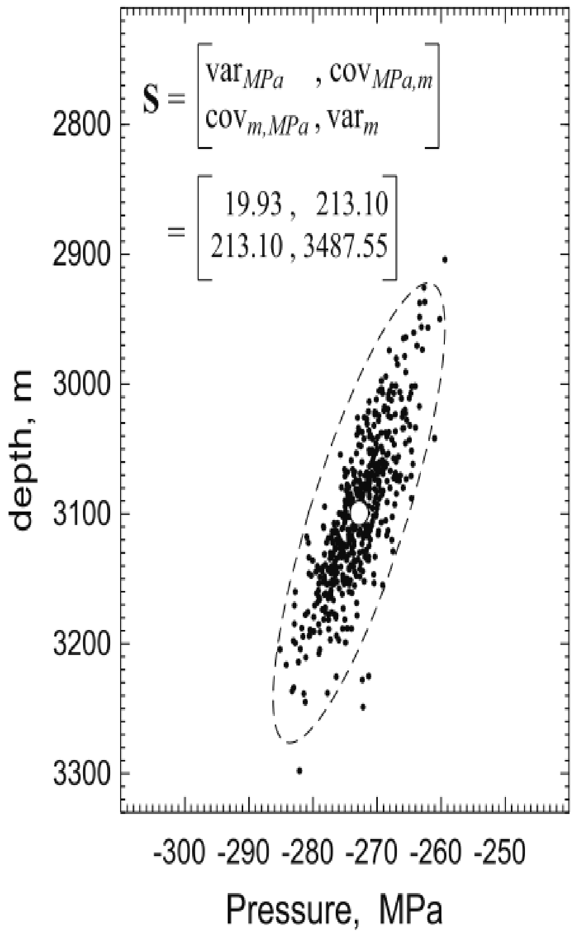

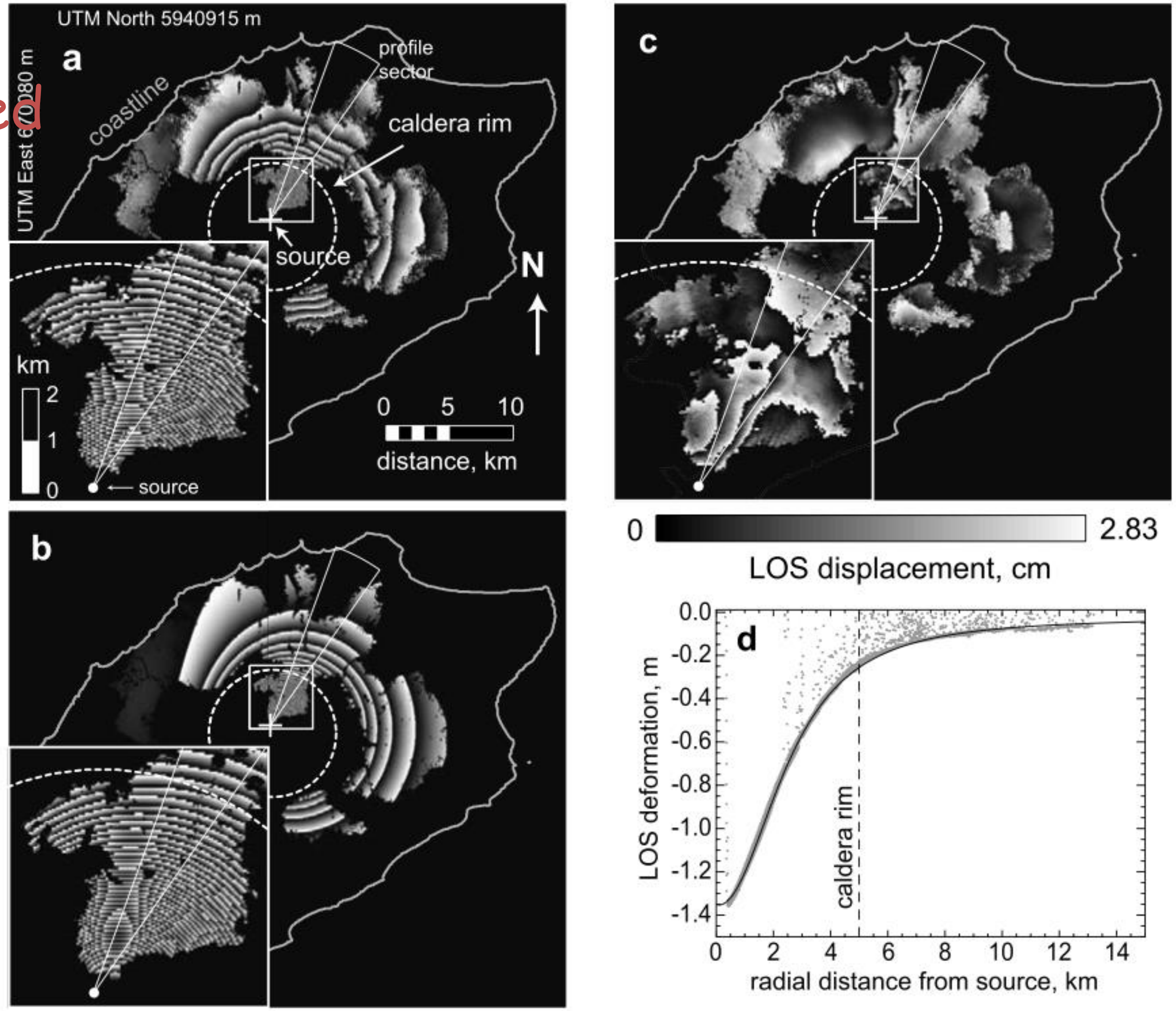

Effect of Topography

Long Valley Caldera

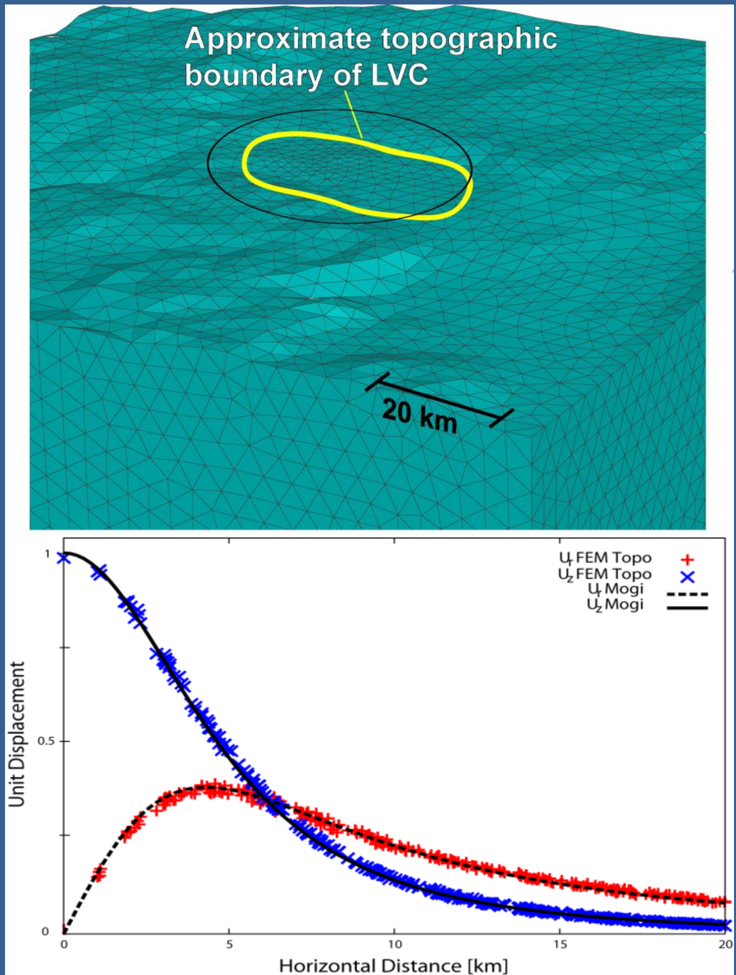

Feng and Newman; in prep

Doesn't matter much

Deep source, modest topography

Mt. Etna

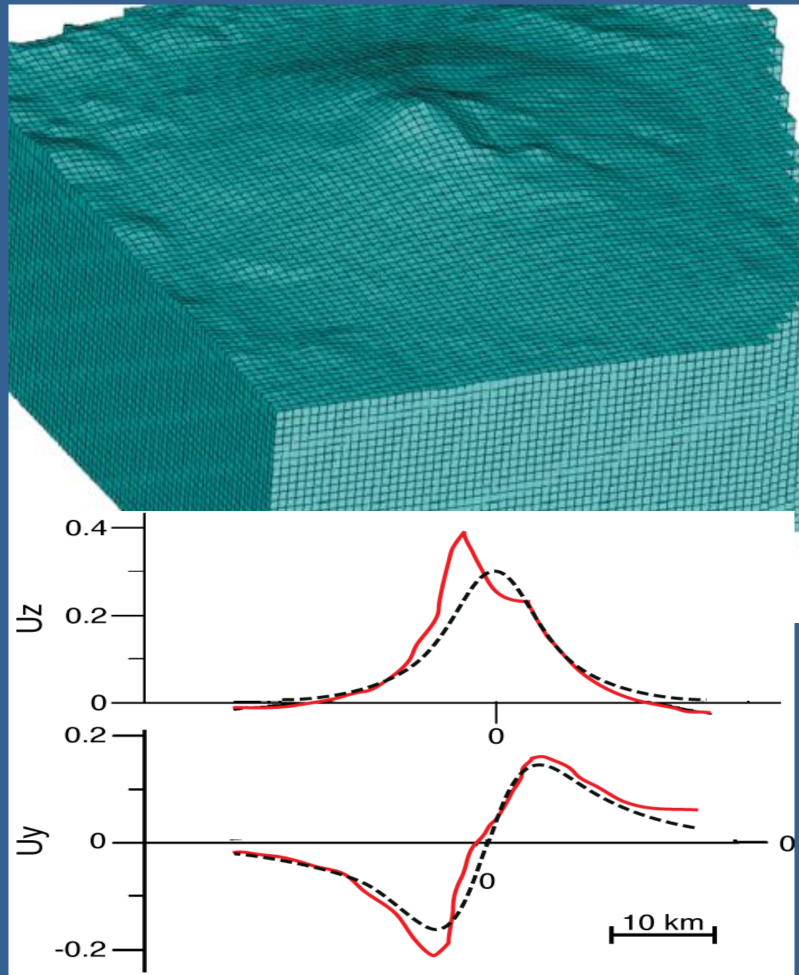

Lungarini et al, JVGR, 2005

More important

Shallow source, steep topography

2 b) Role of Poisson's Ratio

- Studies often assume v=0.25
- Bulk Crust (0.25 < 0.34) [Christensen 1996]
  - Corresponds to 30% difference in deformation
  - Poroelastic Effect (due to pore fluids in upper crust) can increase to 40%

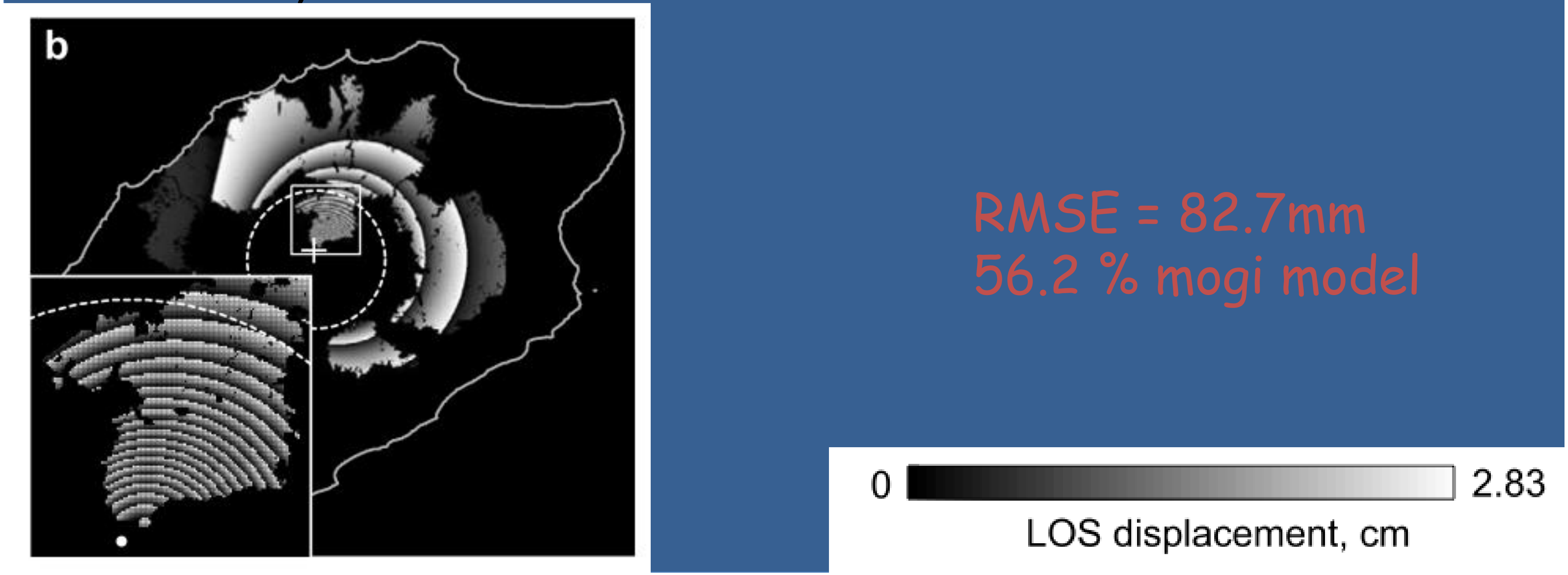

RMSE = 82.7mm
56.2 % mogi model

Impact of Layered Rheology on deformation

5 km depth small spherical pressure source

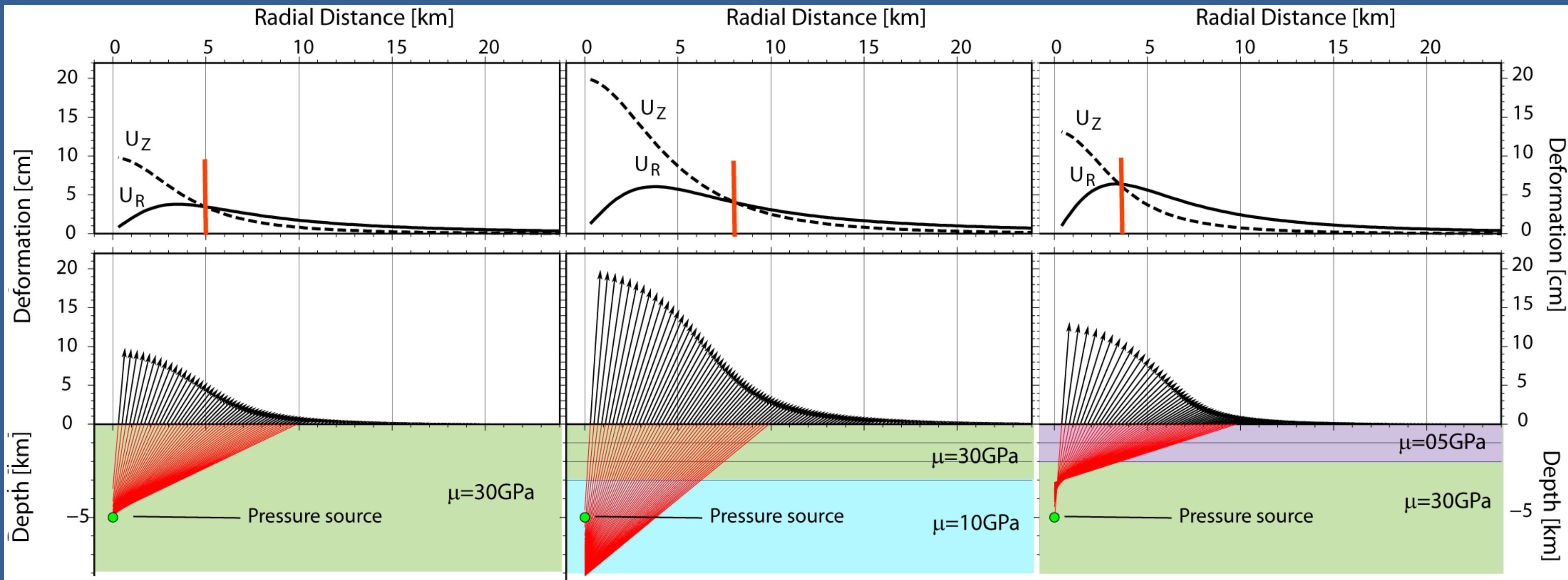

Newman et al., EOS, 2005

Mogi-like

Weaker at depth
- Increased uplift
- Appears deeper

Weaker near surface
- Increased uplift
- Appears shallow

Finite Element Models (FEM)

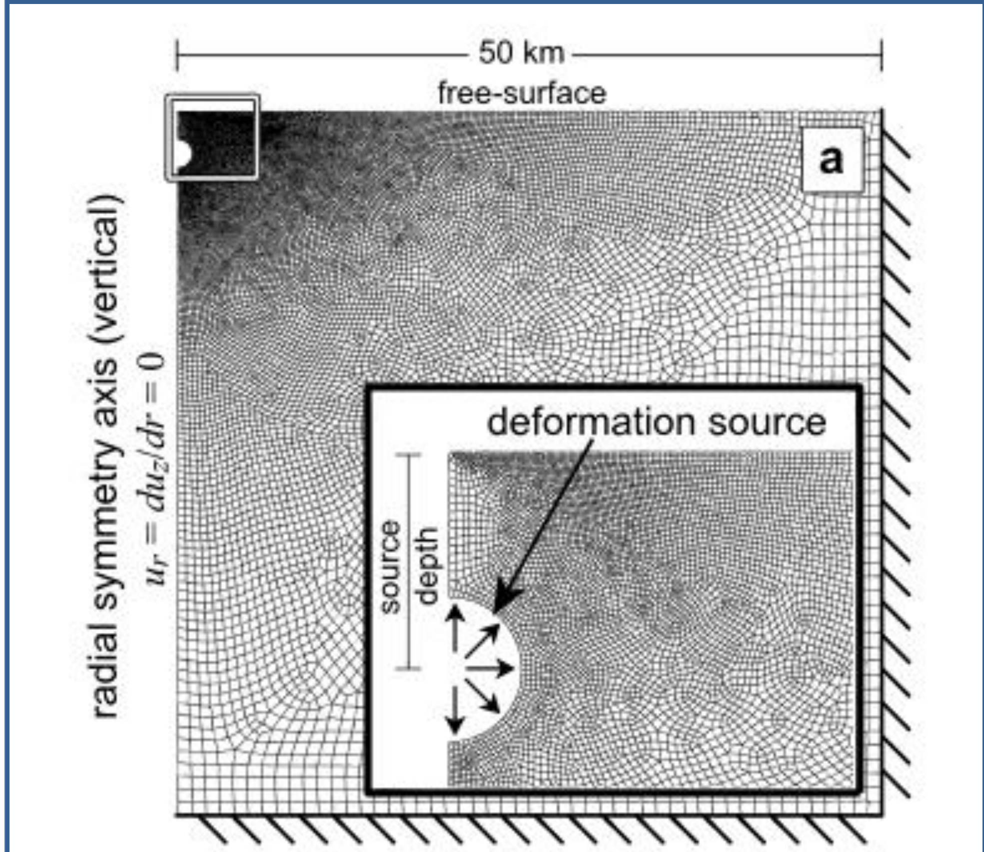

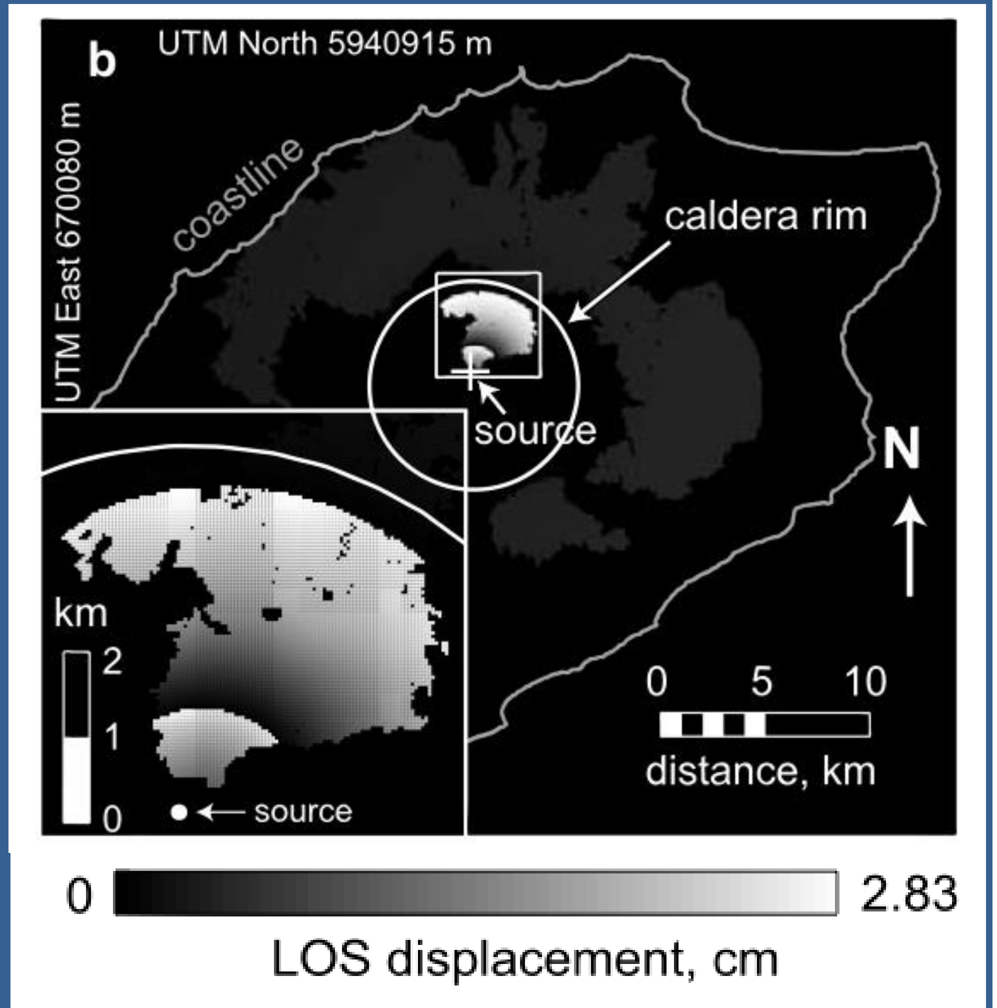

Source radius=1000m

Finite element models are a technique for obtaining approximate solutions to partial differential equations over complex domains

2 d) Heterogeneous Materials

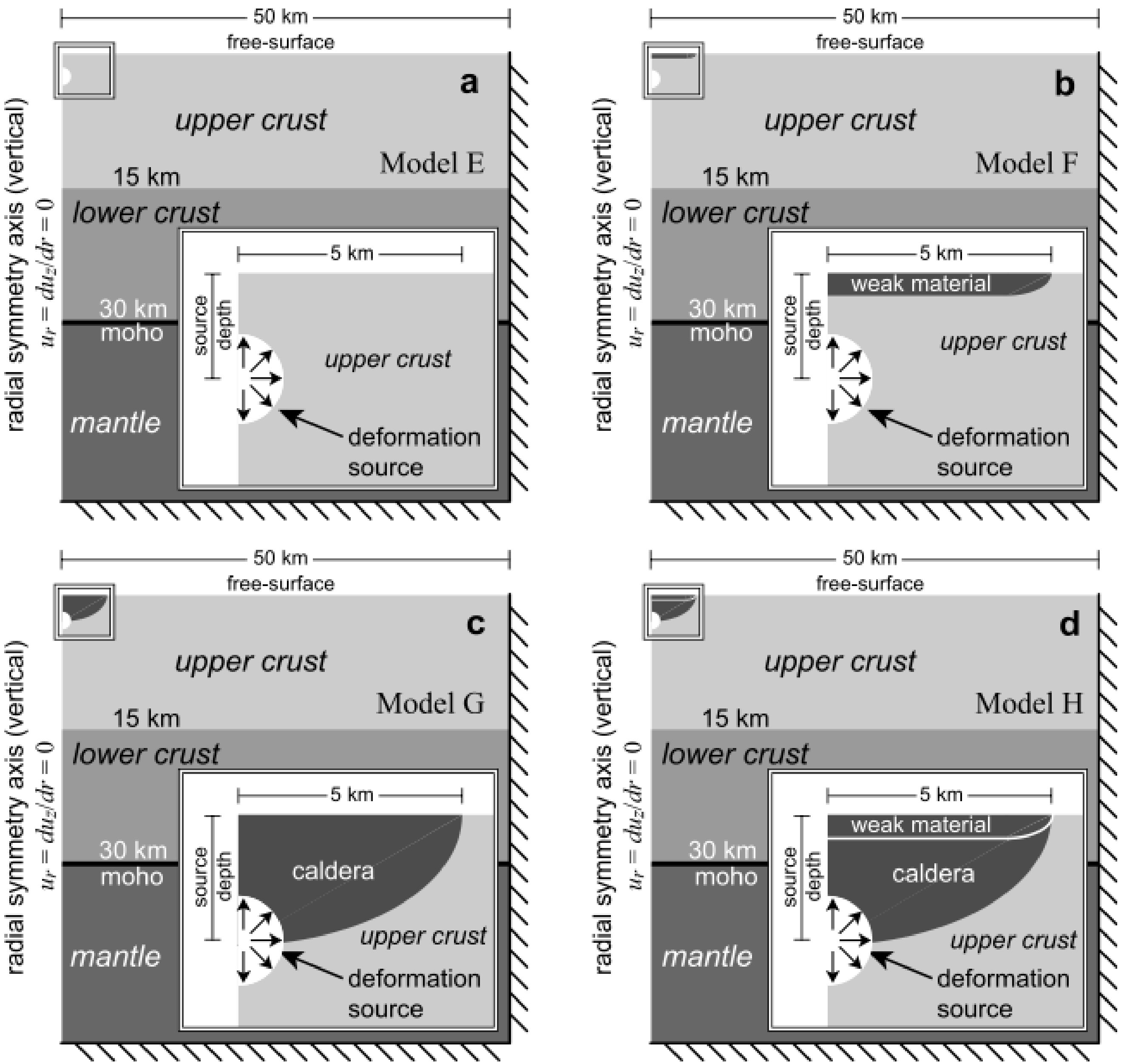

RMSE = 10.5-168.
88.0 - 54.1%

Fault/magma chamber interaction

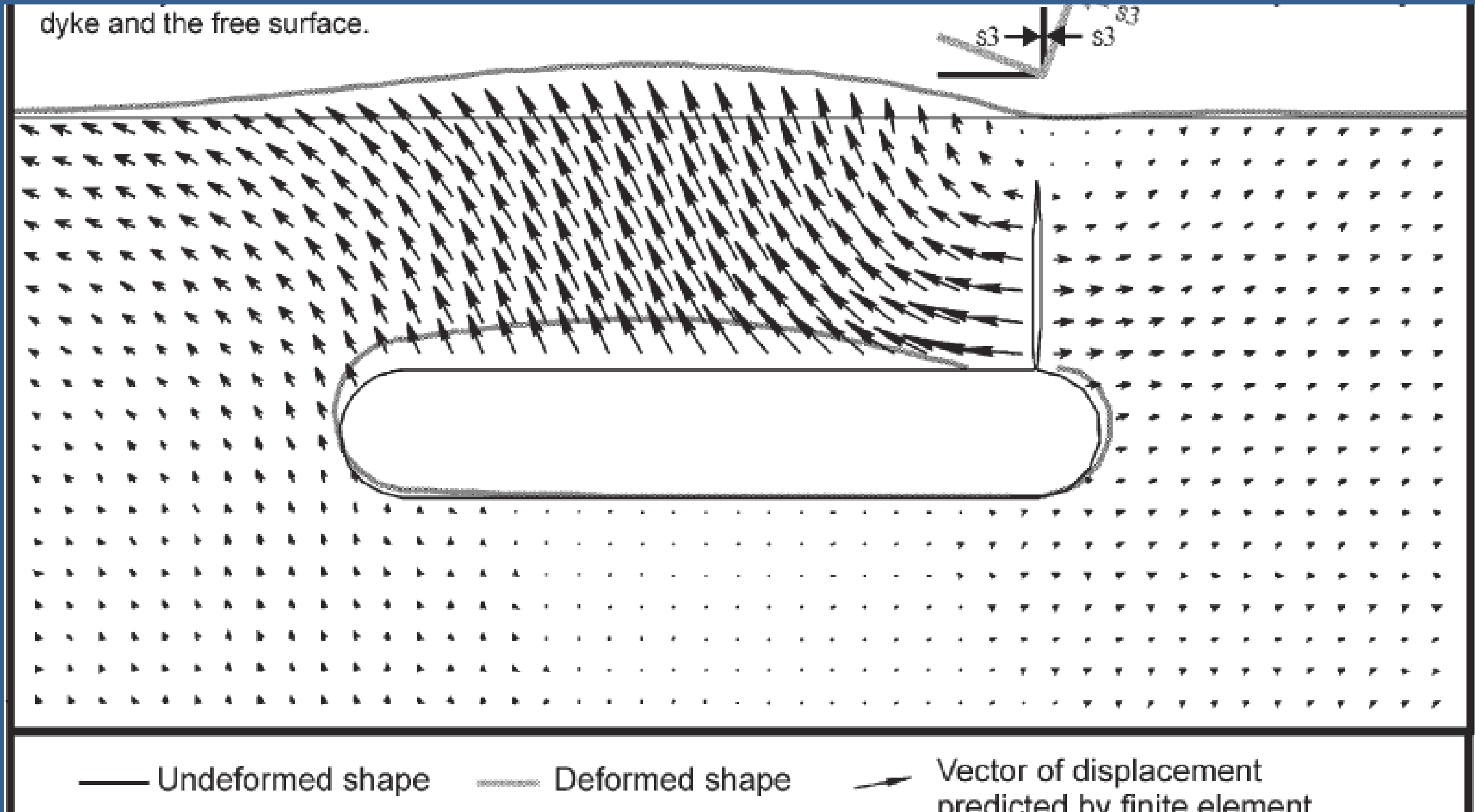

Saunders, B. Volc, 2005

Summary of Assumptions

(Masterlark, 2007)

- **Half-Space** (Add topography)
  - Only important w/ significant relief
- **Poisson-Solid** (Vary poisson's ratio)
  - Very important
- **Isotropic** (Try anisotropic matieral)
  - Somewhat important
- **Homogeneous** (Add heterogeneous subdomains)
  - Very important

Masterlark 2007 Conclusions

1. "Deformation source parameters, precisely estimated from inversion of deformation data, can be significantly inaccurate due to HIPSHS assumtions"

[My comment: HIPSHS aren't the only important assumptions]

1. Mogi models is suitable for *qualitative* assessment of volcano deformation

Summary: What range of models fit your data?

Some different model parameters to test:

- Chamber geometry
- Homogeneous vs. 1D, 2D, and 3D elastic models
- Poisson's ratio
- Include faults and realistic topography
- Isotropic vs. Anisotropic models
- Magma compressibility
- Thermally self-consistent model
- Viscoelastic models

Who cares?

- Impacts: Magma chamber depth, location & volume

Important for understanding relation between deformation and other parameters: seismicity, volumes erupted, gas flux, etc.

Philosophical comments on modeling

We want our models to be as realistic as possible.

Realism is computationally expensive and doesn't "matter" for certain applications (e.g., De Natale & Pingue, 1996; Masterlark, 2007).

Uncertainty about what "real" subsurface properties are. We need to explore a suite of models instead of only a handful. This is also computationally expensive.

We need some systematic exploration of different levels of realism in a variety of volcanic settings.

Effects of source geometry on inferred depth at volcanoes of the central Andes

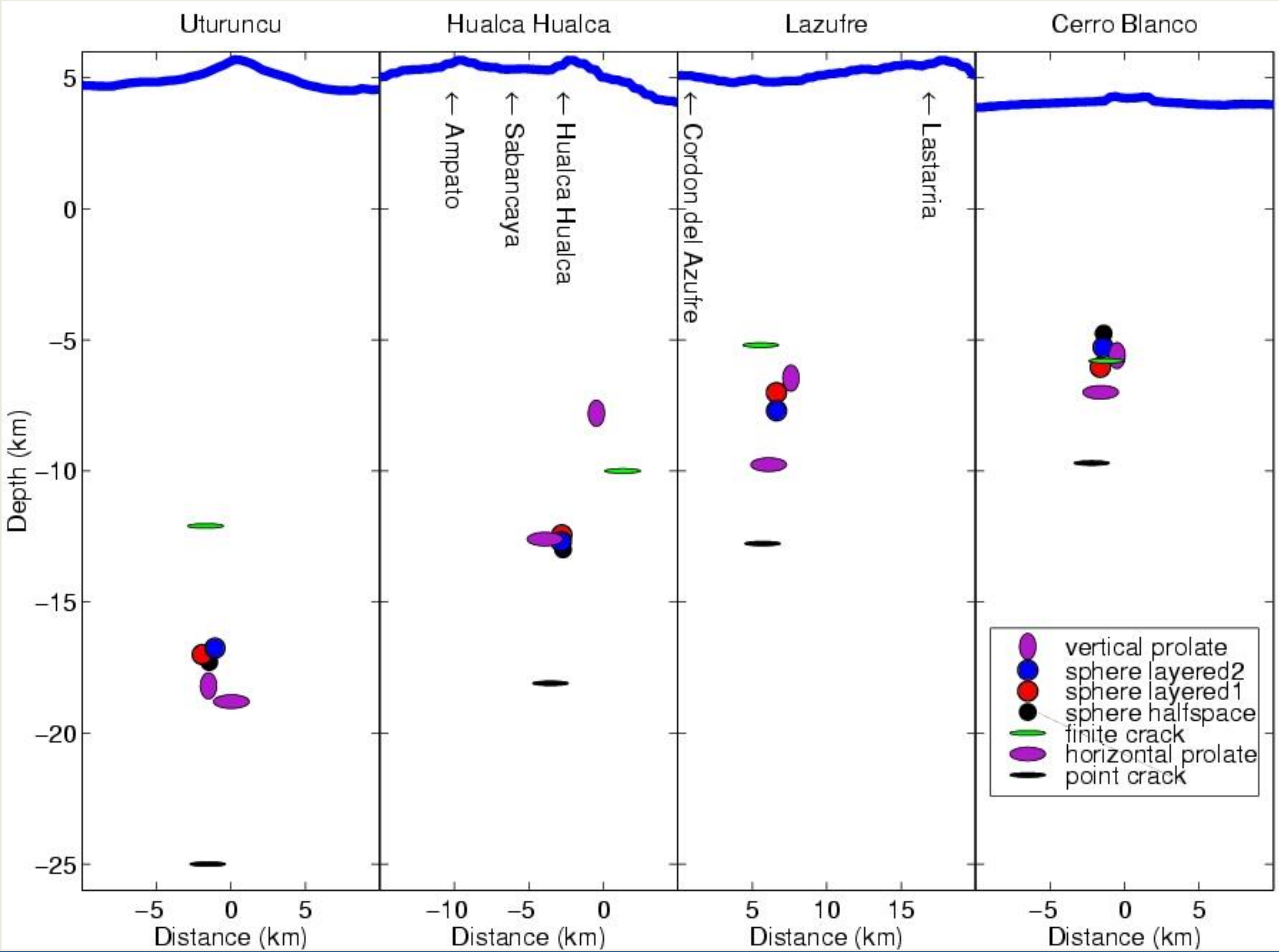

Pritchard & Simons, G-cubed, 2004

General: Choosing Model Complexity

- Case 1: Data overload

(e.g., Campi Flegrei)

  - Datasets
    - Seismicity
    - Velocity/rigidity structure
    - Mapped faults
    - Atmospheric water vapor content
  - Computationally expensive to include a perfectly realistic model....

- Case 2: Not enough data

(e.g., random Andean volcano)

  - Sparse information
  - No continuous GPS
  - Sporadic remote sensing
  - Computationally expensive to explore all possible models....

- Case 1: (high info)
  - How do we use all this information?
  - When do we have to include all info?
  - When does it make sense to simplify?

- Case 2 (low info)
  - What bias do we introduce by using inadequate models?
  - How should we present this error?
  - Which problems can we still address?

Magma ascent from the source to the surface

Magma generation

Modes of melting (approach, change solidus):

- increase temperature
  (convective heating by magmatic underplating,
  latent heat of crystallization
  → granitic magmas in plutons)

- decrease pressure (decompression of rising mantle material → partial melting of mantle)

- change composition → change melting point
  (by adding H_2O or CO_2 in subduction zones,
  wet spots)

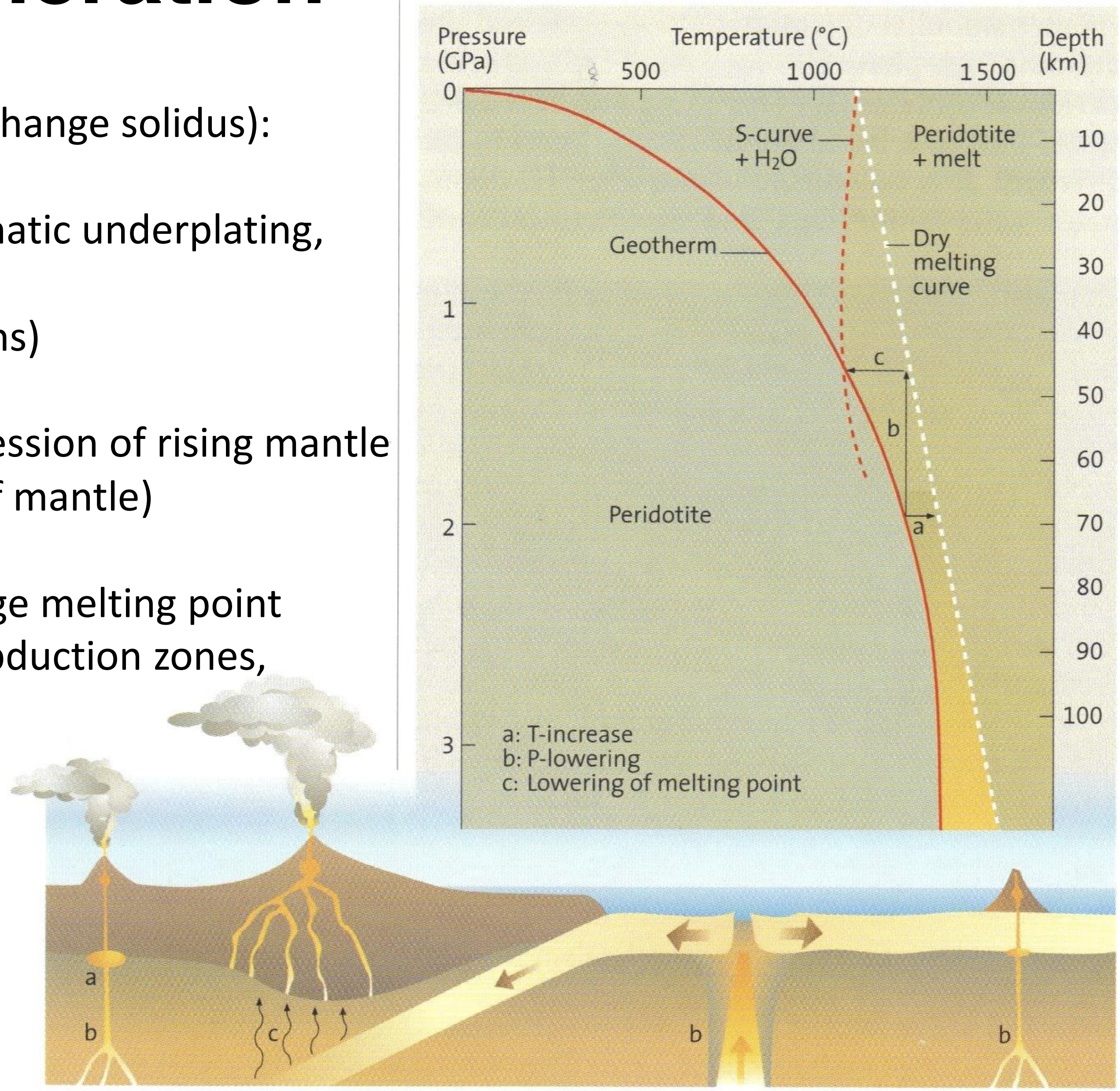

intracontinen-tal volcanism | subduction zones | mid-ocean ridges | hot/wet spots

Volcanic plumbing system

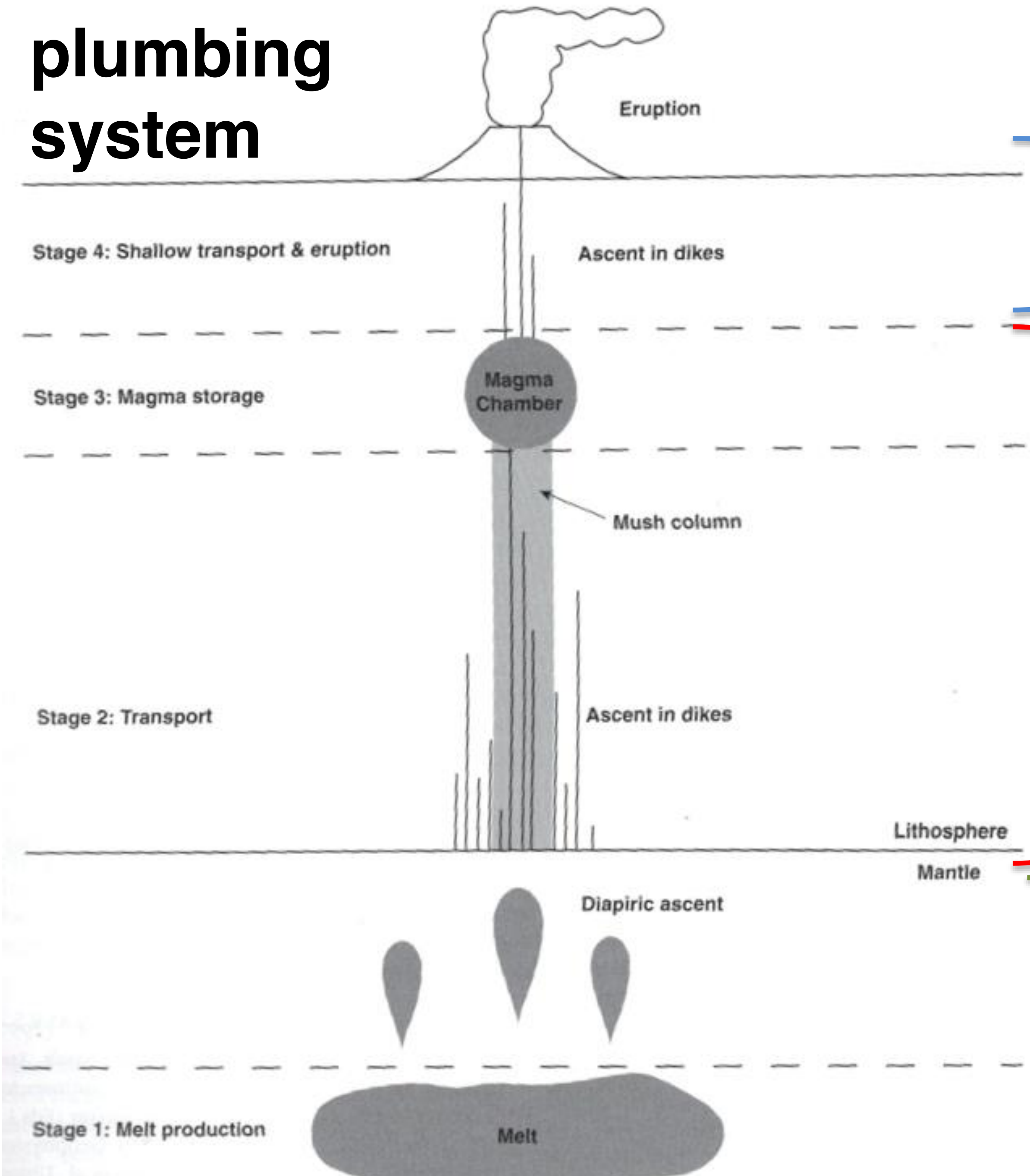

Parfitt & Wilson, Physical Volcanology

GPS, tilt
Seismic

magma ascent to the surface

InSAR

magma storage

magma ascent through the lower, middle crust

petrology, modelling

magma ascent through the mantle

How does the magma rise to the Moho?

Three mechanisms:

A) Diapirs	B) Dikes	C) Flow in fractures

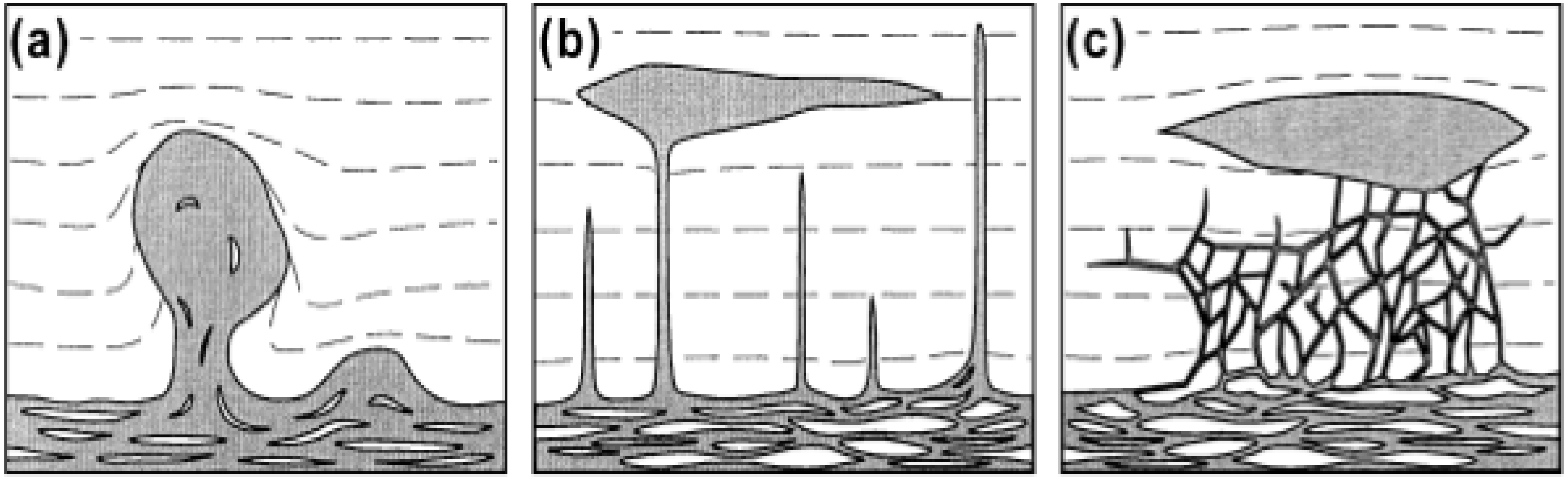

melt ascent rate controlled by:

A) Diapirs	B) Dikes	C) Flow in fractures
viscosity of surrounding rock	viscous drag of magma inside dike	permeability of network
unknown observed in crust	likely	unlikely (works only for T_{rock} >= $T_{melt, solidus}$ imagine water flowing through cracks in ice)

Bons et al., 2004

Magma focussing through dike coalescence

coalesence depends on:
- dike spacing (magma production rate)
- differential horizontal stress

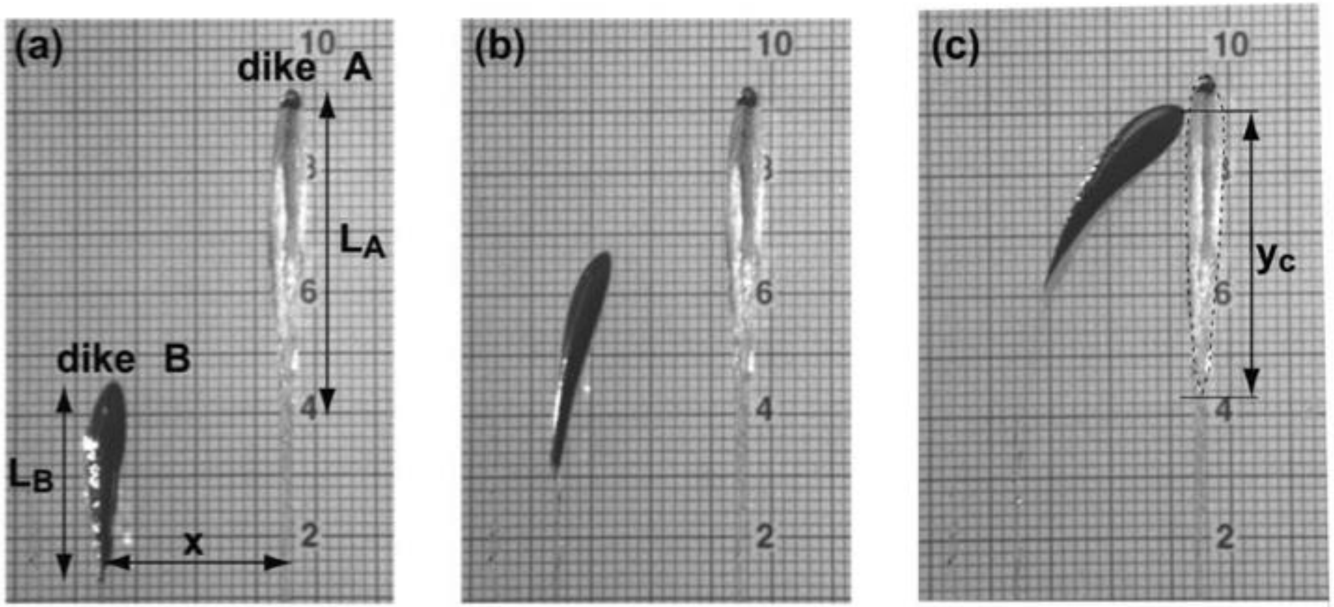

Ito and Martel, 2002

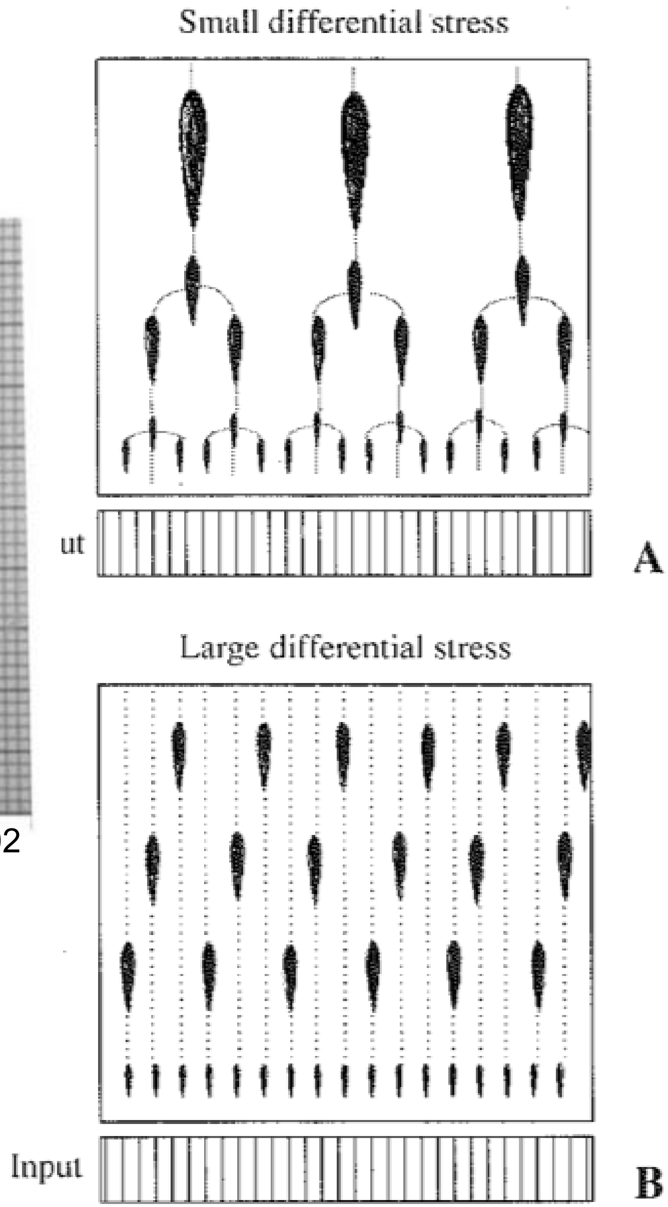

- big dikes “eat” small dikes
- stress at depth affect coalescence and magma supply rate

Magma focussing through dike coalescence

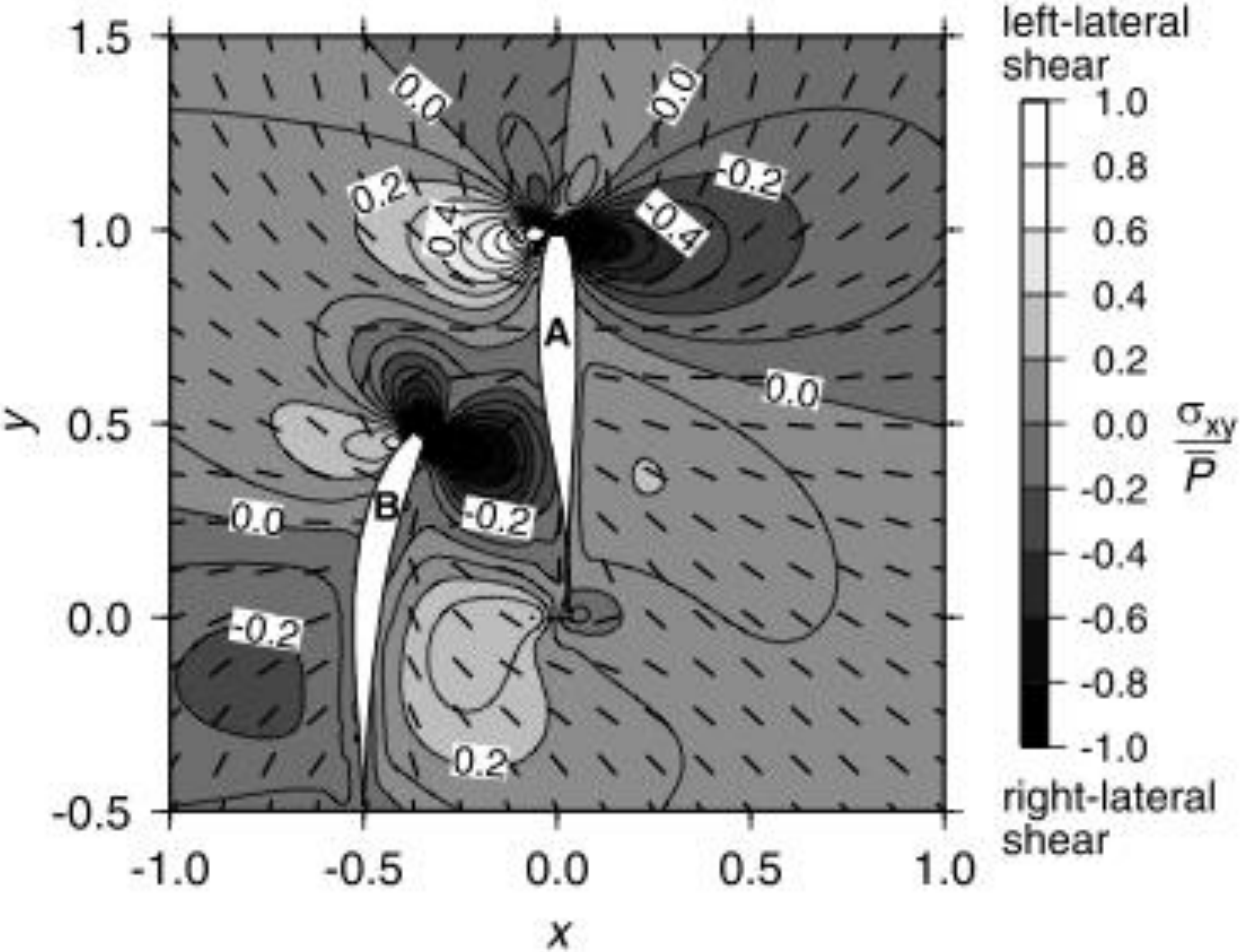

ticks: trajectories of min. tensile stress Ito and Martel, 2002

Volcanoes on thin crust (hot spot volcanoes) → magma ascent in multi-year batches

1. Kilauea Hawaii: increased magma supply during 2004-2009

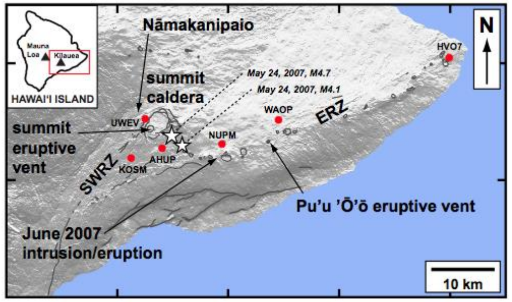

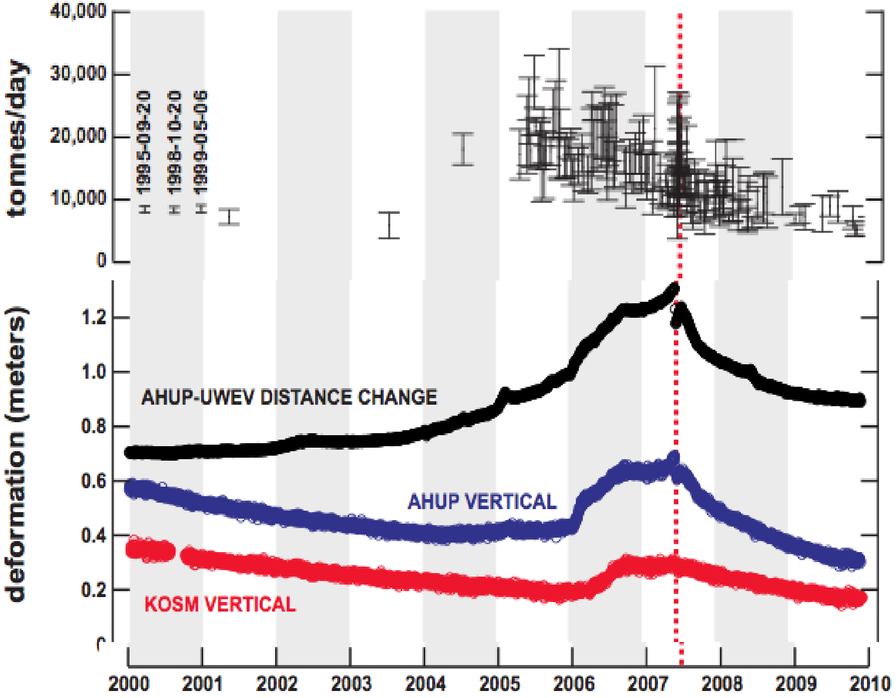

Poland et al., Nature Geo., 2012

2. Galapagos volcanoes

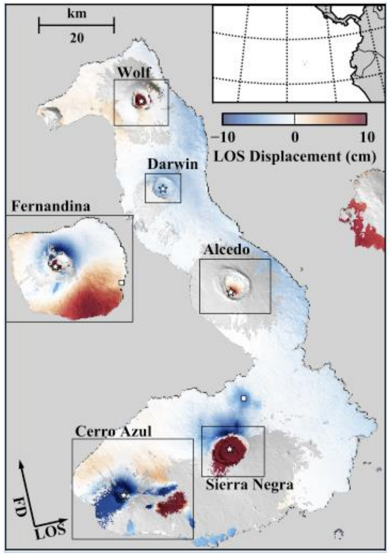

Inflation periods
Wolf : 10 yrs
Alcedo: 2 yrs
Sierra Negra: 8 yrs

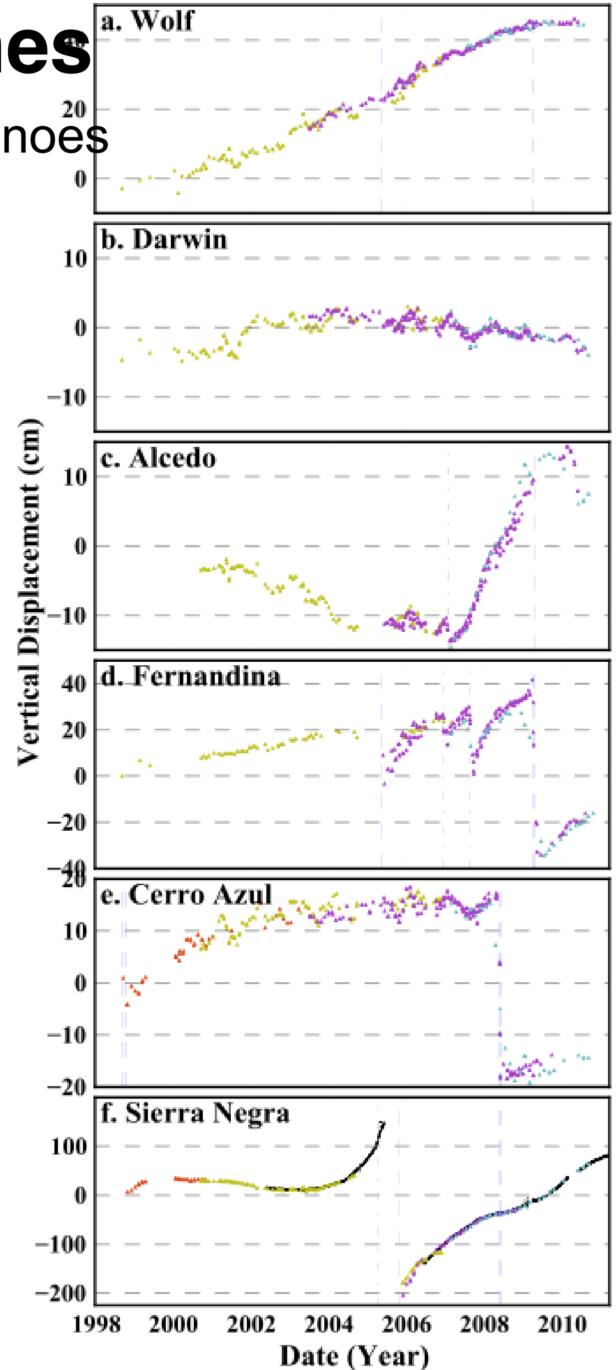

Baker and Amelung, in prep.

Magma body at the Moho: Socorro, NM

2-3 mm/yr uplift rate for at least 100 years (Finnegan & Pritchard, 2009; Pearse &Fialko, 2010)

Figure from: USGS

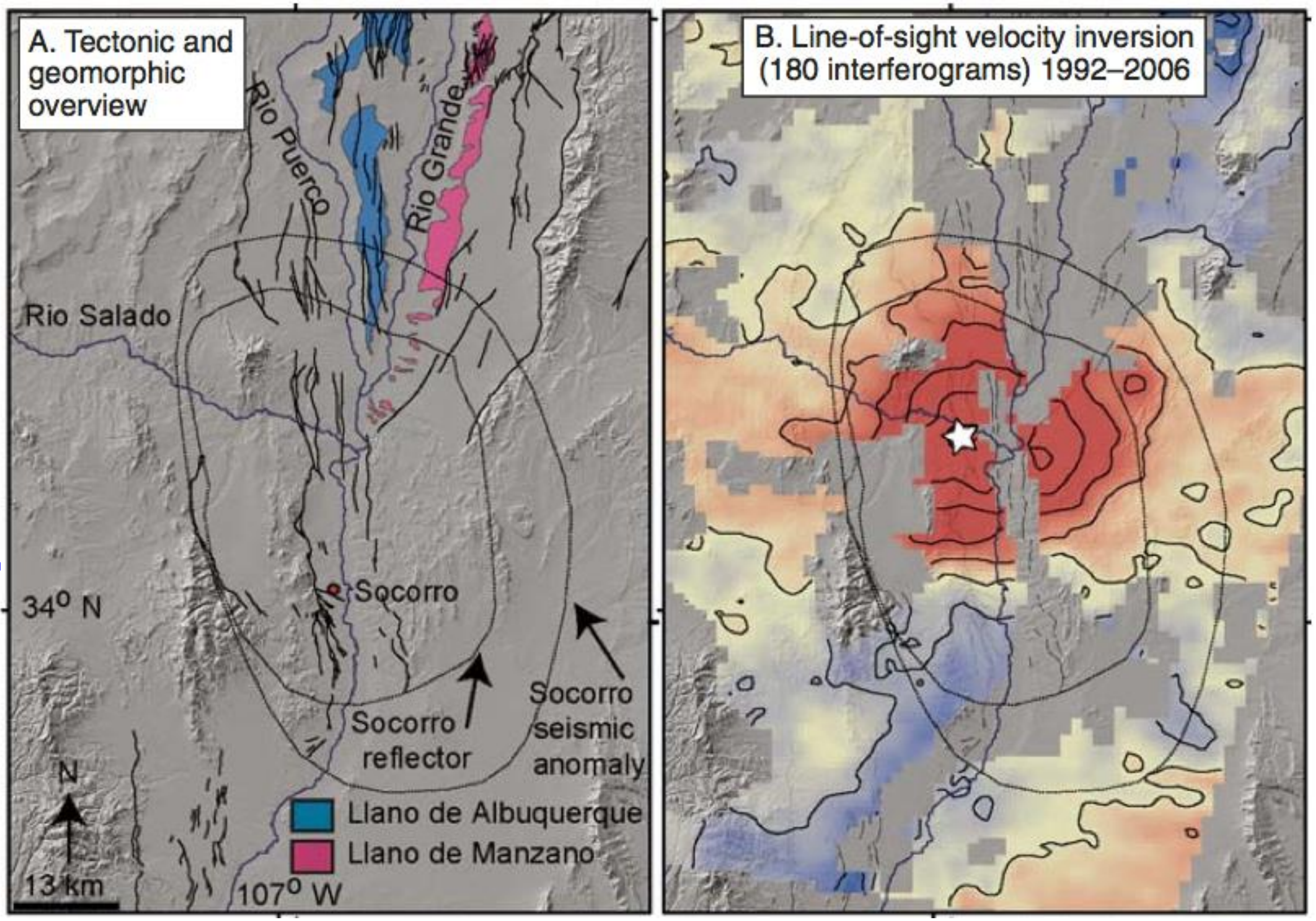

Magma body in the lower crust: Altiplano-Puna

REPORTS

Sombrero Uplift Above the Altiplano-Puna Magma Body: Evidence of a Ballooning Mid-Crustal Diapir

Yuri Fialko* and Jill Pearse†

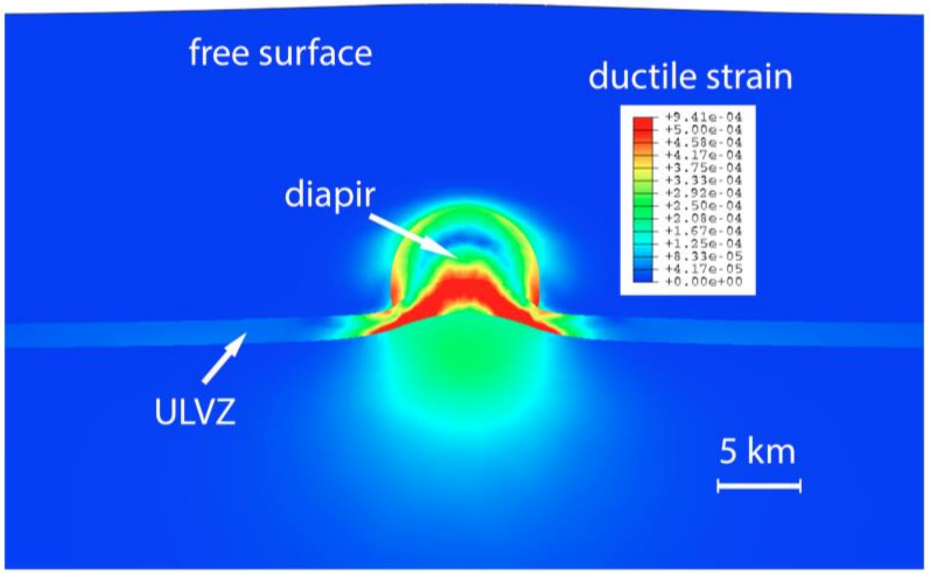

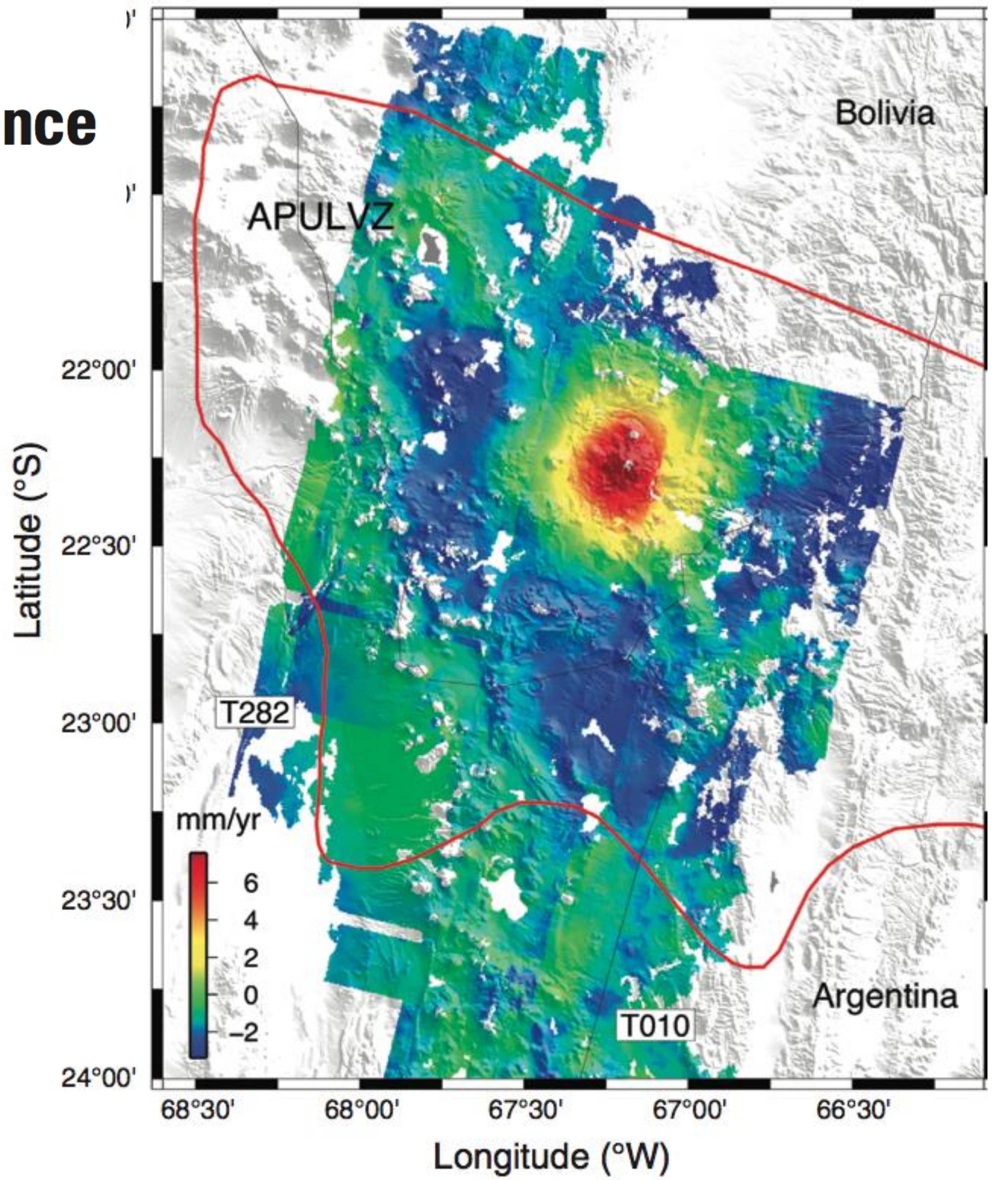

- up to 10 mm/yr uplift in center
- uplift area > 70 km diameter
- surrounded by fringe with 1 mm/yr subsidence

Magma ascent from lower crustal to upper crustal reservoirs

- crust acts as a ***magma filter*** (primary basalt → intermediate, silicic magmas)
- two processes:
  1. partial crystallization of basalt sills (arrived from depth)
  2. partial melting of pre-existing rocks
- melt fraction and composition depends on heat and H2O transfer in lower crust.
- magma attains super-liquidus state
- ascent to shallow levels in dikes
- Viscosity increase by degassing and crystallization of ascending magma
- generation of volcano-feeding shallow reservoirs

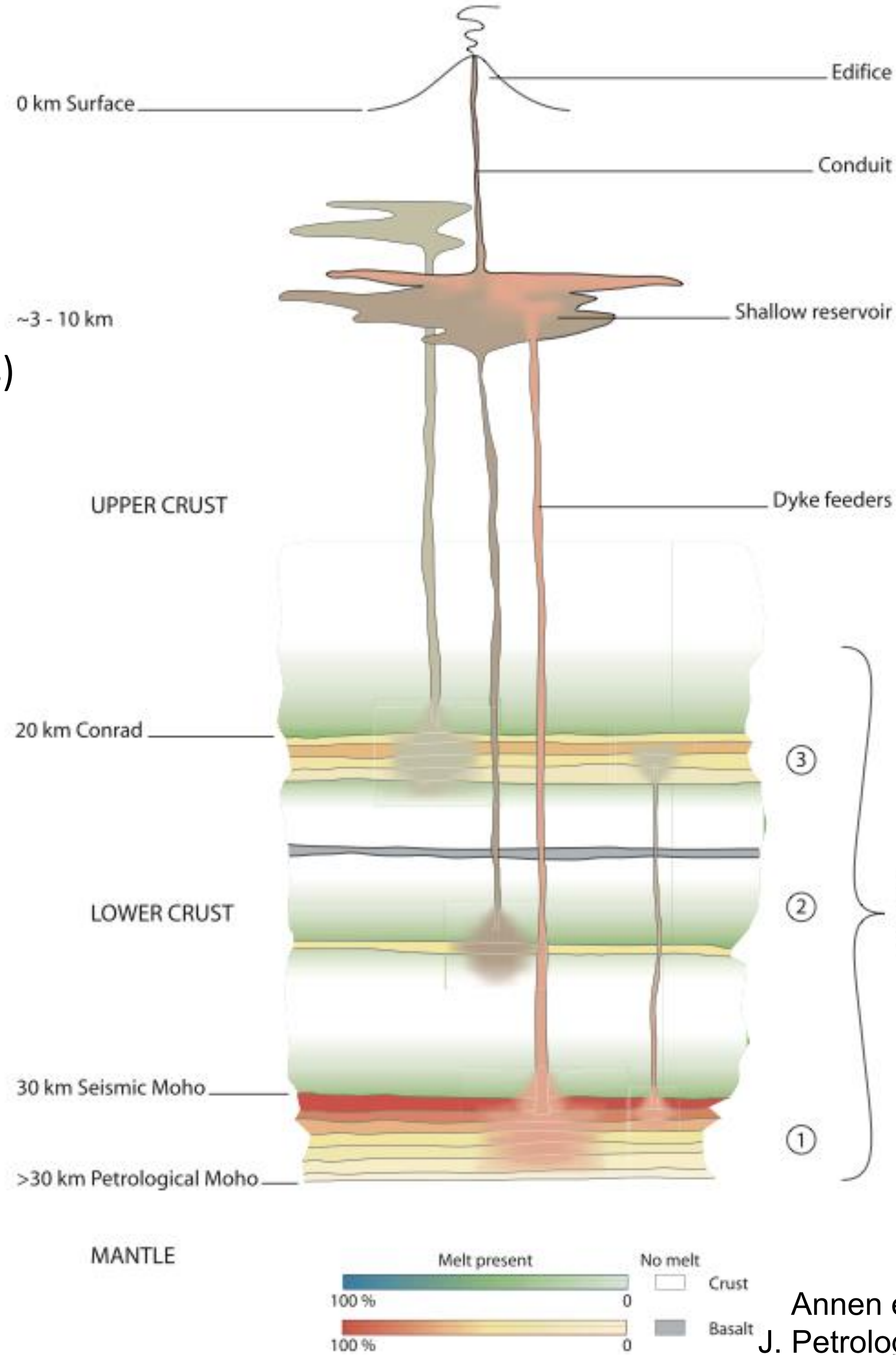

Annen et al., J. Petrology, 2006

What controls magma ascent ?

Classical ***"top-down"*** view of plumbing system. Magma ascent controlled by

- buoyancy
- mechanical rock properties (layering)

Dike arrest by stress traps

A stiff layer above a soft layer may arrest dikes.

stress field in layered media

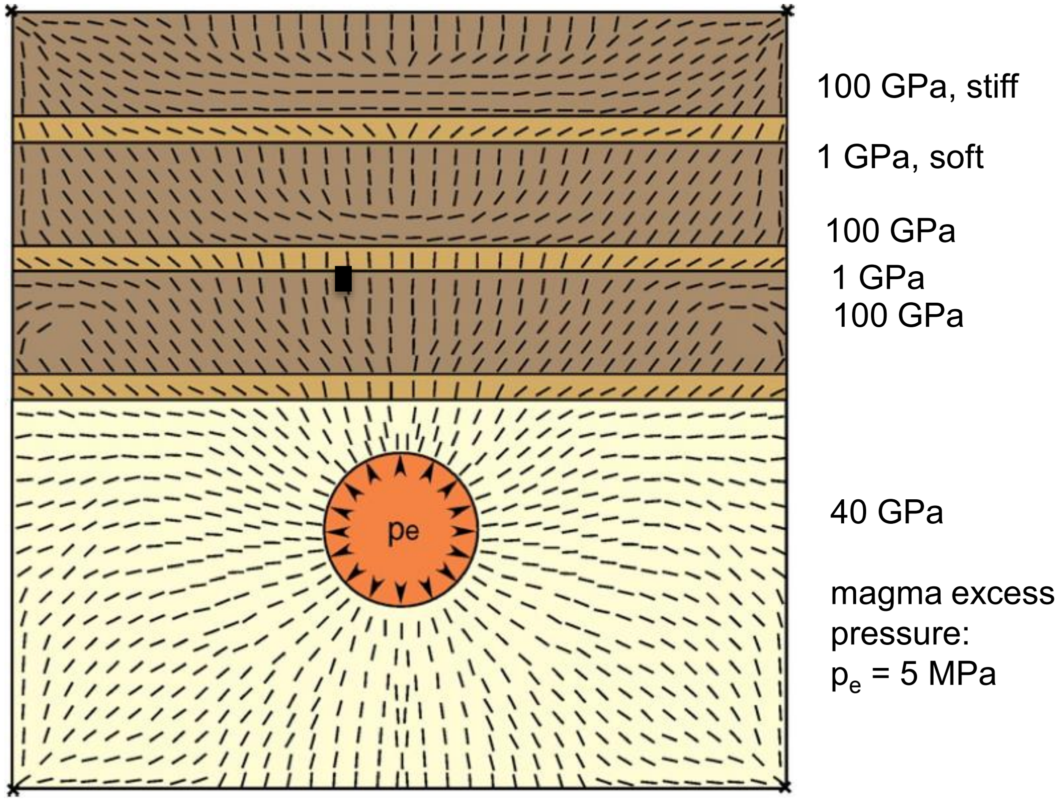

σ_1 trajectories

dikes propagate perpendicular to σ_3, parallel to σ_1

Gudmundsson book, Fig. 6.21

What controls magma ascent ?

Classical ***"top-down"*** view of plumbing system. Magma ascent controlled by

- buoyancy
- mechanical rock properties (layering)

Alternative ***"bottom-up"*** view of self-organized volcanic plumbing. Magma ascend controlled by stress due to:

- magma chambers at Moho
- chambers in crust.
- volcanic edifice.

- capture of ascending dikes. Capture radius depends on
  - magma overpressure P_0 (high P_0 → large capture radius)
  - tectonic stress important (extension → smaller capture radius)
  - viscoelastic relaxation of stress

Stress due to

1. edifice　　2. chamber

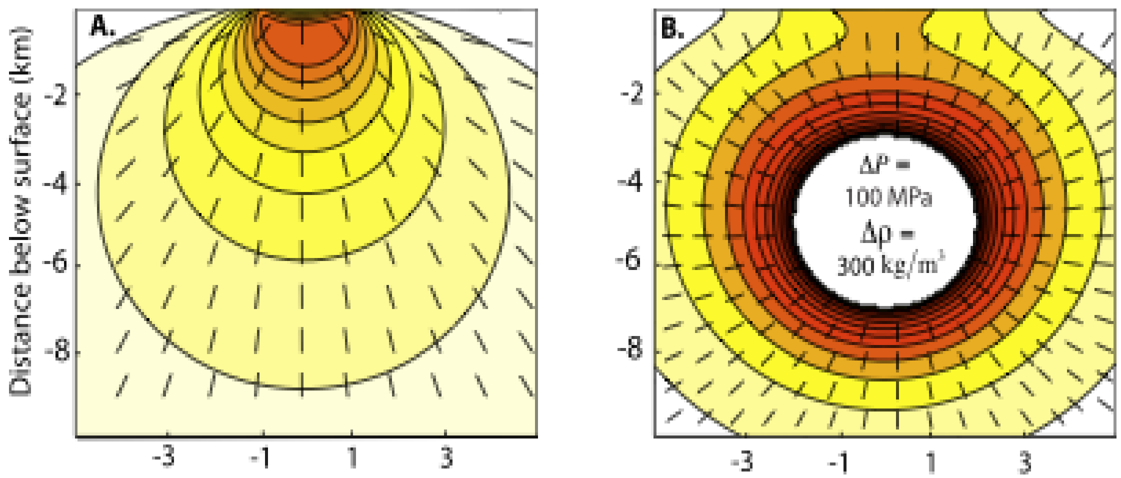

Karlstrom, Dufek, Manga, JGR, 2009

How do magma storage reservoirs look like?

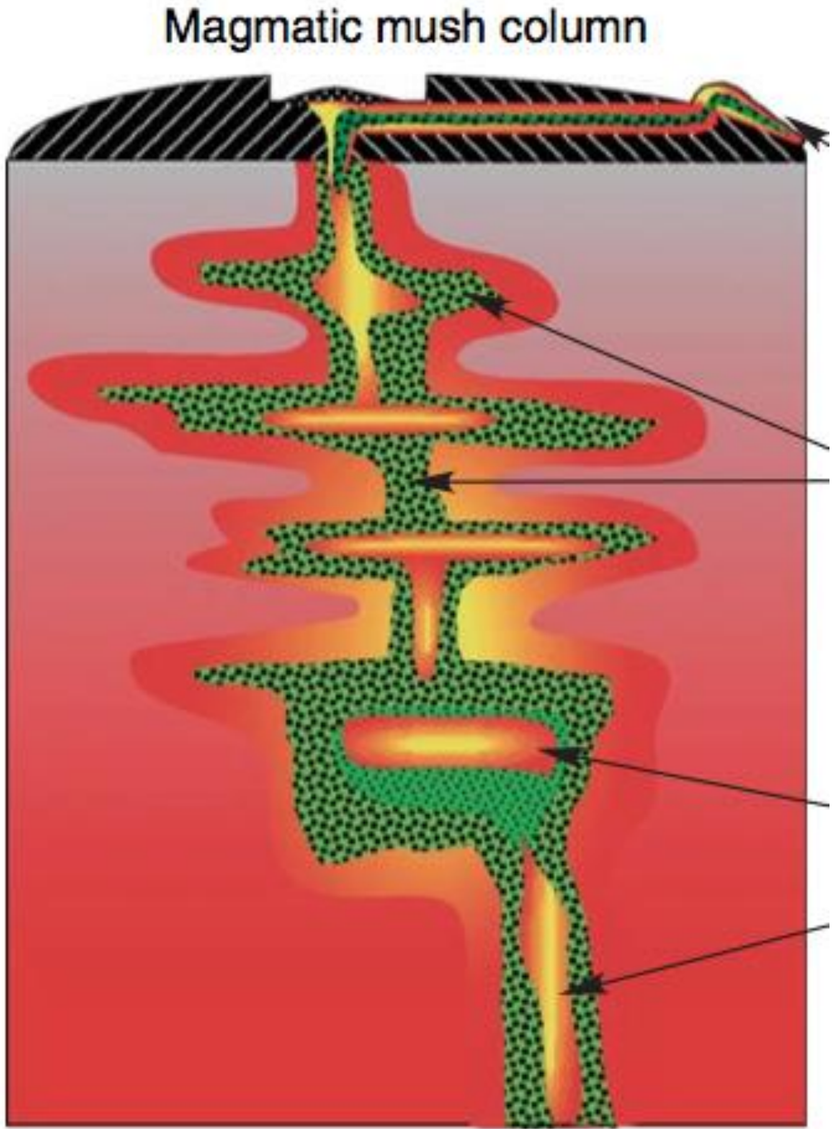

B. Marsh, Treatise of Geophysics, 2007

green colors: mush with 50-90% crystals
red-yellow: mush with <50% crystals, possibly eruptible

Ferrar Diorite, Dry Valleys, Antarctica

petrologic evidence for "solidification fronts" (mush with varying crystal content)

stacked-sill system containing magma mush with 1-5% to 90-95% crystal content

How do magma storage reservoirs look like?

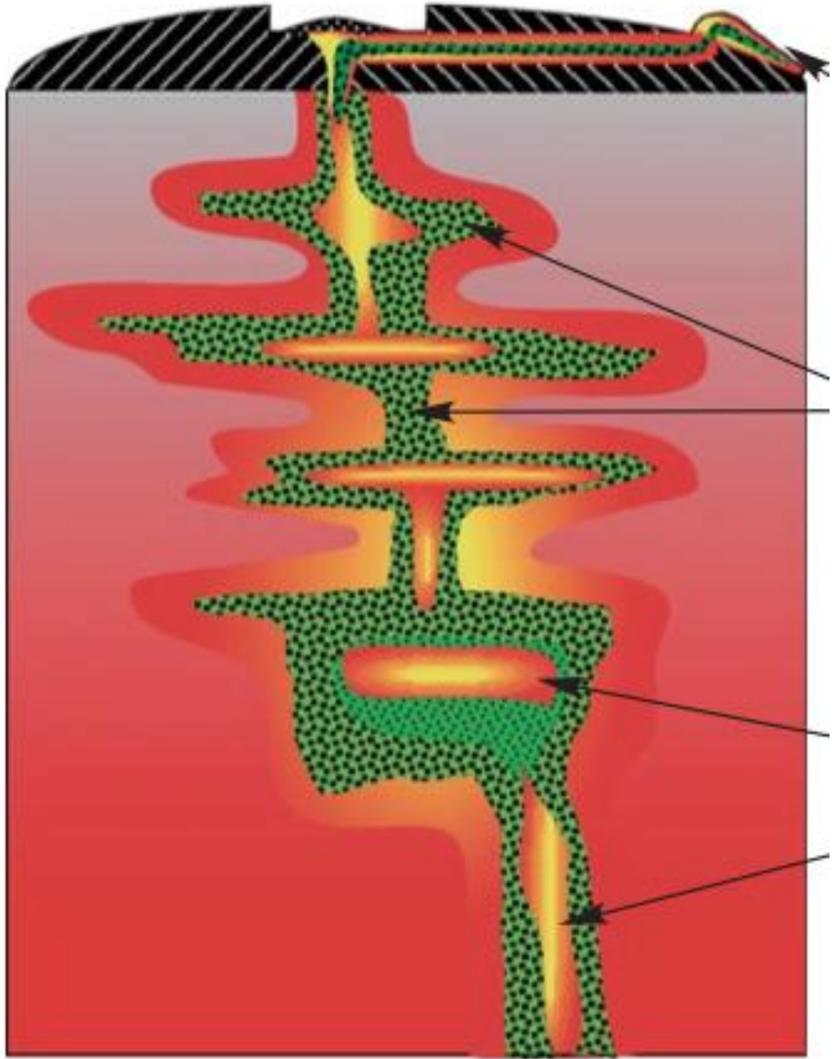

B. Marsh, Treatise of Geophysics, 2007

green colors: mush with 50-90% crystals
red-yellow: mush with <50% crystals, possibly eruptible

Long valley magma storage system
(upper crustal portion)

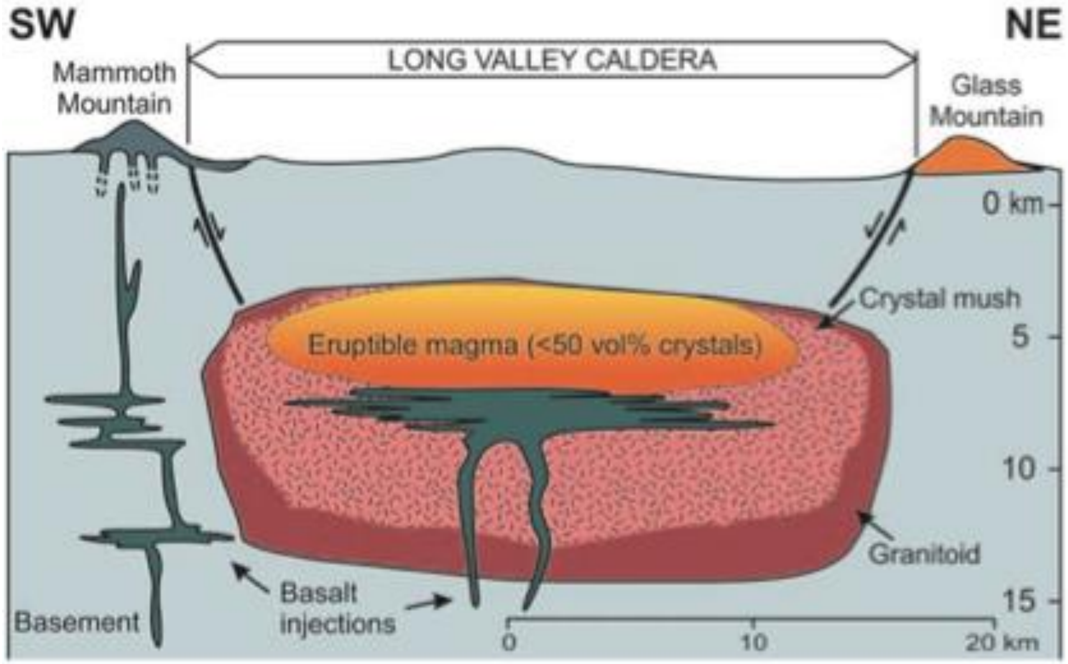

Bachmann and Bergantz, 2008

- only a small fraction of a magmatic system consists of eruptible magma (< 50% crystals)
- note: there is more crystal mush *above* the eruptible magma then shown in the sketch

How do magma storage reservoirs look like?

Solidification front concept

cooler

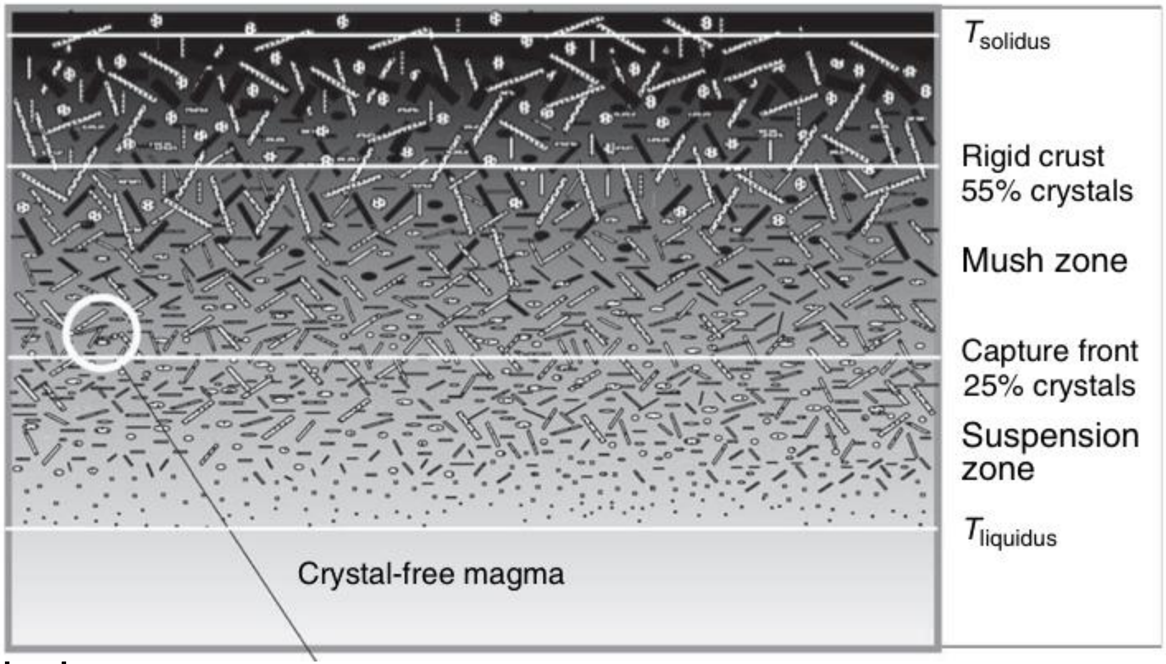

hot

- after intrusion, solidification front rapidly moves inward and then slows down.
- behind *capture front* crystals don't move
- only phenocrysts from *suspension zone* are available to settle.
- crystal growth and settling is "slow". Solidification front may move faster and capture falling crystals

Important: phenocryst content of injected Magma.

→ No crystals in thin sills, dikes

How do magma storage reservoirs look like?

Solidification front concept

cooler

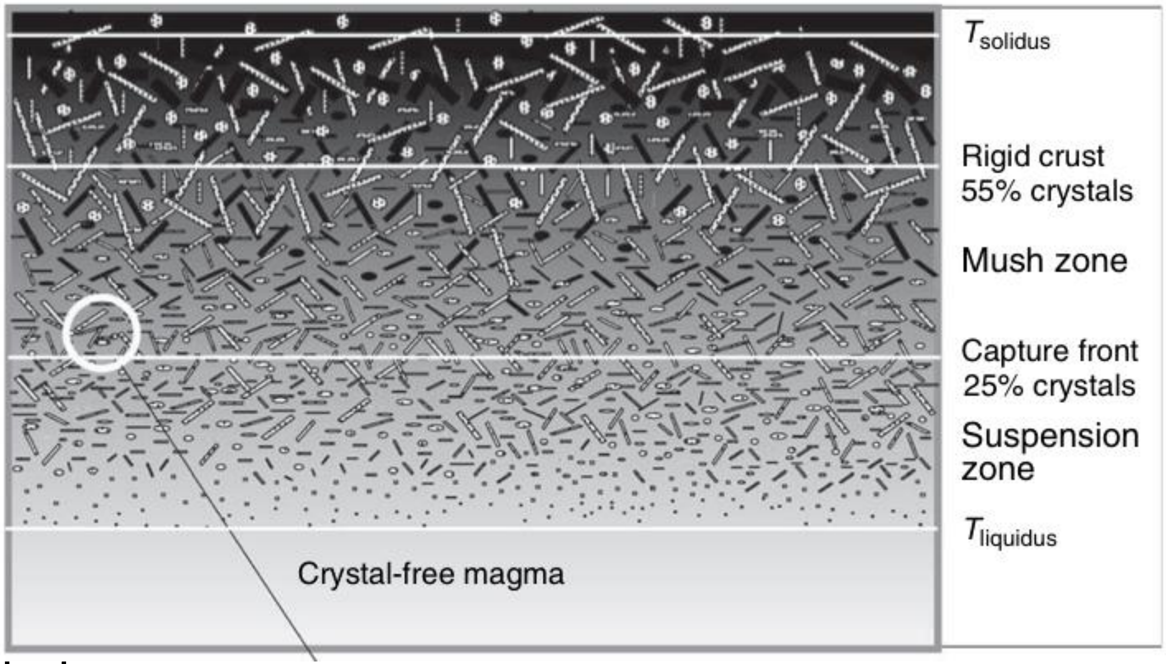

hot

Important: phenocryst content of injected Magma.

Maximum crystal packing….

- magma: crystals have higher density than liquid (opposite for soda)